# On the Need for Locational Signals in a Capacity Market

## Procurement Costs, Redispatch, and Adequacy Under Network Constraints

Master Thesis

Alexander Hutner

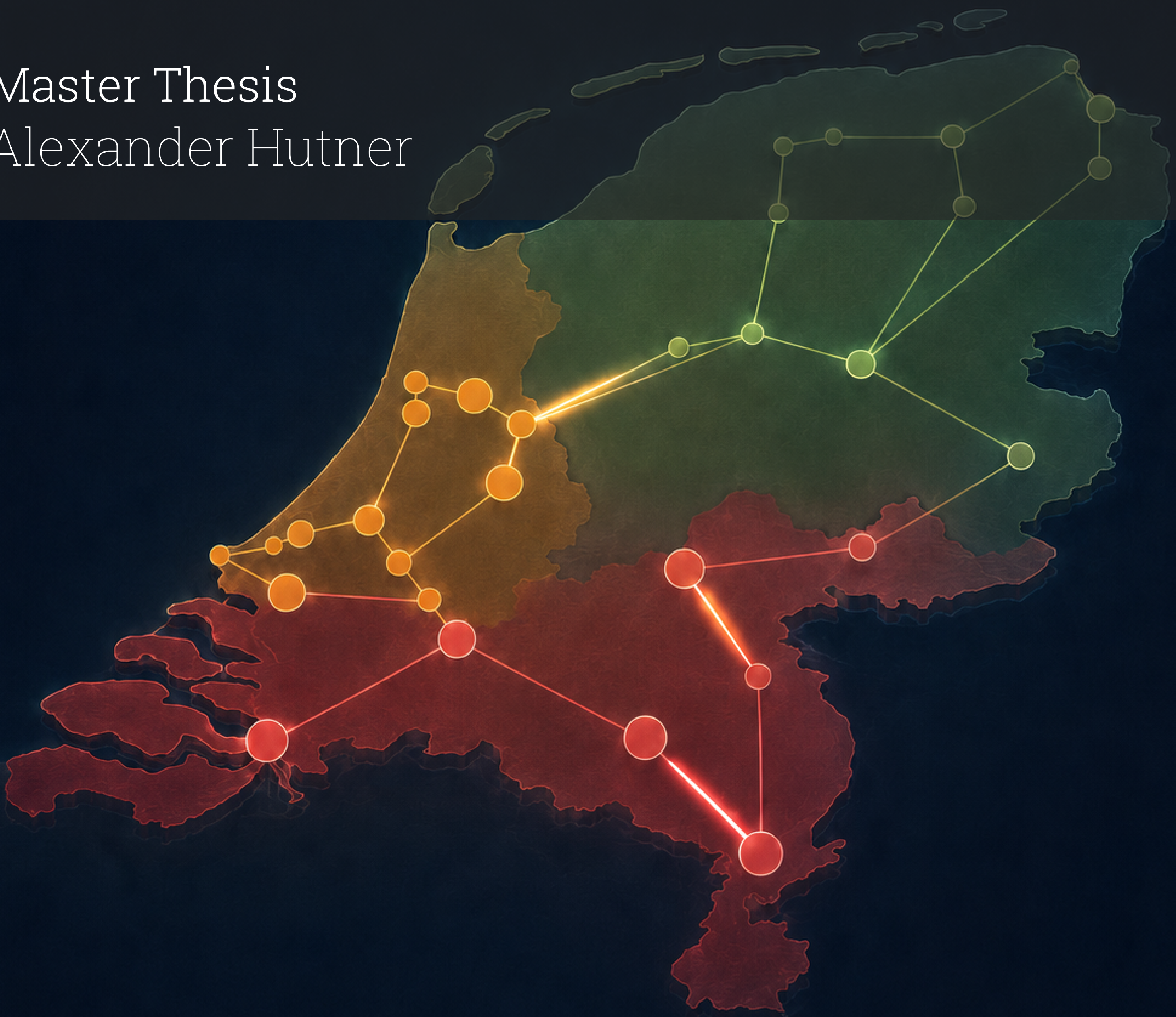

Delft University of Technology

TU Delft

# On the Need for Locational Signals in a Capacity Market

## Procurement Costs, Redispatch, and Adequacy Under Network Constraints

by

Alexander Hutner

to obtain the degree of Master of Science
at the Delft University of Technology,
to be defended publicly on Thursday July 9th, 2026 at 10:30 AM.

| | | |
|---|---|---|
| Student number: | 6291317 | |
| Project duration: | February 2026 – July 2026 | |
| Thesis committee: | Dr. ir. K. Bruninx, | Chair & First Supervisor |
| | Dr. Y. Huang, | Second Supervisor |
| | A. Kelly | Advisor |

Cover: Image generated by ChatGPT (Model GPT-5.5) based on Figure 4.1 and Figure 4.3 of this thesis.
Style: TU Delft Report Style, with modifications by Daan Zwaneveld

An electronic version of this thesis is available at http://repository.tudelft.nl/.
The associated data files and code for the model implementation are available on a public GitHub repository:https://github.com/alexhtn163/locational-signals-cm.

TU Delft

# Preface

Here I sit, the night before my deadline. Another long day of working on my thesis until late, only that this time it will be the last. It was a journey of highs and lows. Sometimes those were only minutes apart, sometimes days (for better or worse). The heatwave of the past weeks proved itself to have both advantages and disadvantages for my work. Disadvantage: my room turned into an oven. Getting enough sleep in an oven is indeed fairly challenging. Advantage: my room turned into an oven. Staying at the library from morning until late was the only option for survival. The survival of my laptop, on the other hand, was at times in question due to sweat raining from the library ceiling and an exploding socket. But without further ado, let me start thanking the people who contributed to the success of this thesis and, more generally, to my student life, before my brain runs out of digital ink.

First of all, I want to thank my supervisors, Kenneth Bruninx and Yilin Huang, for providing me with great feedback and guiding me throughout the process. A huge thank-you also goes to my advisor, Alison Kelly, with whom I worked most closely during this thesis. Thank you for constantly sharing your ideas and advice with me, not only regarding the content of this thesis, but also on everything surrounding the final phase of my studies.

Instead of continuing with a long list of names, which would inevitably lead to me forgetting someone important, I will write a general thank-you in which, hopefully, the right people will be able to find themselves. Over the past years, I have had the privilege of getting to know so many amazing people. Some stuck around for longer, some for a shorter time. Nonetheless, you all had a positive and lasting impact on me, and I was always surrounded by people who made me feel at home, no matter where I was. To all the people I enjoyed drinks with, shared frustrations with, locked in to study with, went to watch football with, spent hours at the beach with, listened to me ramble on about niche movies they probably did not care about but listened regardless, introduced me to even more great people, and, most importantly, were patient with me when I once again did not reply to texts or calls: thank you (and once again, especially sorry to everybody who tried to text me during these past few weeks).

Und als Letztes noch an meine Familie: Papa, Mama und Maxi. Meine Entscheidungen waren vermutlich nicht immer die einfachsten oder naheliegendsten. Zu jedem Zeitpunkt hatte ich dennoch eure volle Unterstützung und euer Verständnis, und zu keinem Zeitpunkt habe ich Zweifel von euch erfahren. Ohne diese Sicherheit wären viele meiner Entscheidungen deutlich schwerer gefallen. Dafür und für alles, was ihr mir auf meinem bisherigen Weg ermöglicht habt, bin ich euch unendlich dankbar.

*Alexander Hutner*
*Delft, July 2026*

# Summary

With the rise of renewables in Europe, conventional generators are increasingly struggling to recover their costs on the energy market. However, due to the intermittency of renewables, controllable generation is still needed. To secure resource adequacy, capacity mechanisms have become a common instrument. Furthermore, that capacity must also be located where the transmission network can deliver it when renewable output is low.

European zonal energy markets do not value the location of generators, because each energy market zone is cleared as if there were no internal transmission constraints. Internal congestion is instead resolved after the market has cleared through redispatch, which has become a frequent and costly corrective measure.

So far, capacity mechanisms in Europe are also indifferent to generator location within a country. They procure sufficient capacity in total without ensuring that it is available where the network needs it. In a zonal market, this omission has real consequences, because capacity sited in low-cost but network-constrained locations can increase redispatch needs or make redispatch infeasible during scarcity. A locational signal within the capacity mechanism could direct investment towards more useful locations. By restricting where capacity may be procured, however, such a signal may also raise capacity-market expenditure. Although several studies argue that locational capacity mechanisms improve congestion outcomes, they either combine multiple locational signals or embed capacity-market cost within aggregate system-cost measures, and therefore cannot isolate this trade-off. This leads to the research question:

*To what extent do locational signals in capacity markets shape the trade-off between capacity procurement costs and congestion outcomes in a zonal energy market?*

To answer this question, the thesis develops a sequential two-stage model consisting of a market-equilibrium stage followed by a cost-based redispatch stage. Generators decide their dispatch and capacity offers, new generators additionally decide their investment, and demand agents procure capacity against a system-wide requirement and, under the locational design, against zonal requirements. In the model, redispatch revenues do not influence generator investment. The energy market also does not offer any locational signal, and the capacity market only does so at the level of the defined zones. Several first-stage equilibria can therefore share identical energy and capacity costs while siting capacity at different nodes, and each siting implies a different redispatch outcome in the second-stage problem. A single equilibrium solution would hide this variation.

The thesis addresses this through solution-space exploration. The equilibrium is reformulated and solved repeatedly under PTDF-based objective weights that push investment along different network directions, exploring a range of market-equivalent siting outcomes together with their redispatch consequences. This is the main methodological contribution, as it makes explicit the side of the trade-off that existing studies leave inside a black box: the capacity-market cost of a locational signal, evaluated jointly with its congestion outcomes. The model is first verified on a small proof-of-concept system and then applied to the Dutch transmission network consisting of 34 nodes and eight representative days. Two case studies are constructed on this network but with different inherited generation. The first removes most legacy gas, so that new investment supplies the majority of the required capacity and the mechanism largely determines where it is built. The second retains the existing gas fleet, leaving only a small residual deficit on which the signal can act. Each case compares a country-wide capacity requirement against a three-zone requirement and varies cross-zonal participation from none to full.

The results show that a locational signal improves physical deliverability more consistently than it reduces costs, while its effect on capacity-market expenditure remains conditional. Across both case studies, the zonal requirement redirects capacity towards deficient zones and substantially improves the ability of the system to restore network feasibility during scarcity. Its effect on capacity-market

expenditure depends strongly on the inherited fleet: in the first case it raises expenditure by only a few percent, whereas in the second the increase is much larger because only a small amount of new capacity is required under country-wide procurement and accepted legacy units also receive the zonal price.

Redispatch volume and cost alone prove incomplete measures of performance, because neither decreases monotonically with the strength of the signal. Feasibility responds far more clearly. The country-wide design leaves scarcity events that cannot be resolved, while strict zonal procurement eliminates grid-related load shedding in the second case. Limited cross-zonal participation can recover part of the additional cost where a neighboring zone holds surplus capacity, but excessive participation weakens the signal and returns the system towards the country-wide siting pattern. No single design or participation level is therefore optimal. A locational capacity mechanism does not remove congestion or substitute for grid expansion. It can shift part of the burden from ex-post redispatch towards the ex-ante procurement of deliverable capacity, and in doing so reframes the policy question from how much capacity to procure towards how much of it must be local to remain deliverable when the network is constrained.

# Contents

# List of Figures

# List of Tables

# Nomenclature

## Sets and Indices

| Symbol | Description | Unit |
|---|---|---|
| $t \in \mathcal{T}$ | Time step, with $\mathcal{T}$ as the set of all time steps | – |
| $i \in \mathcal{I}$ | Investable controllable generator, with $\mathcal{I}$ as the set of investable generators | – |
| $j \in \mathcal{J}$ | Legacy generator, with $\mathcal{J}$ as the set of legacy generators | – |
| $g \in \mathcal{G}$ | Generator, with $\mathcal{G} = \mathcal{I} \cup \mathcal{J}$ as the set of all generators | – |
| $n \in \mathcal{N}$ | Network node, with $\mathcal{N}$ as the set of all nodes | – |
| $l \in \mathcal{L}$ | Transmission line, with $\mathcal{L}$ as the set of all lines | – |
| $z \in \mathcal{Z}$ | Capacity-market zone, with $\mathcal{Z}$ as the set of all zones | – |
| $(a, b) \in \mathcal{P}$ | Unordered pair of capacity-market zones connected by cross-zonal participation | – |
| $k$ | Exploration-vector index | – |
| $\omega \in \mathcal{A}$ | Generic actor, with $\mathcal{A}$ as the set of actors in the primal-dual formulation | – |
| $\mathcal{G}_n$ | Set of generators located at node $n$ | – |
| $n(g)$ | Network node of generator $g$ | – |
| $n(i)$ | Network node of investable generator $i$ | – |
| $z(g)$ | Capacity-market zone of generator $g$ | – |
| $z(i)$ | Capacity-market zone of investable generator $i$ | – |
| $z(j)$ | Capacity-market zone of legacy generator $j$ | – |
| $\mathcal{W}$ | Set of positive and negative PTDF-based exploration vectors | – |

## Decision Variables and Market Prices

| Symbol | Description | Unit |
|---|---|---|
| $\lambda_t^e$ | Energy-market clearing price in time step $t$ | €/MWh |
| $\lambda_z^c$ | Capacity-market clearing price in zone $z$ | €/MW |
| $q_{t,i}$ | Energy-market dispatch of investable generator $i$ in time step $t$ | MW |
| $q_{t,j}$ | Energy-market dispatch of legacy generator $j$ in time step $t$ | MW |
| $q_{t,g}$ | Energy-market dispatch of generator $g$ in time step $t$ | MW |
| $c_i$ | Installed capacity of investable generator $i$ | MW |
| $c_i^{cm}$ | Capacity offered by investable generator $i$ in the capacity market | MW |
| $c_j^{cm}$ | Capacity offered by legacy generator $j$ in the capacity market | MW |
| $c_g^{cm}$ | Capacity offered by generator $g$ in the capacity market | MW |
| $D_t$ | Aggregate demand served in the energy market in time step $t$ | MW |
| $ls_t^{em}$ | Load shedding in the energy market in time step $t$ | MW |
| $c_z^{dem}$ | Capacity procured in capacity-market zone $z$ | MW |

| | | |
|---|---|---|
| $f_{ab}$ | Signed cross-zonal capacity contribution between zones $a$ and $b$ | MW |
| $\eta_z$ | Net cross-zonal capacity contribution received by zone $z$ | MW |
| $r_{t,g}^{+}$ | Upward redispatch of generator $g$ in time step $t$ | MW |
| $r_{t,g}^{-}$ | Downward redispatch of generator $g$ in time step $t$ | MW |
| $ls_{n,t}^{grid}$ | Grid-related load shedding at node $n$ in time step $t$ | MW |
| $p_{n,t}^{inj}$ | Nodal power injection at node $n$ in time step $t$ | MW |
| $p_{l,t}^{flow}$ | Active power flow on line $l$ in time step $t$ | MW |
| $q_{t,g}^{mkt}$ | Market dispatch of generator $g$ before redispatch | MW |
| $q_{t,g}^{final}$ | Final dispatch of generator $g$ after redispatch | MW |

## Dual Variables

| Symbol | Description | Unit |
|---|---|---|
| $\mu_{t,i}^{q}$ | Dual variable of the dispatch upper bound of investable generator $i$ | €/MW |
| $\mu_{i}^{cap}$ | Dual variable of the maximum installable-capacity constraint of investable generator $i$ | €/MW |
| $\mu_{i}^{cm}$ | Dual variable of the capacity-market offer bound of investable generator $i$ | €/MW |
| $\mu_{t,j}^{q}$ | Dual variable of the dispatch upper bound of legacy generator $j$ | €/MW |
| $\mu_{j}^{cm}$ | Dual variable of the capacity-market offer bound of legacy generator $j$ | €/MW |
| $\xi_t$ | Dual variable of the energy-demand balance constraint | €/MW |
| $\kappa_t$ | Dual variable of the upper bound on served energy demand | €/MW |
| $\nu_z$ | Dual variable of the zonal capacity requirement constraint | €/MW |
| $\lambda^{c,sys}$ | Dual variable of the system-wide capacity requirement | €/MW |
| $\rho_z$ | Dual variable of the non-negative zonal requirement guard | €/MW |
| $\phi_{ab}^{lo}$ | Dual variable of the lower cross-zonal contribution bound | €/MW |
| $\phi_{ab}^{hi}$ | Dual variable of the upper cross-zonal contribution bound | €/MW |
| $\overline{\beta}_{t,g}^{q}$ | Dual variable of the upward redispatch limit of generator $g$ | €/MW |
| $\overline{\beta}_{t,g}^{-}$ | Dual variable of the downward redispatch limit of generator $g$ | €/MW |
| $\overline{\gamma}_{n,t}$ | Dual variable of the upper bound on grid-related load shedding | €/MW |
| $\lambda_t^{RD}$ | Dual variable of the redispatch balance constraint in time step $t$ | €/MW |
| $\underline{\rho}_{l,t}$ | Dual variable of the lower thermal line-flow limit | €/MW |
| $\overline{\rho}_{l,t}$ | Dual variable of the upper thermal line-flow limit | €/MW |
| $\phi_{l,t}$ | Dual variable of the power-flow definition on line $l$ in time step $t$ | €/MW |

## Binary Variables for Disjunctive Linearization

| Symbol | Description | Unit |
|---|---|---|
| $r^{q,I}_{t,i}$ | Binary variable for the complementarity of $q_{t,i}$ and its stationarity condition | binary |
| $r^{q,J}_{t,j}$ | Binary variable for the complementarity of $q_{t,j}$ and its stationarity condition | binary |
| $r^{c}_{i}$ | Binary variable for the complementarity of $c_i$ and its stationarity condition | binary |
| $r^{cap}_{i}$ | Binary variable for the complementarity of the installable-capacity slack and $\mu^{cap}_i$ | binary |
| $r^{cm,I}_{i}$ | Binary variable for the complementarity of $c^{cm}_i$ and its stationarity condition | binary |
| $r^{cm,J}_{j}$ | Binary variable for the complementarity of $c^{cm}_j$ and its stationarity condition | binary |
| $r^{\mu q,I}_{t,i}$ | Binary variable for the complementarity of $\mu^{q}_{t,i}$ and the dispatch-limit slack | binary |
| $r^{\mu q,J}_{t,j}$ | Binary variable for the complementarity of $\mu^{q}_{t,j}$ and the dispatch-limit slack | binary |
| $r^{\mu cm,I}_{i}$ | Binary variable for the complementarity of $\mu^{cm}_i$ and the capacity-offer slack | binary |
| $r^{\mu cm,J}_{j}$ | Binary variable for the complementarity of $\mu^{cm}_j$ and the capacity-offer slack | binary |
| $r^{ls}_{t}$ | Binary variable for the complementarity of energy-market load shedding | binary |
| $r^{dem}_{z}$ | Binary variable for the complementarity of $c^{dem}_z$ and its stationarity condition | binary |
| $r^{\nu}_{z}$ | Binary variable for the complementarity of $\nu_z$ and the zonal requirement slack | binary |
| $r^{\rho}_{z}$ | Binary variable for the complementarity of $\rho_z$ and the requirement-guard slack | binary |
| $r^{sys}$ | Binary variable for the complementarity of the system-wide capacity requirement | binary |
| $r^{lo}_{ab}$ | Binary variable for the complementarity of the lower cross-zonal contribution bound | binary |
| $r^{hi}_{ab}$ | Binary variable for the complementarity of the upper cross-zonal contribution bound | binary |
| $r$ | Generic binary variable in the disjunctive reformulation | binary |

# Parameters and Derived Quantities

| Symbol | Description | Unit |
|---|---|---|
| $W_t$ | Weight of time step $t$ in the objective functions | h |
| $W^{\max}$ | Maximum time-step weight, $\max_{t\in\mathcal{T}} W_t$ | h |
| $W^{tot}$ | Sum of all time-step weights, $\sum_{t\in\mathcal{T}} W_t$ | h |
| $VOLL^{em}$ | Value of lost load based on the energy-market price cap | €/MWh |
| $VOLL^{grid}$ | Value of lost load due to grid constraints | €/MWh |
| $vc_i$ | Variable cost of investable generator $i$ | €/MWh |
| $vc_j$ | Variable cost of legacy generator $j$ | €/MWh |
| $vc_g$ | Variable cost of generator $g$ | €/MWh |
| $fc_i$ | Fixed cost of investable generator $i$ | €/MW |
| $\overline{cap}_i$ | Maximum installable capacity of investable generator $i$ | MW |

| | | |
|---|---|---|
| $\overline{cap}_j$ | Installed capacity of legacy generator $j$ | MW |
| $\overline{cap}_g$ | Installed or maximum installable capacity of generator $g$, depending on generator type | MW |
| $a_{t,j}$ | Availability factor of legacy generator $j$ in time step $t$ | – |
| $\alpha_i$ | De-rating factor of investable generator $i$ in the capacity market | – |
| $\alpha_j$ | De-rating factor of legacy generator $j$ in the capacity market | – |
| $\alpha_g$ | De-rating factor of generator $g$ in the capacity market | – |
| $\overline{q}_{t,g}$ | Maximum available generation of generator $g$ in time step $t$ | MW |
| $D_t^{\max}$ | Maximum aggregate demand in time step $t$ | MW |
| $d_{n,t}$ | Demand at node $n$ in time step $t$ | MW |
| $s_n$ | Share of aggregate demand located at node $n$ | – |
| $d_{n,t}^{served}$ | Nodal demand remaining after energy-market load shedding | MW |
| $d_z^c$ | Capacity requirement of zone $z$ | MW |
| $d^c$ | System-wide capacity requirement | MW |
| $MEC_{ab}$ | Maximum entry capacity between zones $a$ and $b$ | MW |
| $\sigma$ | Cross-zonal participation factor applied to $MEC_{ab}$ | – |
| $\overline{f}_{ab}$ | Absolute cross-zonal contribution bound, equal to $\sigma MEC_{ab}$ | MW |
| $F_l$ | Thermal capacity limit of transmission line $l$ | MW |
| $x$ | Mark-up added to redispatch cost to avoid unnecessary redispatch | €/MWh |
| $f_{l,t}^{mkt}$ | Pre-redispatch market flow on line $l$ in time step $t$ | MW |
| $PTDF$ | Power transfer distribution factor matrix | – |
| $PTDF_{l,n}$ | Power transfer distribution factor of node $n$ on line $l$ | – |
| $IM$ | Incidence matrix of the network | – |
| $im_{l,n}$ | Entry of the incidence matrix for line $l$ and node $n$ | – |
| $X_l$ | Reactance of line $l$ | p.u. |
| $B_l$ | Susceptance of line $l$ | p.u. |
| $B_d$ | Diagonal matrix of line susceptances | p.u. |
| $w_n^{(k)}$ | PTDF-based exploration weight of node $n$ in exploration vector $k$ | – |
| $\overline{\lambda^c}$ | Upper bound on the capacity-market price, equal to $\max_{i\in\mathcal{I}} fc_i$ | €/MW |

# Cost-Comparison Quantities

| Symbol | Description | Unit |
|---|---|---|
| $C^{expl}$ | Redispatch-based secondary objective of the full primal-dual formulation, including grid-related load shedding | € |
| $C^{CM}$ | Capacity-market expenditure | € |
| $C^{RD}$ | Net redispatch cost excluding grid-related load shedding | € |
| $E^{grid\text{-}LS}$ | Grid-related load shedding | MWh |
| $C^{grid\text{-}LS}$ | Monetary value of grid-related load shedding, $VOLL^{grid}E^{grid\text{-}LS}$ | € |
| $C^{combined}$ | Combined capacity-market and congestion-cost measure | € |
| $VOLL^{grid,*}$ | Break-even valuation of grid-related load shedding | €/MWh |

| | | |
|---|---|---|
| $L$ | Superscript denoting a locational capacity-market design in the break-even comparison | – |
| $CW$ | Superscript denoting the country-wide capacity-market design in the break-even comparison | – |

## Generic Optimization Notation

| Symbol | Description | Unit |
|---|---|---|
| $\boldsymbol{x}$ | Generic primal decision-variable vector | depends on formulation |
| $f(\boldsymbol{x})$ | Generic objective function | depends on formulation |
| $h(\boldsymbol{x})$ | Generic equality-constraint function | depends on formulation |
| $g(\boldsymbol{x})$ | Generic inequality-constraint function | depends on formulation |
| $\lambda$ | Generic dual variable of equality constraints | depends on constraint |
| $\mu$ | Generic non-negative dual variable of inequality constraints | depends on constraint |
| $\mathcal{L}$ | Generic Lagrangian function | € |
| $\mathcal{L}_i$ | Lagrangian of investable generator $i$ | € |
| $\mathcal{L}_j$ | Lagrangian of legacy generator $j$ | € |
| $\mathcal{L}^{CD}$ | Lagrangian of the capacity-demand agent | € |
| $\mathcal{L}^{RD}$ | Lagrangian of the redispatch operator | € |
| $P_\omega(\boldsymbol{x}_\omega)$ | Primal objective value of actor $\omega$ | € |
| $D_\omega(\mu_\omega)$ | Dual objective value of actor $\omega$ | € |
| $u$ | First non-negative member of a generic complementarity pair | depends on variable |
| $v$ | Second non-negative member of a generic complementarity pair | depends on expression |
| $K^u$ | Upper bound on $u$ in the generic disjunctive reformulation | depends on variable |
| $K^v$ | Upper bound on $v$ in the generic disjunctive reformulation | depends on expression |

## Constants for Disjunctive Constraints

| Symbol | Description | Unit |
|---|---|---|
| $K^q$ | Bound on generator dispatch | MW |
| $K^{ls}$ | Bound on energy-market load shedding | MW |
| $K^c$ | Bound on installed capacity of an investable generator | MW |
| $K^{cm}$ | Bound on a capacity-market offer | MW |
| $K^{dem}$ | Bound on zonal capacity procurement and its requirement slacks | MW |
| $K^{sys}$ | Bound on the slack of the system-wide capacity requirement | MW |
| $\widetilde{K}^{q,I}$ | Bound on the dispatch-limit slack of an investable generator | MW |
| $\widetilde{K}^{q,J}$ | Bound on the dispatch-limit slack of a legacy generator | MW |
| $\widetilde{K}^{cap}$ | Bound on the installable-capacity slack | MW |

| | | |
|---|---|---|
| $\widetilde{K}^{cm,I}$ | Bound on the capacity-offer slack of an investable generator | MW |
| $\widetilde{K}^{cm,J}$ | Bound on the capacity-offer slack of a legacy generator | MW |
| $\widetilde{K}^{f}_{ab}$ | Bound on the slack of either cross-zonal contribution limit | MW |
| $\widehat{K}^{\lambda^e}$ | Upper bound on the energy-market price | €/MWh |
| $\widehat{K}^{\lambda^c}$ | Upper bound on the capacity-market price | €/MW |
| $\widehat{K}^{\mu^q}$ | Bound on generator dispatch-limit dual variables | €/MW |
| $\widehat{K}^{\mu^{cm}}$ | Bound on capacity-offer dual variables | €/MW |
| $\widehat{K}^{\mu^{cap}}$ | Bound on the maximum installable-capacity dual variable | €/MW |
| $\widehat{K}^{\nu}$ | Bound on the zonal requirement dual variable $\nu_z$ | €/MW |
| $\widehat{K}^{\rho}$ | Bound on the requirement-guard dual variable $\rho_z$ | €/MW |
| $\widehat{K}^{\phi}$ | Bound on the cross-zonal contribution-bound dual variables | €/MW |
| $\widehat{K}^{\lambda^{c,sys}}$ | Bound on the system-wide capacity-requirement dual variable | €/MW |
| $\overline{K}^{q,I}$ | Bound on the dispatch-stationarity expression of an investable generator | €/MW |
| $\overline{K}^{q,J}$ | Bound on the dispatch-stationarity expression of a legacy generator | €/MW |
| $\overline{K}^{c}$ | Bound on the capacity-investment stationarity expression | €/MW |
| $\overline{K}^{cm}$ | Bound on the capacity-offer stationarity expression | €/MW |
| $\overline{K}^{dem}$ | Bound on the capacity-demand stationarity expression | €/MW |
| $\overline{K}^{ls}$ | Bound on the load-shedding stationarity expression | €/MW |

# 1 Introduction

Sustainability is one of the three key challenges of European energy policy (European Commission, 2025). The European Union and its member states are therefore expanding renewable capacity to decarbonize the power system (IRENA, 2025). However, most renewable energy sources are intermittent, meaning that controllable generation is still needed when renewable output is low. At the same time, renewables increasingly reduce the operating hours of controllable generators (IEA, 2016). In theory, scarcity prices should provide sufficient incentives for investment, but price caps constrain these prices (Fabra, 2018). As a result, controllable generators may no longer recover their fixed costs, known as the “missing-money” problem (Duan et al., 2020). Investment is further affected by the long lifetimes and high upfront costs of power plants. The risk of overinvestment discourages investment, even when capacity remains necessary for security of supply (Cruickshank et al., 2016). Capacity mechanisms have consequently become a common option within the EU. They remunerate generation assets for making capacity available rather than only for providing energy, thereby supporting continued investment in controllable generation (Aurora Energy Research, 2025; European Union, n.d.; Finon & Roques, 2013).

A second challenge arises from the spatial shift in generation and consumption. Conventional power plants were typically located close to load centers, and transmission networks were developed around these locations. Renewables, by contrast, are primarily built where resources are available, increasing the need for transmission capacity (Janda et al., 2017). Within a single bidding zone, the electricity market generally treats the network as unconstrained. This “copper-plate” representation does not reflect internal bottlenecks. Congestion must therefore be resolved through corrective congestion management measures, which increase system costs (Trepper et al., 2015). In Germany, redispatch costs almost quadrupled to €4.2 billion per year between 2019 and 2022 (BDEW, 2023).

Two main solutions aim to address transmission-grid congestion at its root. The first is to split national electricity markets into multiple bidding zones so that electricity prices better reflect physical grid constraints. However, political resistance has so far prevented implementation in many European countries. A common concern is that some zones could face higher electricity prices and therefore experience a regional disadvantage (Eicke & Schittekatte, 2022). The second solution is to expand the transmission network. Grid expansion, however, also faces rising material and labor costs, local resistance, and long permitting periods. Regulated grid expansion has historically not been able to match the pace of generation-capacity expansion and shifts in load (ENTSO-E, 2026). Both solutions therefore encounter substantial hurdles in Europe.

Locational signals in capacity mechanisms could provide an additional way of influencing where controllable capacity is located. Currently, however, capacity mechanisms are assessed primarily in terms of aggregate adequacy, while internal grid congestion is not considered. EU regulation allows capacity mechanisms only under specific adequacy conditions and explicitly excludes congestion management measures from their scope (European Union, n.d.). Nevertheless, ENTSO-E (2025) highlight the potential of locational signals in capacity mechanisms to reduce congestion. Nieto and Fraser (2007) also point out that aggregate capacity mechanisms could worsen congestion and capacity concerns. This raises the question of whether locational capacity procurement can improve the deliverability of procured capacity, and how this affects procurement costs and congestion outcomes. The question is particularly relevant in Europe, where capacity mechanisms are regulated at EU level and primarily justified through resource adequacy. Any locational extension would therefore have to be assessed within this existing policy and regulatory framework.

## 1.1. Knowledge gap & research question

The literature on capacity mechanisms and congestion management remains fragmented. Existing studies generally examine capacity mechanisms or congestion management and locational signals separately. Where the two topics are connected, locational elements in capacity mechanisms have received only limited systematic attention within the current European market design. In particular, their potential role in reducing congestion and ensuring that procured capacity can be delivered during scarcity situations remains unclear. The relevant literature is reviewed in detail in Chapter 2. This section uses the connecting literature and its limitations to formulate the knowledge gap and research question.

The capacity mechanism literature primarily focuses on aggregate resource adequacy. It examines how investment uncertainty, market design, and cross-border effects influence the performance and design of capacity mechanisms (de Vries & Heijnen, 2008; Ehrenmann & Smeers, 2011; Fraunholz et al., 2023). In recent years, particular attention has been given to the European integration of national capacity mechanisms and the effects of cross-border participation (ENTSO-E, 2025; Fraunholz et al., 2023; Hladik et al., 2020). However, this literature mainly considers whether sufficient capacity exists at the aggregate level. It pays less attention to where this capacity is located within a bidding zone and whether it can be delivered when internal grid constraints are binding.

The congestion management literature starts from the spatial limitations of zonal electricity markets. The copper-plate assumption neglects internal grid constraints and, together with the geographically uneven deployment of renewables, can contribute to increasing congestion and redispatch needs (Eicke & Schittekatte, 2022; Hladik et al., 2020). Splitting bidding zones has therefore been extensively studied as a way to provide locational investment signals through electricity prices (Eicke et al., 2020; Fraunholz et al., 2020; S. Oliveira et al., 2023). However, a bidding-zone split can negatively affect resource adequacy and faces considerable political resistance (Eicke & Schittekatte, 2022; Fraunholz et al., 2020). Locational signals have also been proposed outside the energy market price, for example through locational components in renewable-support schemes (Thomaßen & Fuhrmanek, 2025). These studies show that investment locations can be influenced through market design, but they do not directly examine the trade-off created by locational signals in capacity mechanisms.

Markets in the US, such as PJM, already use capacity market zones with locational signals (Lawson, 2025). There is therefore extensive experience on locational capacity markets in these regions. However, the surrounding electricity market design differs significantly from the one commonly applied in Europe because US markets generally use nodal rather than zonal pricing (IEA, 2025). Similarly, Chile combines a nodal energy market with a nodal capacity market (Eicke et al., 2020). Findings from these markets cannot therefore be directly applied to the European context, where congestion within bidding zones is resolved through redispatch. Nevertheless, they indicate which effects should be considered when introducing locational signals into European capacity mechanisms. In PJM, for example, the separation into smaller capacity market zones has reduced competition and increased capacity prices (McCullough et al., 2020).

Only a limited number of European studies directly connect locational capacity mechanisms with congestion outcomes. Lété et al. (2026) examine market-based redispatch under zonal pricing. They show that this combination can lead to investment in “ghost plants” that are built to extract arbitrage rents between the zonal energy price and the nodal redispatch price. A locational capacity market can remove these arbitrage profits and restore the long-run efficiency of the system. Hladik et al. (2020) examine congestion management in Germany and find that introducing a locational capacity mechanism can improve congestion outcomes. However, they consider only one specific market setup, making it difficult to isolate the effect of the capacity mechanism from the other elements of the design.

Thomassen and Fuhrmanek (2025) provide a broader study of locational investment signals, including locational components in capacity mechanisms. They describe locational capacity mechanisms as a no-regret option in the current zonal market setup because they reduce overall consumer costs and improve the feasibility of redispatch. However, the study introduces several locational investment signals simultaneously and does not explicitly model capacity market costs. It is therefore not possible to isolate the effect of the locational capacity mechanism itself or to observe the trade-off between capacity market and redispatch costs.

A further difference exists between the practical motivation for locational capacity mechanisms and their assessment in the literature. Implemented locational mechanisms base their requirements primarily on security and reliability analyses. Their main purpose is not necessarily to minimize redispatch volumes or costs, but to ensure that sufficient capacity physically exists in the right location for the system to be operated safely. By contrast, Thomassen and Fuhrmanek (2025) and Hladik et al. (2020) focus mainly on redispatch outcomes. However in an earlier publication, Thomassen et al. (2024) also question whether locational elements in capacity mechanisms can reduce redispatch at all. Locational signals may therefore be more important for enabling feasible redispatch than for minimizing its volume.

Taken together, the literature leaves two connected gaps. First, existing studies do not provide a systematic and isolating comparison between country-wide and locational capacity market designs. Second, one side of the central trade-off is generally not modeled explicitly. Capacity market costs are instead included within broader system-cost measures, creating a black box around the interaction with changing redispatch costs. Redispatch feasibility is also not consistently treated as a separate outcome. A systematic comparison is therefore needed to examine how locational capacity market designs affect capacity market costs, redispatch volumes and costs, and load shedding caused by grid constraints.

This leads to the following research question:

*To what extent do locational signals in capacity markets shape the trade-off between capacity procurement costs and congestion outcomes in a zonal energy market?*

## 1.2. Sub-questions

To answer the research question, the project is structured following the bathtub model from Chappin (2021). While the bathtub model consists of more steps, they are concentrated into four research stages for this project. First, SQ1 and SQ2 build the conceptual model from literature. SQ1 focuses on understanding the basic system and its interactions, while SQ2 dives into the experimental design. SQ3 consists of formulating the formal model, reformulating it so the solution space can be explored, and implementing and running it as a computational model. Lastly, SQ4 represents the analysis and interpretation of the model results.

#### Conceptual Model - System

*SQ1: Which actors, decisions, and interactions must be represented in a zonal energy market with cost-based redispatch and a capacity mechanism?*

***Method:*** Desk research
***Data Requirements:*** Foundational literature on electricity market structure and operation
***Data Sources:*** Academic databases such as Web of Science and Scopus
***Analysis Tools:*** Zotero to keep track of literature; Miro (n.d.) to create a visualization of the conceptual model
***Deliverable:*** A base conceptual model made up of the core actors and their interactions. This model establishes the fundamental components of the system (e.g. generators, demand, grid constraints) and its operational processes that will be formalized later. A visual representation of the actors and their interactions supports the formulation of the formal model.

#### Conceptual Model - Intervention & Experimental Design

*SQ2: Which forms of locational signals exist in capacity mechanisms, and how do they function?*

***Method:*** Literature review
***Data Requirements:*** Base model from SQ1; academic journal articles and authoritative policy reports

on locational signals in capacity market design
***Data Sources:*** SQ1; academic databases such as Web of Science and Scopus
***Analysis Tools:*** Zotero to keep track of literature
***Deliverable:*** SQ2 provides the experimental design. Literature is scanned to provide an overview of the possibilities that exist for locational signals in capacity markets and how they work. From the variants explored, a set of designs is chosen for this project. The choice is made based on the compatibility with the system design in SQ1. The reason to split the conceptual model into two sub-questions is that SQ1 concerns the basic functioning of our current electricity market design, while SQ2 introduces possible interventions to that system from literature. To answer SQ2, a detailed understanding of the current market must be established first in SQ1. Otherwise, the experimental design could carry over false assumptions from a flawed base model.

### Formal & Computational Model

*SQ3: How do locational signals affect capacity procurement, capacity siting, and congestion outcomes across the investigated scenarios?*

***Method:*** Mathematical model formulation; Computational simulation
***Data Requirements:*** The conceptual model from SQ1 and SQ2;
***Data Sources:*** SQ1; SQ2; PyPSA-Eur (Hörsch et al., 2018)
***Analysis Tools:*** Julia and the JuMP package for mathematical modeling (Kwon, 2019; Lubin et al., 2023); Git for version control; Python to retrieve data on the Netherlands from PyPSA-Eur; solver to compute the model solutions
***Deliverable:*** Based on the conceptual model, the formal capacity expansion model is then built. There already is extensive literature on modeling electricity markets with capacity mechanisms (Askeland et al., 2019; Höschle, Le Cadre, Smeers, et al., 2018; Lorenczik, 2019; Menegatti & Meeus, 2024) and redispatch (Kenis et al., 2024; Kunz & Zerrahn, 2015; Lété et al., 2022), which can serve as a guide. Emphasis in this part is on the exploration of the solution space. The reason lies in how capacity siting is determined in the model. The deciding factors on where capacity is built are among others land availability, labor costs and local resistance. Those are difficult to include in electricity market models (Thomassen & Fuhrmanek, 2025). Several locations can therefore be equivalent from the perspective of the energy and capacity markets, leading to multiple equilibria and solver dependency in the solution. As capacity siting is the driver behind the congestion outcomes, relying on one solver-selected equilibrium could distort the comparison. The model therefore explores spatially different equilibria with the same energy- and capacity market outcomes. The exploration proved challenging in terms of keeping solving times feasible. At the end, a two-stage solution method was developed in which a PTDF-based objective creates diverse capacity-siting outcomes before redispatch is solved separately. Before it is applied, the model is verified on a small three-node network as a proof of concept. The formal model is then implemented in Julia using JuMP (Lubin et al., 2023) and run on data for the Dutch system. The metrics compared across the scenarios are capacity procurement and expenditure, capacity siting, redispatch volumes and costs, and grid-related load shedding. Generally, all data sources and modeling choices are documented to make the results transparent and clearly show what drives the outcomes, avoiding a ”black box” analysis later. Necessary data from the Dutch system for the model includes:

- Renewables Data: An hourly time-series of renewable capacity factors
- Generator Data: Investment costs (€/MW/year), operational costs (€/MWh), and location
- Network Data: A map of Dutch transmission lines, their capacities and connection points
- Demand Data: An hourly time-series of the Dutch electricity demand

Crucially, all data is needed in the same spatial resolution as the network data. Only then, can redispatch and locational signals be accurately modeled. In line with the copper plate assumption of the current electricity market design, demand data is only available for the whole of the Netherlands and generator data is independent from grid connection points. To get the spatial resolution in data, several methods are available, e.g. distributing demand over nodes based on inhabitants and economic activities. Instead of following the manual approach, a PyPSA-Eur run is configured to represent the Dutch network including buses, links, generators and demand (Hörsch et al., 2018). Using its snakemake workflow, PyPSA-Eur then transforms the data into the desired spatial granularity, ensuring the data matches across all kinds of data.

### Analysis & Interpretation

*SQ4: What trade-offs and design implications follow for locational signaling in capacity markets?*

***Method:*** Synthesis of model results
***Data Requirements:*** Full set of results from SQ3
***Data Sources:*** SQ3
***Deliverable:*** This is a primarily qualitative step, interpreting the quantitative results in the context of the policy debate and the literature review. The analysis will focus on the relative differences between market designs, not absolute forecasts. Concretely, it compares how the capacity mechanism costs, redispatch and grid-related load shedding move against each other across the locational signal designs. This ensures the findings are presented as conditional insights, directly linked to the core assumptions of the model. It involves identifying causal mechanisms within the model that explain the observed outcomes. This results in a set of evidence-based conclusions that directly answer the main research question and provide recommendations on the design and implementation of locational capacity mechanisms.

## 1.3. Research approach

The research question concerns the functioning of a complex electricity system under alternative market designs. Specifically, the interaction between a zonal energy market and capacity mechanism design. Answering this question thus requires the systematic comparison of different system designs that cannot be observed in real-world systems. Energy market and system models are widely used to provide such insights in systems where real-world experimentation is infeasible (Pfenninger et al., 2014), therefore a modeling approach is chosen for this research.

In this case, the focus is on market design and system-level outcomes rather than detailed engineering representations of individual technologies. In energy system and market modeling it is important to emphasize that their role is not prediction, but the generation of insights by formulating assumptions and exploring how changes in the system design affect certain outcomes (Pfenninger et al., 2014). Furthermore, modeling and simulation are suitable for analyzing systems with interacting actors, long-term investment horizons, feedback in market interactions and physical constraints. The model is crucial for understanding those interactions at the system level, where outcomes result from decentralized decisions from individual actors instead of central coordination (Subramanian et al., 2018).

Looking back at the research question and knowledge gap, a model can provide what is needed to systematically observe the system-level effects (capacity procurement, redispatch, and grid-related load shedding) originating from individual actors' decision making in different capacity market designs, offering a comparison between them.

When it comes to the limitation of this research approach, computational constraints are the main cause. The computational intensity limits the level of detail and therefore accuracy of the model. Thus, modeling choices regarding the level of detail are needed. Following Kotzur et al. (2021), the approach is to start with as simple a model as possible and only add detail where the research question demands it. This is especially relevant in models that require a high temporal and spatial granularity. In combination those can quickly let the model explode in size (Kotzur et al., 2021).

As the focus of this study is on the comparison between market designs rather than the prediction of absolute outcomes, modeling choices prioritize traceability of results over accuracy of individual components. This means that factors of additional complexity such as strategic behavior, risk aversion and demand response are excluded where they affect all scenarios equally and therefore do not drive the differences between them.

A challenge is that results are conditional on those choices as well as system boundaries and parameter values. This carries the risk of turning the model into a 'black box' which hides the mechanisms driving the results (Pfenninger et al., 2018). Two mitigation measures are implemented to minimize that risk: a) Results are treated as conditional insights for comparison, not forecasts. The analysis focuses on differences between the scenarios while absolute results are secondary. b) The model is kept transparent: the assumptions and modeling choices are made explicit, and both the data and the model are openly available in a public Git repository.

## 1.4. Societal and CoSEM relevance

As discussed earlier, having enough capacity on an aggregate level is only one part of security of supply. If grid constraints prevent that capacity from delivering during scarcity events, its contribution is limited. Locational signals in a capacity mechanism therefore matter because they can guide where new controllable capacity is built, ensuring both resource and transmission adequacy.

The question is also relevant for the costs of the energy transition. A locational signal may reduce redispatch needs and grid-related load shedding, but it can also increase capacity market costs by restricting where and how much capacity is procured. These costs eventually affect consumers, whether through capacity payments, grid tariffs, or the cost of congestion management. This thesis therefore studies how different capacity market designs shift costs and risks between ex-ante capacity procurement and ex-post congestion management, including redispatch and grid-related load shedding. A locational capacity mechanism is not treated as a replacement for grid expansion or bigger energy market reform, but as a possible mitigation while these solutions remain slow or politically difficult to implement. In a broader sense, it therefore also concerns the general success of the energy transition. Public support for the energy transition is tied to affordability (Middlemiss et al., 2020). If public support fades, the transition itself is in danger.

This is where the CoSEM perspective becomes relevant. The problem is rooted in a technical issue, namely renewable intermittency and grid congestion. But it cannot be assessed in technical terms alone, because the market and the grid are coupled. The rules of the capacity mechanism affect investment and dispatch decisions, while the transmission network determines what these decisions mean for system operation. Changing the locational signal can therefore improve one part of the system while creating costs elsewhere. Stricter local procurement can make capacity more useful for the grid, but also more expensive. Allowing more cross-zonal participation can lower procurement costs, but puts more weight on the transmission network and on redispatch. The design cannot be assessed from one perspective alone.

Several actors are involved and their objectives do not fully align. Generators decide where to invest based on expected revenues and costs. The market operators aim to procure enough capacity and clear the markets at low cost. The transmission system operator is responsible for restoring network feasibility after the energy market has cleared. Regulators set the rules connecting these actors. Consumers do not take part in these decisions directly, but depend on the outcome and eventually carry the costs. A change in the capacity mechanism therefore affects both private investment incentives and public outcomes such as congestion, security of supply, and system costs.

The methodology also follows a CoSEM perspective. Instead of optimizing the electricity system from the viewpoint of one central planner, the model starts from the decisions and constraints of individual actors. These actor problems are combined into a market equilibrium, after which redispatch is solved as a separate system operation. This makes it possible to trace how a regulatory design choice changes private decisions and how these decisions lead to system-level outcomes. One market equilibrium would not be enough for this purpose. Different siting outcomes can have the same energy- and capacity market costs, while their consequences for the grid differ substantially.

The thesis therefore does not search for one technically optimal design. It compares how the different designs move costs between capacity procurement and congestion management. This is also the policy problem behind the model: improving deliverability can raise procurement costs, while cheaper procurement can compromise deliverability.

## 1.5. Contribution and structure of the report

Across the four sub-questions, the main contribution of this thesis is the model it builds to study how locational capacity market designs affect capacity procurement, redispatch, and adequacy under network constraints.

The system links decisions at different scales. Capacity investment is a long-term and spatial choice.

The energy market clears over many periods. Redispatch acts on the detailed network. These are not separate problems: the capacity mechanism and the energy market are interdependent, and redispatch then corrects the cleared dispatch for the network limits. Capturing all three at a resolution fine enough to see congestion lets the model explode in size. Keeping it solvable took most of the modeling effort. The market is solved as one equilibrium, redispatch as a separate stage, and the equilibrium is reformulated to keep solving times feasible at case-study scale.

The report follows the sub-questions. Chapter 2 reviews the literature on locational signals in capacity mechanisms. It explains why such signals are used, sorts them into design archetypes, and selects the design that is compared with country-wide procurement in the rest of the thesis (SQ2). Chapter 3 sets up the methodology. It first describes the actors and their interactions (SQ1), then formalizes them into the equilibrium model, and develops the solution method that keeps the model solvable (SQ3). The methodological contribution sits here. Chapter 4 applies the model to two case studies of the Dutch system. The two case studies differ in the size of the underlying legacy system. One therefore requires substantially more new capacity and allows more freedom in capacity siting, while the other already has an almost sufficient system with less room for capacity movement. Chapter 5 presents the results. It reports the capacity requirements and siting, followed by capacity market cost, redispatch, and grid-related load shedding for each design (SQ3). Chapter 6 discusses these results: their limitations, how they fit the literature, and what they imply for locational signal design (SQ4). Chapter 7 concludes by answering the sub-questions and the research question.

# 2

# Locational Signals in Capacity Mechanisms

This chapter develops the locational capacity mechanism design used in the model. It first discusses why locational signals are introduced and groups existing designs into three archetypes. It then reviews the limited literature connecting locational capacity mechanisms with redispatch and discusses the role of cross-zonal participation. The chapter concludes by translating these findings into the design compared in this thesis.

## 2.1. The rationale behind locational signals in capacity mechanisms

The general argument for locational signals in capacity mechanisms is that transmission constraints affect the value of capacity (Cruickshank et al., 2016). Three more specific rationales can be distinguished. Existing mechanisms mainly use locational signals to protect security of supply by ensuring that procured capacity can be delivered. The reduction of congestion management needs appears mostly in consultation documents and academic studies. A third rationale, the co-development of generation and transmission, is mentioned less explicitly but connects the other two to the broader discussion on coordinating grid and generation expansion.

### 2.1.1. Increase of security of supply

The argument found most clearly in practice is that procured capacity must be able to deliver during scarcity. In an aggregate CM, the capacity of each generator is valued as if internal transmission constraints did not exist. The lowest-bidding generators can therefore clear the auction even when bottlenecks prevent their output from reaching the areas where it is needed. Resource adequacy must consequently also be considered at a sub-regional level (Spees et al., 2013).

This issue also extends to disinvestment. A low aggregate capacity price may signal a generator to leave the market even though its capacity remains locally necessary because of transmission constraints (Benedettini, 2013). Locational components are used to represent this difference in value. Depending on the market design, separate zones are created or individual load pockets are distinguished from the rest of the system (Gill et al., 2025). An import-constrained area may require a minimum amount of local capacity. In an export-constrained area, the amount of capacity that can count towards the wider system requirement may instead be limited.

A locational signal can also ensure that enough capacity is available in the right part of the system to make redispatch feasible (Thomassen & Fuhrmanek, 2025). The capacity mechanism then moves beyond aggregate resource adequacy, also affecting deliverability or transmission adequacy. PJM provides an illustrative example. Its Installed Reserve Margin meets a system-wide reliability criterion without considering internal transmission constraints. Additional reliability requirements are imposed for Locational Deliverability Areas (PJM, 2025).

Gill et al. (2025) extend this reasoning beyond the electricity network. Other location-dependent infrastructures can also prevent a group of generators from delivering. Their example is the gas network: if many generators in one area depend on the same component, its failure can compromise security of supply.

### 2.1.2. Reduction of congestion management measures

Beyond ensuring deliverability, literature and policy documents also discuss locational capacity mechanisms as a way to reduce ex-post congestion management. Both Hladik et al. (2020) and Thomassen and Fuhrmanek (2025) introduce locational signals with this objective. Thomassen and Fuhrmanek (2025) split the energy market bidding zones and let the capacity market follow the same spatial structure. They argue that capacity market zones should be at least as granular as the energy market. Otherwise, the capacity market may weaken the locational signal already provided by energy prices.

Thomassen et al. (2024), however, question whether a locational capacity signal can materially reduce redispatch. Newly procured plants are likely to be near the end of the merit order and may therefore have little effect on ordinary energy market dispatch. Hladik et al. (2020) do observe lower redispatch in a scenario with a nodal capacity market beneath the German single bidding zone. Their design allocates new capacity according to congestion indicators: high positive redispatch is interpreted as local generation scarcity, directing capacity towards those nodes.

Taken together, the literature does not point to one single role for locational capacity signals. They can be introduced to preserve or strengthen existing locational price signals, or they can be constructed directly from congestion indicators to reduce redispatch. At the same time, Thomassen et al. (2024) question how strongly newly procured capacity can affect redispatch when it is rarely dispatched in the energy market. Whether congestion reduction should determine the locational signal therefore remains open.

### 2.1.3. Co-development of generation and transmission

The third rationale is the coordination of generation and transmission expansion. In Europe, private actors can generally choose the location of new generation within broad planning and permitting constraints. Renewable generation is mainly sited according to resource availability (Thomaßen & Fuhrmanek, 2025), while other generators are also guided by their private costs rather than by where the network benefits most (Nieto & Fraser, 2007). Transmission expansion by the regulated TSO is then expected to follow these investment decisions (Gill et al., 2025).

In practice, grid development has often not matched the pace or location of new generation. Recent German policy proposals, for example, consider removing redispatch compensation for newly built renewables in areas identified as grid-constrained by the TSO (Siemer, 2026)[1]. The underlying idea is that generation and transmission should be developed more jointly rather than treating grid expansion as a reaction to generation siting.

Locational capacity market signals can contribute to this coordination (Gill et al., 2025). Capacity may be directed around transmission constraints to protect security of supply, or towards locations that reduce congestion outside scarcity periods. Co-development therefore connects the deliverability and congestion rationales, even though it is less often stated as an explicit objective of existing capacity mechanisms.

### 2.1.4. Key differences between EU and US

A central difference between the US and Europe is the spatial relationship between the capacity and energy markets. In the US, capacity market zones usually aggregate several nodes of an already locational energy market. In Europe, locational capacity arrangements are generally more granular than the single-price energy market zone beneath them.

The US setup reflects two considerations. First, smaller capacity zones reduce liquidity and can increase local market power (Cruickshank et al., 2016; McCullough et al., 2020). In an extreme case, a

[1]While the proposal itself had not been released at the time of writing, the Ministry of Economic Affairs confirmed the leaked information and its intention to include the plans in the official proposal.

zone has a pivotal supplier without whom the local requirement cannot be met. Withholding by that supplier can then strongly affect the local capacity price (McCullough et al., 2020). Second, fragmentation can increase procurement when separate zones or mechanisms do not recognize the contribution of neighboring capacity (Bucksteeg et al., 2019). Cross-zonal participation is one way to limit this effect, as discussed in Section 2.4.

A comparable aggregation across European countries faces substantial political and institutional barriers. Capacity mechanisms remain closely connected to national adequacy preferences, economic conditions, and security-of-supply responsibilities (Hickey et al., 2021; Roques, 2019). Even where rules exist for simultaneous system stress, countries may be reluctant to rely fully on neighboring systems (Bucksteeg et al., 2019). Full integration is therefore difficult, while cross-border participation offers a more limited form of coordination (Menegatti & Meeus, 2024). These concerns are less pronounced within the area of one US system operator, where the same institutions and market rules apply across the relevant zones.

The appropriate capacity market granularity therefore depends on the energy market beneath it. Where nodal prices already guide investment, larger capacity zones can preserve liquidity while local requirements are added only where transmission constraints threaten deliverability during system stress. In a European single-price zone, internal locational value is not reflected in the energy price. A locational capacity component can then be used to ensure that procured capacity is available where it can deliver.

Taken together, the comparison does not point to one universally preferable spatial design. Where the energy market already provides locational prices, capacity zones can remain broader and focus on deliverability. Where it does not, a locational capacity component may have to provide part of that signal itself. The archetypes in the next section organize the main ways in which this relationship is implemented.

## 2.2. Archetypes of capacity mechanisms with locational signals

Real-world implementations and academic proposals can be grouped according to how the spatial structure of the capacity mechanism relates to the underlying energy market. Table 2.1 summarizes three archetypes. A fuller overview of the individual market designs is provided in Appendix A.

**Table 2.1:** Archetypes of capacity mechanisms with locational signals, clustered by their spatial relationship to the energy market. Per market implementation detail is given in Appendix A.

| | **A — mirrors energy market** | **B — aggregates energy market nodes** | **C — local procurement beneath an aggregate market** |
|---|---|---|---|
| **Relation to energy market** | Same spatial granularity; CM follows the energy market's own nodes or zones | CM zones aggregate several energy market nodes, nested or flat | Additional local procurement is layered beneath an aggregate energy and capacity market |
| **How zones are defined** | Inherited directly from the energy market (nodal or zonal) | Aggregated from nodes on transmission constraints; nested (PJM), flat (ISO-NE, CAISO) or hybrid (NYISO, MISO) | Ad-hoc, TSO-selected constrained areas layered on one system-wide zone |
| **How the locational signal arises** | From the energy market itself; the CM only mirrors it | From CM auction clearing (PJM, ISO-NE) or a bilateral quantity obligation (MISO, NYISO, CAISO) | Selective TSO intervention or a one-off tender, not a systematic price |
| **Used in** | Chile (nodal), Italy (zonal) | PJM, ISO-NE, MISO, NYISO, CAISO | Ireland, France (Brittany), Germany (south) |
| **Key weakness** | Requires the energy market to price locationally (nodal or zonal); no signal to mirror in a single-price zone | Smaller zones raise market power; cross-country fragmentation risks over-procurement | Targeted, not integrated: treats symptoms, not the CM design itself |

### 2.2.1. Archetype A - CM mirroring the energy market

The first archetype is a capacity mechanism that applies the same spatial granularity as the energy market. The locational signal emerges from the energy market, which the capacity market follows by having a different price for capacity per zone or node. Chile is one of the examples that uses this archetype. In general, Chile has a unique energy market design compared to European markets, as it uses a nodal market with locational prices. Furthermore, generators do not bid in the wholesale market, but declare their technical and cost parameters to the central authority, which then dispatches plants in ascending cost order (Serra, 2022). These characteristics are carried over into the capacity mechanism. Capacity payments are different across all 49 nodes of the underlying energy market (Eicke et al., 2020). Instead of an auction, the central authority again calculates prices and volumes administratively ex-post (ECCO International, 2024; Eicke et al., 2020).

The example for this archetype in Europe is Italy and its zonal capacity auction. The auction accounts for transmission constraints and produces a different capacity price for each bidding zone, mirroring the zonal structure of the day-ahead energy market (Papavasiliou, 2021). The crucial point is that Italy can use this archetype because its day-ahead market is already split into bidding zones, so a locational signal exists for the capacity auction to mirror. The Italian network structure helps explain why this arrangement is suitable. The peninsula is built around parallel north–south links with few interconnections in between (ENTSO-E, n.d.), so it is far less meshed than most European grids. Because important constraints follow relatively clear north–south boundaries, the bidding zones can represent part of the underlying locational value. In a more meshed network, transmission constraints are less likely to align with simple zonal borders.

### 2.2.2. Archetype B - CM aggregating energy market nodes

The defining feature of this archetype is that the underlying energy market is spatially more granular than the capacity market: capacity zones aggregate energy nodes, but only as far as transmission constraints allow. It is the structure found across US markets, and the variation within the group lies in how the zones are shaped.

PJM uses nested Locational Deliverability Areas (LDAs) (PJM, 2025). Starting from the system-wide Regional Transmission Organization (RTO) zone, sub-zones split into progressively finer ones, as Figure 2.1 shows. As explained in subsection 2.1.1, the aggregate zone's reliability target delivers resource adequacy, while each constrained sub-zone adds a local requirement that delivers transmission adequacy. The standard critique of this nesting is market power: the finer the sub-zones, the more often a pivotal supplier emerges who can withhold capacity to inflate the local price (McCullough et al., 2020).

- RTO=> **Western PJM**
- RTO => Western PJM => **ComEd**
- RTO => Western PJM => **AEP**
- RTO => Western PJM => **Dayton** (may be listed as DAY)
- RTO => Western PJM => **Duquesne** (may be listed as DLCO or DUQ)
- RTO => Western PJM => **APS**
- RTO => Western PJM => **ATSI**
- RTO => Western PJM => ATSI => **Cleveland** (may be listed as ATSI-Cleveland)
- RTO => Western PJM => **DEOK**
- RTO => Western PJM => **EKPC**
- RTO => Western PJM => OVEC

**Figure 2.1:** Example of the nested structure in the PJM market (PJM, 2025).

ISO-NE and CAISO instead use flat zones: one rest-of-system zone from which only constrained zones are separated (Draghi et al., 2025; ISO New England, 2026; Spees et al., 2013). NYISO and MISO sit between the two, mostly flat but with some nesting (MISO, 2026; NYISO, 2023). Across all of them the same logic recurs: a system-wide reliability target, a local requirement for each constrained zone set against that zone's import capability, and a feasibility check that re-clears the auction if the procured capacity cannot physically be delivered. The detailed per market rules (local requirements, import and export limits, and feasibility tests) are collected in Appendix A.

How the locational price arises depends on procurement. PJM and ISO-NE clear central forward auctions, so the locational signal is the zonal auction price (ISO New England, 2026; Lawson, 2025; PJM, 2025). MISO, NYISO and CAISO procure mostly bilaterally, with the auction only a residual or fallback mechanism, so there the locational signal works through the obligation to procure locally rather than through a cleared price (Draghi et al., 2025; MISO, 2026; NYISO, 2026; Papavasiliou, 2021; Spees et al., 2013).

### 2.2.3. Archetype C - Local procurement beneath an aggregate market

The third archetype is found mainly in Europe. Rather than splitting the main capacity mechanism into stable locational zones, it adds selective local procurement beneath an otherwise aggregate market.

In Ireland, transmission constraints are not represented directly in the auction. Resources in favorable parts of the system can nevertheless be accepted at their bid price even when they are out of the money and do not contribute to the main capacity target (Papavasiliou, 2021). Procurement can therefore exceed the target. The locational signal results from a selective TSO decision rather than from a systematic zonal price.

France operates an aggregate capacity mechanism without an integrated treatment of internal bottlenecks (Papavasiliou, 2021). A separate locational tender was introduced for the import-constrained Brittany region, but this was a targeted intervention layered on top of the system-wide mechanism (Eicke et al., 2020). Germany similarly combines a system-wide strategic reserve with separate local capacity procurement. Plants in the south were procured to provide redispatch services and did not participate in other markets (Eicke et al., 2020; Papavasiliou, 2021).

Outside Italy, European capacity mechanisms therefore generally do not contain an integrated locational component. Several countries nevertheless procure capacity separately in transmission-constrained areas. These arrangements show that missing locational signals are recognized, but they address the issue through additional interventions rather than through the capacity market design itself.

## 2.3. Locational capacity mechanisms and redispatch in literature

Locational capacity mechanisms are most established in markets that already use locational energy prices, as in Archetype B. There, local capacity requirements mainly ensure that procured capacity can be delivered during system stress. Ordinary congestion is already reflected in the energy market. In European single-price zones, internal congestion is instead managed through redispatch, while the capacity mechanisms generally lack an integrated locational component. Only a small number of studies therefore examine how a locational capacity mechanism interacts with congestion outcomes under a more aggregate energy market.

Hladik et al. (2020) focus on the future of congestion management in Germany. They test several market designs for their ability to reduce congestion, including a nodal capacity market beneath the single-zone energy market. Nodes with high positive redispatch are interpreted as having scarce generation, and new capacity is directed towards them. The study observes lower redispatch volumes under this design.

The study does not, however, report capacity mechanism costs. The authors also identify a limitation of their congestion indicator: a node with positive redispatch already has enough capacity to increase output, while nearby nodes without this ability may be more in need of investment. In addition, the mechanism is not anchored in an explicit reliability target. It is primarily used to steer investment towards congested locations. The study therefore shows that a locational capacity mechanism can reduce redispatch, but not how the resulting design affects procurement or adequacy.

Thomassen and Fuhrmanek (2025) also analyze locational capacity mechanisms in Europe, but as one element of a broader package that includes bidding-zone reform and locational renewable support. The effects of the capacity mechanism cannot therefore be isolated. Moreover, the capacity zones follow the new energy market split, which differs from the combination of a locational capacity mechanism and one aggregate energy market zone studied here. The capacity mechanism is represented through revenue-gap payments rather than through explicit market clearing, so its procurement costs are not observed. The study nevertheless supports the view that locational capacity can reduce congestion or make redispatch feasible.

The third paper is Lété et al. (2026). They model generation investment under zonal electricity pricing with market-based redispatch and show that "ghost plants" can be built to profit from the difference between the zonal energy price and nodal redispatch prices. A locational capacity market can offset these arbitrage incentives by rewarding capacity where it is genuinely needed. This is a specific market-based redispatch problem, and the paper does not evaluate the capacity mechanism trade-off studied here. It does, however, provide a clear explanation of why locational investment signals matter in a zonal energy market.

The strategic redispatch incentive identified by Lété et al. (2026) is specific to market-based redispatch. Under cost-based redispatch, generators are compensated at cost and do not receive the same arbitrage incentive. The redispatch design therefore matters when interpreting the role of a locational capacity mechanism.

The literature gap is therefore twofold. The studies reviewed do not report the procurement cost of an integrated, reliability-anchored locational capacity mechanism, and they do not examine how different levels of cross-zonal contribution change its outcomes. As the capacity market costs are not explicitly modeled, overprocurement of more expensive capacity is therefore not an issue. Where there is no issue, there is no solution. Thus cross-zonal participation is out of their scope.

## 2.4. Cross-zonal participation

When local capacity requirements are assessed independently, they may ignore capacity that can be delivered from neighboring zones. In the wider literature, cross-zonal or cross-border participation is used to recognize this contribution and can reduce both local procurement and total procurement costs (Bucksteeg et al., 2019; Cepeda, 2018). The European debate usually concerns participation between countries (Menegatti & Meeus, 2024), but the same principle can be applied to internal capacity zones.

Two main forms are distinguished. Under implicit participation, the expected contribution of neighboring resources is deducted from the importing zone's requirement without those resources bidding directly or receiving remuneration in that market (Höschle, Le Cadre, & Belmans, 2018; Roques, 2019). Under explicit participation, neighboring generators or interconnectors participate directly and receive remuneration up to a de-rated interconnection capacity (Höschle, Le Cadre, & Belmans, 2018). In both cases, the reliability of the credited contribution is central. Höschle, Le Cadre, and Belmans (2018) show that overestimating it can lower the reserve margin below the adequacy target, while underestimating it causes additional investment and higher costs. Adekola et al. (2026) find a similar trade-off: implicit participation lowers costs but can also lead to energy not served.

Both forms require a rule for how much capacity can be credited across a boundary. A de-rated transfer limit provides a relatively simple representation, while a flow-based approach can account more directly for simultaneous network interactions (Adekola et al., 2026).

## 2.5. Conclusion

The review leads to a nested capacity market design adapted to a European single-price energy market. A system-wide requirement provides aggregate resource adequacy, while local requirements are added for transmission-constrained zones to ensure that part of the procured capacity is located where it can contribute during scarcity. The structure follows the deliverability logic of Archetype B, while retaining the zonal energy market and cost-based redispatch used in Europe.

Cross-zonal participation is included to recognize that capacity in one zone may contribute to the requirement of another. The model follows the logic of implicit participation because generators do not bid across zones or receive separate cross-zonal remuneration. To keep the overall zonal obligation fixed, the contribution is represented as a signed reallocation between zones rather than as a one-sided deduction. The permitted reallocation is bounded by $\sigma \cdot MEC$, with $\sigma$ varying how strongly zones can

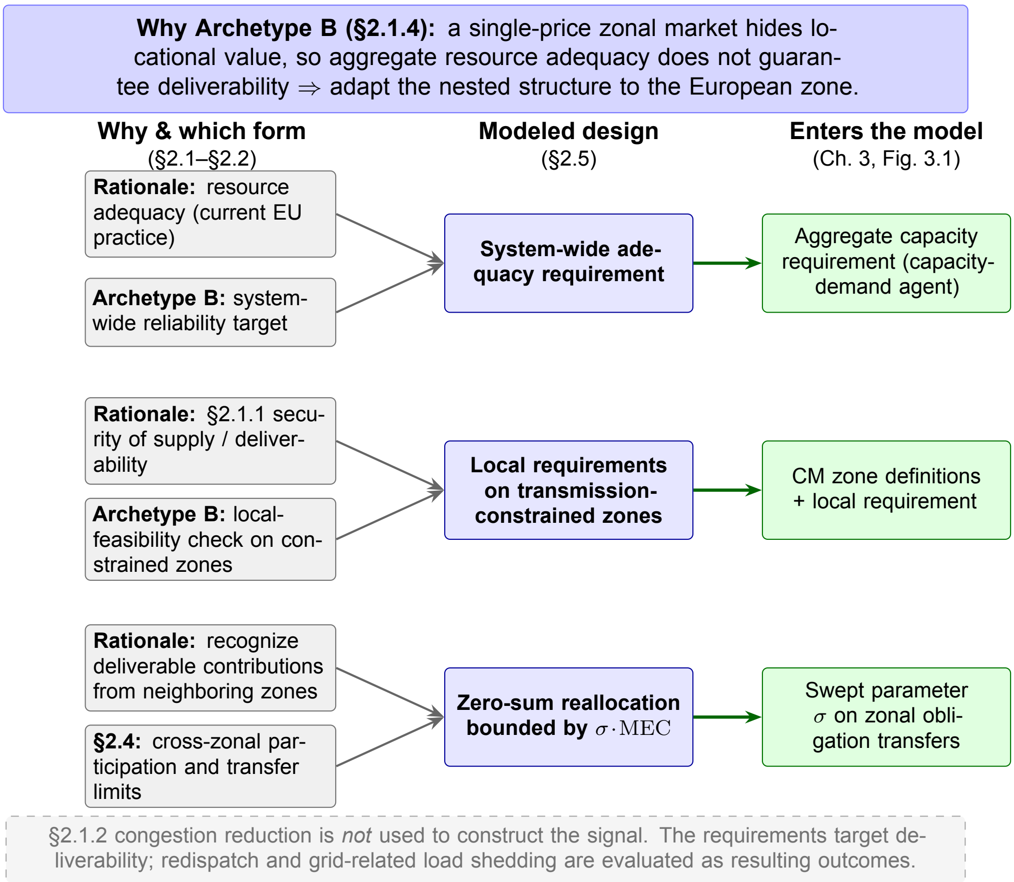


**Figure 2.2:** The modeled design follows from the review. Each element is derived from a rationale (§2.1) and an archetype (§2.2, grey arrows) and enters the model of Chapter 3 (green arrows).

rely on neighboring capacity.

Figure 2.2 summarizes how the selected design enters the model. The system-wide and local requirements are represented by the capacity-demand agent, the zonal structure defines where capacity is procured, and $\sigma \cdot MEC$ determines how far the obligation can be shifted across zones. The model then compares the procurement-cost implications of these locational requirements with the resulting redispatch and adequacy outcomes.

# 3
# Methodology

The modeling method applied in this study is mathematical programming. This chapter presents the conceptual and formal model, ending with a proof of concept on a small system before the model is applied to the Dutch case study. The conceptual model is developed first by defining the actors, the three market processes, and the interactions between them. Afterwards, the individual optimization problem of each actor is formalized together with its objective, decision variables, and inputs. The market-clearing conditions linking the actors are stated as well.

The actor problems are then combined into a Mixed Complementarity Problem (MCP). The MCP represents the complete game and includes the energy market, capacity market, investment decisions, and redispatch. Since the resulting complementarity system can have multiple equilibria, different reformulations are considered to explore its solution space. A full primal-dual formulation is introduced first. Because embedding redispatch creates a large number of bilinear terms, the model is subsequently decomposed into a first-stage market equilibrium and a second-stage redispatch problem. The first-stage equilibrium is initially retained as a primal-dual MPEC. It is then transformed into a Mixed-Integer Linear Problem (MILP) by directly linearizing its complementarity conditions. Based on computational performance, the sequential solution method consisting of a first-stage MILP and a second-stage LP is selected for the case study.

## 3.1. Conceptual model

The core processes of the model are the capacity market, the energy market, and the redispatch mechanism. This section describes how these processes operate and how the actors connect through them. The complete conceptual structure is summarized in Figure 3.1. The individual optimization problems follow in Section 3.2.

The capacity market secures sufficient firm capacity through centralized, volume-based procurement. The system operator sets an administratively determined target volume, and capacity is procured until that target is met. Accepted generators receive the market-clearing price. The design is extended with the locational elements identified in Chapter 2 by introducing a nested structure with one system-wide requirement and several zonal requirements. Capacity in one zone can contribute to the requirement of another zone within predefined transfer limits.

The capacity market is the intervention point of this study. Investable generators compare their expected revenues from the energy and capacity markets with their fixed costs. The spatial definition of the capacity requirements therefore affects where new capacity can recover its costs and, consequently, where investment takes place.

The energy market represents the zonal market design applied in most European countries (Gomez et al., 2019). The bidding zone covers the entire modeled system, and internal transmission constraints are not considered during market clearing. Generators offer their available output at marginal cost. Under the assumption of perfect competition, this is the dominant bidding strategy. The market dispatches generators in ascending marginal cost order until supply equals served demand. The outcome consists of a uniform energy price and a dispatch schedule for every generator. Lastly, the energy market operates with a price cap, that prevents controllable generators to regain their fixed costs during scarcity events (Fabra, 2018). The price cap therefore motivates the introduction of the capacity market in the first place.

Since the energy market does not consider the internal grid, its dispatch may violate transmission limits. Redispatch is the ex-post correction of this market outcome (Poplavskaya et al., 2020). The redispatch operator calculates the flows resulting from the market dispatch and changes generator output where necessary. Some generators increase output through upward redispatch, while others reduce output through downward redispatch. If the available redispatch options are insufficient to restore network feasibility, grid-related load shedding is used as a last resort.

Cost-based redispatch is chosen instead of market-based redispatch for two reasons. First, it avoids the additional complexity of strategic behavior in the redispatch market (Grimm et al., 2022; Martin et al., 2022). Second, without redispatch anticipation and strategic behavior, cost-based and market-based redispatch produce the same physical outcome (Hirth & Schlecht, 2020). Cost-based redispatch also means that generators do not earn an additional profit from being redispatched. Upward redispatch covers the additional variable costs, while downward redispatch compensates the generator for the foregone energy market margin. Redispatch therefore does not create an additional locational investment signal in the model.

The capacity mechanism and the energy market are interdependent. Although capacity procurement takes place before delivery in practice, generators base their investment decisions on expected energy market revenues. At the same time, their investment decisions determine the generation available in the energy market. The expected energy price therefore affects investment, while investment changes the market supply curve.

Redispatch is operationally sequential. The redispatch operator takes the energy market dispatch as given and changes it only to restore network feasibility. Capacity siting affects the market dispatch, which in turn determines the available redispatch options and the resulting congestion outcomes. This chain, from capacity siting through energy market dispatch to redispatch, is the mechanism through which locational capacity market signals affect congestion.

Within the complete game, the redispatch operator is nevertheless represented as an actor. Its optimization problem is included together with those of the generators and demand agents, while the market dispatch enters its problem as an input. The complete MCP therefore contains the energy market, capacity market, investment decisions, and redispatch. Only when the computational solution methods are introduced is this game decomposed into a first-stage market equilibrium and a separate second-stage redispatch problem.

The generator decisions can be summarized as follows. Renewable generators offer their available generation in the energy market and do not participate in the capacity market. Legacy controllable generators participate in both markets, but their installed capacity is fixed. Investable controllable generators additionally choose their available capacity. Their investment decision depends on expected energy- and capacity market revenues relative to fixed costs. Since redispatch is cost-neutral, redispatch revenues do not enter this decision. Investable generators are therefore the actors through which a locational capacity market signal changes the spatial distribution of capacity.

The setup assumes perfect information, perfect competition, and risk-neutral decision-making. Risk aversion is often included in capacity-expansion problems and can contribute to the need for a capacity mechanism (Fraunholz et al., 2023). In this study, however, the existence of the capacity mechanism is taken as given. The focus lies on its locational design. Risk aversion is therefore excluded to keep the model as simple as possible.

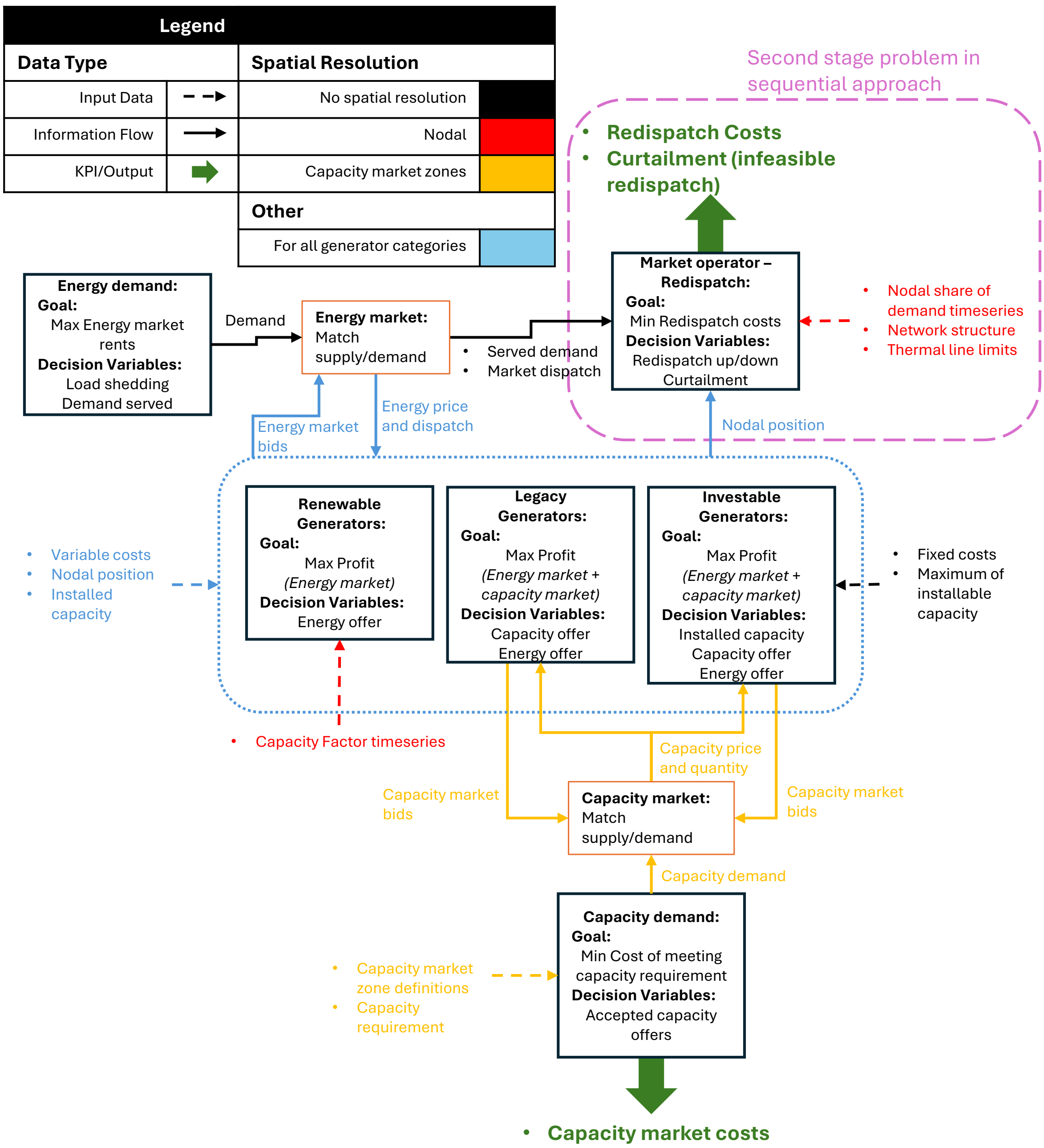


**Figure 3.1:** Conceptual model showing the actors, their objectives, and their interactions.

## 3.2. Individual actor problems

The term actor is used broadly. An actor can be an individual entity, such as a generator, or an aggregation, such as the capacity demand agent. Actors are distinguished by their objectives and constraints. This section formalities the optimization problem of each actor and defines the variables and parameters connecting it to the rest of the system.

The energy and redispatch models are indexed by timesteps $t \in \mathcal{T}$, each representing one hour. Representative days are used instead of a full year. The parameter $W_t$ gives the number of original hours represented by timestep $t$. It multiplies objective terms representing annual revenues, costs, or energy volumes. Physical constraints apply separately to every representative hour and are therefore not multiplied by $W_t$. Variables shown in brackets next to constraints are the corresponding dual variables.

### 3.2.1. Power generators

Each power generator maximizes its own profit. Three types of generator are distinguished. Renewable and controllable generators differ in their operational characteristics, while legacy and investable generators differ in whether installed capacity is a decision variable. Table 3.1 summaries their decisions and constraints.

**Table 3.1:** Generator classification: decision variables and constraints by type.

| Generator type | Dispatch type | Decision variables | Key constraints |
|---|---|---|---|
| Legacy | Controllable | Energy market offer | Generation bounded by installed capacity |
| | | Capacity market offer | Capacity offer bounded by installed capacity multiplied by the de-rating factor |
| | Renewable | Energy market offer | Generation bounded by installed capacity multiplied by the time-varying availability factor |
| | | — | No capacity market participation |
| Investable | Controllable | Available capacity | Capacity bounded by maximum installable capacity |
| | | Energy market offer | Generation bounded by available capacity |
| | | Capacity market offer | Capacity offer bounded by de-rated available capacity |

The investable generator $i \in \mathcal{I}$ chooses energy market dispatch $q_{t,i}$, available capacity $c_i$, and capacity market offer $c_i^{cm}$. Its parameters are variable cost $vc_i$, fixed cost $fc_i$, maximum installable capacity $\overline{cap}_i$, and capacity market de-rating factor $\alpha_i$. The energy price $\lambda_t^e$ and zonal capacity price $\lambda_{z(i)}^c$ are taken as given.

$$
\begin{aligned}
\max_{q_{t,i}\geq 0,\, c_i \geq 0,\, c_i^{cm}\geq 0} \quad & \sum_{t\in\mathcal{T}} W_t(\lambda_t^e - vc_i)q_{t,i} - fc_i c_i + \lambda_{z(i)}^c c_i^{cm} && && \text{(3.1a)}\\
\text{s.t.} \quad & q_{t,i} \leq c_i && (\mu_{t,i}^q) \quad \forall t && \text{(3.1b)}\\
& c_i \leq \overline{cap}_i && (\mu_i^{cap}) && \text{(3.1c)}\\
& c_i^{cm} \leq \alpha_i c_i && (\mu_i^{cm}) && \text{(3.1d)}
\end{aligned}
$$

The legacy generator $j \in \mathcal{J}$ does not make an investment decision. Its installed capacity $\overline{cap}_j$ is fixed. Dispatch is limited by installed capacity multiplied by the time-dependent availability factor $a_{t,j}$. For controllable generators, $a_{t,j} = 1$. The capacity market de-rating factor $\alpha_j$ equals zero for renewable generators and one for the controllable legacy generators included in the capacity mechanism.

$$
\begin{aligned}
\max_{q_{t,j}\geq 0,\, c_j^{cm}\geq 0} \quad & \sum_{t\in\mathcal{T}} W_t(\lambda_t^e - vc_j)q_{t,j} + \lambda_{z(j)}^c c_j^{cm} && && \text{(3.2a)}\\
\text{s.t.} \quad & q_{t,j} \leq a_{t,j}\overline{cap}_j && (\mu_{t,j}^q) \quad \forall t && \text{(3.2b)}\\
& c_j^{cm} \leq \alpha_j \overline{cap}_j && (\mu_j^{cm}) && \text{(3.2c)}
\end{aligned}
$$

The investable and legacy generators jointly form the set

$$\mathcal{G} = \mathcal{I} \cup \mathcal{J} \tag{3.3}$$

Whenever both types are included in one equation, the index $g \in \mathcal{G}$ is used.

## 3.2.2. Demand agents

The demand agents are divided into energy demand and capacity demand. Both interact with the generators through market-clearing conditions, but their objectives and constraints differ.

### Energy demand

The energy-demand agent serves demand up to its willingness to pay. Its decision variables are served demand $D_t$ and energy market load shedding $ls_t^{em}$. The inelastic demand parameter is $D_t^{\max}$, while $VOLL^{em}$ represents the willingness to pay and the administrative energy market price cap.

$$
\begin{aligned}
\max_{D_t \geq 0,\, ls_t^{em} \geq 0} \quad & \sum_{t \in \mathcal{T}} W_t (VOLL^{em} - \lambda_t^e) D_t && && \text{(3.4a)}\\
\text{s.t.} \quad & D_t + ls_t^{em} = D_t^{\max} && (\xi_t) \quad && \forall t \quad \text{(3.4b)}\\
& D_t \leq D_t^{\max} && (\kappa_t) \quad && \forall t \quad \text{(3.4c)}
\end{aligned}
$$

### Capacity demand

The capacity demand agent procures firm capacity in every zone and for the system as a whole. The system-wide requirement represents aggregate resource adequacy. The zonal requirements add a simplified locational deliverability condition by requiring capacity to be procured within different parts of the system. They do not constitute a complete transmission-adequacy assessment, since intra-zonal constraints and the simultaneous deliverability of several cross-zonal contributions are not represented in the capacity market clearing.

The agent chooses procured capacity $c_z^{dem}$ in every zone and a signed capacity contribution $f_{ab}$ for each unordered zone pair $(a, b) \in \mathcal{P}$. Its parameters are the zonal capacity requirements $d_z^c$, the system requirement $d^c$, and the Maximum Entry Capacity $MEC_{ab}$. The parameter $\sigma$ determines the share of each MEC that can be used for cross-zonal participation.

The signed net contribution received by zone $z$ is

$$\eta_z = \sum_{(a,b) \in \mathcal{P}: a = z} f_{ab} - \sum_{(a,b) \in \mathcal{P}: b = z} f_{ab} \tag{3.5}$$

For a pair $(a, b)$, a positive $f_{ab}$ represents a contribution from zone $b$ to zone $a$. The contribution in the opposite direction is represented by a negative value, so the same contribution cannot be counted twice.

$$
\begin{aligned}
\min_{c_z^{dem} \geq 0,\, f_{ab}} \quad & \sum_{z \in \mathcal{Z}} \lambda_z^c c_z^{dem} && && \text{(3.6a)}\\
\text{s.t.} \quad & c_z^{dem} \geq d_z^c - \eta_z && (\nu_z) \quad && \forall z \quad \text{(3.6b)}\\
& \sum_{z \in \mathcal{Z}} c_z^{dem} \geq d^c && (\lambda^{c,sys}) \quad && \text{(3.6c)}\\
& d_z^c - \eta_z \geq 0 && (\rho_z) \quad && \forall z \quad \text{(3.6d)}\\
& -\sigma MEC_{ab} \leq f_{ab} \leq \sigma MEC_{ab} && (\phi_{ab}^{lo}, \phi_{ab}^{hi}) \quad && \forall (a,b) \in \mathcal{P} \quad \text{(3.6e)}
\end{aligned}
$$

Equation (3.6b) defines the effective zonal requirement after cross-zonal contributions. Equation (3.6c) preserves the system-wide adequacy floor. Equation (3.6d) prevents the effective requirement of a zone from becoming negative, while Equation (3.6e) limits the contribution between each pair of zones.

### 3.2.3. Redispatch operator

The redispatch operator minimizes the cost of restoring network feasibility after the energy market has cleared. Its decision variables are upward redispatch $r^{+}_{t,g}$, downward redispatch $r^{-}_{t,g}$, and grid-related load shedding $ls^{grid}_{n,t}$.

The energy market dispatch $q_{t,g}$ is taken as given by this actor. Available output is denoted by $\overline{q}_{t,g}$. For an investable generator, $\overline{q}_{t,i} = c_i$. For a legacy generator, $\overline{q}_{t,j} = a_{t,j}\overline{cap}_j$.

Energy market load shedding is distributed across nodes according to their demand shares. Let $s_n$ denote the share of system demand at node $n$. The nodal demand remaining after energy market load shedding is

$$d^{served}_{n,t} = d_{n,t} - s_n ls^{em}_t \tag{3.7}$$

The redispatch objective contains a mark-up $x$ on both upward and downward redispatch. Following Kenis et al. (2024), this prevents additional redispatch that is not needed to restore network feasibility. The mark-up affects the optimization but is excluded from the redispatch-cost measure reported in the results. Its sensitivity is examined in Table 3.14.

$$\begin{aligned}\min_{r^{+}_{t,g}\geq 0,\; r^{-}_{t,g}\geq 0,\; ls^{grid}_{n,t}\geq 0} \quad \sum_{t\in\mathcal{T}} W_t \Bigg[ \sum_{g\in\mathcal{G}} \big((vc_g + x)r^{+}_{t,g} + (-vc_g + x)r^{-}_{t,g}\big) \\ + VOLL^{grid} \sum_{n\in\mathcal{N}} ls^{grid}_{n,t} \Bigg]\end{aligned} \tag{3.8a}$$

$$\begin{aligned}
\text{s.t.} \quad & r^{+}_{t,g} \leq \overline{q}_{t,g} - q_{t,g} && (\overline{\beta}^{q}_{t,g}) && \forall t, g && (3.8b)\\
& r^{-}_{t,g} \leq q_{t,g} && (\overline{\beta}^{-}_{t,g}) && \forall t, g && (3.8c)\\
& ls^{grid}_{n,t} \leq d^{served}_{n,t} && (\overline{\gamma}_{n,t}) && \forall t, n && (3.8d)\\
& \sum_{g\in\mathcal{G}} r^{+}_{t,g} - \sum_{g\in\mathcal{G}} r^{-}_{t,g} + \sum_{n\in\mathcal{N}} ls^{grid}_{n,t} = 0 && (\lambda^{RD}_t) && \forall t && (3.8e)\\
& -F_l \leq p^{flow}_{l,t} \leq F_l && (\underline{\rho}_{l,t}, \overline{\rho}_{l,t}) && \forall l, t && (3.8f)\\
& p^{flow}_{l,t} = \sum_{n\in\mathcal{N}} PTDF_{l,n} p^{inj}_{n,t} && (\phi_{l,t}) && \forall l, t && (3.8g)
\end{aligned}$$

$$\begin{aligned} with \quad p^{inj}_{n,t} = \sum_{g\in\mathcal{G}_n} \big(q_{t,g} + r^{+}_{t,g} - r^{-}_{t,g}\big) \\ - d^{served}_{n,t} + ls^{grid}_{n,t}, \qquad \forall n, t.\end{aligned} \tag{3.8h}$$

Equations (3.8b) and (3.8c) limit redispatch by the available upward headroom and the market dispatch. Equation (3.8d) prevents grid-related load shedding from exceeding the nodal demand still served after the energy market. Equation (3.8e) balances downward redispatch with upward redispatch and grid-related load shedding. Equations (3.8f)–(3.8h) impose the DC power-flow constraints.

### 3.2.4. Market clearing

The actor problems are linked through the energy- and capacity market clearing conditions. The energy market clears when total dispatch equals served demand. The capacity market clears in each zone when procured capacity equals the capacity offered by generators located in that zone.

$$\sum_{g\in\mathcal{G}} q_{t,g} = D_t \qquad (\lambda_t^e) \qquad \forall t \tag{3.9a}$$

$$\sum_{g\in\mathcal{G}:z(g)=z} c_g^{cm} - c_z^{dem} = 0 \qquad (\lambda_z^c) \qquad \forall z \tag{3.9b}$$

The dual variables of these conditions are the energy price $\lambda_t^e$ and the zonal capacity prices $\lambda_z^c$, which the individual actors take as given.

## 3.3. Mixed Complementarity Problem

Each actor solves its own optimization problem subject to its own constraints. The Karush–Kuhn–Tucker conditions of all actor problems can be combined with the market-clearing conditions to form one equilibrium problem. The resulting formulation is a Mixed Complementarity Problem.

The general construction of an MCP is provided in Appendix C.1. The actor-specific Lagrangians and optimality conditions are collected in Appendix C.3. Keeping these derivations in the appendix allows the methodology chapter to focus on how the actor problems are connected and how the resulting equilibrium is solved.

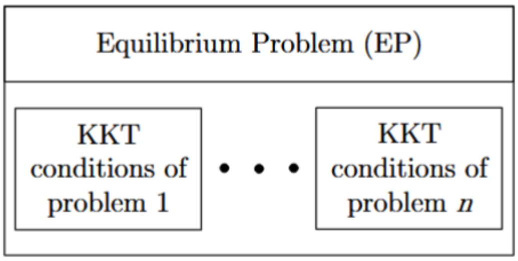


**Figure 3.2:** General structure of equilibrium problems (Gabriel et al., 2013).

The complete MCP combines the optimality conditions of the investable generators, legacy generators, energy-demand agent, capacity demand agent, and redispatch operator. The energy- and capacity market clearing conditions in Equations (3.9a) and (3.9b) connect the market actors. The redispatch problem is linked to the remaining actors through the market dispatch $q_{t,g}$, available output $\overline{q}_{t,g}$, and served nodal demand $d_{n,t}^{served}$.

Redispatch remains operationally sequential because the redispatch operator takes the market outcome as given. Within the complete game, however, its optimality conditions form part of the same complementarity system. The sequential solution methods introduced below decompose this game by solving the energy- and capacity market equilibrium first and the redispatch problem afterwards.

Every individual actor problem is linear and therefore convex. The combined complementarity system nevertheless has a non-convex feasible set. Several equilibria can consequently exist.

This is particularly relevant for capacity siting. Investment is determined by energy and capacity market profitability, while the outcomes are also evaluated through redispatch. Since redispatch is cost-neutral to generators, it does not affect their investment decisions. Several spatial investment patterns can therefore be equivalent for the market actors while producing different network flows and redispatch outcomes. A single solver-selected equilibrium would reveal only one of these possible congestion outcomes.

## 3.4. Solution-space exploration

The solution space is explored to reduce dependence on a single solver-selected equilibrium. The aim is not to assign probabilities to the equilibria. Instead, the exploration searches for spatially different capacity-siting outcomes and reports the resulting minimum–maximum ranges of congestion outcomes.

Three solution methods were developed. The first is a full primal-dual MPEC that retains all actors, including redispatch, in one formulation. The second separates redispatch from the market equilibrium but retains a primal-dual formulation for the first stage. The third keeps the same sequential structure but replaces the first-stage complementarity conditions with disjunctive constraints.

The methods are assessed according to whether they represent the intended actor problems and whether they solve within feasible time at the scale of the case study. The proof of concept compares the methods on a traceable system in Subsection 3.5.2. Computational performance at case-study scale is reported in Section 5.1 and Appendix D.

### 3.4.1. Full primal-dual MPEC

The first solution method reformulates the complete MCP through primal feasibility, dual feasibility, and strong duality following (Dimanchev et al., 2024). For each linear actor problem, these conditions are equivalent to its KKT conditions. Primal feasibility follows from the actor problems in Section 3.2. The corresponding dual-feasibility and strong-duality equations are provided in Appendix C.3.

The individual primal-dual reformulations were verified separately using `Dualization.jl` (Legat et al., 2026). For each actor, the objective value of the primal problem was compared to the objective value of the automated dual problem from `Dualization.jl` and the manual dual problem. All three values being equal proved the correctness of strong duality.

The actor problems are connected through the energy- and capacity market clearing conditions in Equations (3.9a) and (3.9b). A secondary objective is added to select between equilibria that are equivalent for the individual actors. The full formulation is solved once by minimizing and once by maximizing

$$C^{expl} = \sum_{t \in \mathcal{T}} W_t \left[ \sum_{g \in \mathcal{G}} vc_g \left( r^+_{t,g} - r^-_{t,g} \right) + VOLL^{grid} \sum_{n \in \mathcal{N}} ls^{grid}_{n,t} \right]. \tag{3.10}$$

This objective is not part of the original game. It is used only to select between equilibria at different ends of the redispatch-cost range. The redispatch operator itself remains optimal with respect to the mark-up-inclusive objective in Equation (3.8a)

The main computational difficulty enters through the redispatch strong-duality equation in Appendix C.3.5. Its dual objective contains the product

$$f^{mkt}_{l,t} \phi_{l,t}, \tag{3.11}$$

where the pre-redispatch market flow is

$$f^{mkt}_{l,t} = \sum_{n \in \mathcal{N}} PTDF_{l,n} \left[ \sum_{g \in \mathcal{G}_n} q_{t,g} - d^{served}_{n,t} \right] \tag{3.12}$$

Substituting Equation (3.12) into Equation (3.11) gives

$$\begin{aligned} f^{mkt}_{l,t} \phi_{l,t} = & \sum_{n \in \mathcal{N}} \sum_{g \in \mathcal{G}_n} PTDF_{l,n} \underbrace{q_{t,g} \phi_{l,t}}_{\text{bilinear}} \\ & - \sum_{n \in \mathcal{N}} PTDF_{l,n} d^{served}_{n,t} \phi_{l,t} \end{aligned} \tag{3.13}$$

Both $q_{t,g}$ and $\phi_{l,t}$ are endogenous to the full model. The first term therefore creates one bilinear product for every relevant generator–line–timestep combination. Their number grows approximately with

$$|\mathcal{T}| \times |\mathcal{G}| \times |\mathcal{L}|. \tag{3.14}$$

The difficulty is amplified by the PTDF structure. In a meshed network, an injection at one node affects the flows on many lines. The dispatch of almost every generator can therefore become bilinearly coupled with the congestion dual variables of several transmission lines.

Other bilinearities remain in the full primal-dual formulation, including products between energy prices and dispatch and between capacity prices and capacity offers. These products are more local. The PTDF-induced products in Equation (3.13), by contrast, create dense coupling between generators and transmission constraints throughout the network.

For a system with $|\mathcal{T}| = 240$ representative hours, $|\mathcal{G}| = 40$ generators, and $|\mathcal{L}| = 25$ lines, the redispatch strong-duality equation alone introduces up to $240{,}000$ generator–line–timestep products. Reducing the number of nodes, lines, or timesteps lowers this number, but the reduction would have to be substantial before the formulation becomes tractable. This would remove much of the spatial or temporal detail required for the case study.

The individual primal-dual actor formulations remain valid, but coupling them in one model creates a large MPEC dominated by the PTDF-related bilinearities. The next method therefore removes the redispatch block from the first-stage equilibrium and solves it separately.

### 3.4.2. Sequential primal-dual

The sequential primal-dual formulation separates the redispatch operator from the market equilibrium. The first stage retains the same primal-dual formulations of the investable generators, legacy generators, energy-demand agent, and capacity demand agent as the full formulation. These equations are provided in Appendix C.3. The redispatch block in Appendix C.3.5 is omitted from the first stage.

Once the market equilibrium has been solved, the resulting dispatch, available capacities, and energy market load shedding are fixed and passed to the redispatch problem in Equation (3.8). The second stage is therefore an LP.

Since redispatch is not available when the first stage is solved, Equation (3.10) cannot be used as its secondary objective. Instead, one positive and one negative exploration direction are defined for every PTDF row:

$$\mathcal{W} = \{PTDF_{l,\cdot}, -PTDF_{l,\cdot} \mid l \in \mathcal{L}\} \tag{3.15}$$

For every $w^{(k)} \in \mathcal{W}$, the first-stage objective is

$$\max \sum_{i \in \mathcal{I}} w^{(k)}_{n(i)} c_i \tag{3.16}$$

where $n(i)$ denotes the node of investable generator $i$. Positive and negative PTDF rows direct capacity towards different parts of the network. Repeating the model for all vectors in $\mathcal{W}$ therefore produces spatially different siting outcomes. The objective has no economic interpretation and does not assign probabilities to the resulting equilibria.

Separating redispatch removes the dense generator–line bilinearities in Equation (3.13). The first-stage strong-duality equations nevertheless still contain products between endogenous market prices and quantities. The sequential primal-dual formulation is therefore smaller than the full MPEC, but remains non-convex and does not solve within feasible time at case-study scale.

### 3.4.3. Sequential MILP

The sequential MILP retains the same two-stage structure and the same exploration objective in Equation (3.16). The difference lies only in the representation of the first-stage equilibrium. Rather than imposing primal feasibility, dual feasibility, and strong duality, the first-stage KKT conditions are used directly and their complementarity conditions are linearized through binary variables.

### Disjunctive reformulation

Following Gabriel and Leuthold (2010), a complementarity condition

$$0 \leq u \perp v \geq 0 \tag{3.17}$$

is replaced by

$$0 \leq u \leq K^u(1-r), \qquad 0 \leq v \leq K^v r, \qquad r \in \{0,1\} \tag{3.18}$$

At least one of $u$ and $v$ must equal zero. Both can also be zero. The constants $K^u$ and $K^v$ have to be sufficiently large not to exclude feasible equilibria, but unnecessarily large values weaken the MILP formulation.

The bounds used in this study are derived from physical generation capacities, maximum demand, permitted cross-zonal contributions, representative-period weights, and the price limits of the energy and capacity markets. Common category-specific bounds are used instead of separate values for every generator, zone, and timestep. Their definitions and derivations are provided in Appendix C.4. Their adequacy is tested in the proof of concept by multiplying all bounds by 100. Since the market and redispatch outcomes remain unchanged, the selected values do not appear to restrict the relevant solution space.

### First-stage market equilibrium

For every exploration vector $w^{(k)} \in \mathcal{W}$, the first-stage MILP maximizes Equation (3.16). The energy-demand balance in Equation (3.4b) is substituted into the energy market clearing condition in Equation (3.9a). This gives

$$\sum_{g \in \mathcal{G}} q_{t,g} + ls_t^{em} = D_t^{\max} \qquad \forall t \tag{3.19}$$

The capacity market clearing condition is unchanged and is reused directly as Equation (3.9b).

The energy and capacity prices are bounded by

$$0 \leq \lambda_t^e \leq VOLL^{em} \qquad \forall t \tag{3.20a}$$

$$0 \leq \lambda_z^c \leq \overline{\lambda^c} \qquad \forall z \tag{3.20b}$$

$$0 \leq \lambda^{c,sys} \leq \overline{\lambda^c} \tag{3.20c}$$

For investable generators, the complementarity conditions are replaced by

$$0 \le q_{t,i} \le K^q(1 - r^{q,I}_{t,i}) \qquad \forall t, i \tag{3.21a}$$
$$0 \le -W_t(\lambda^e_t - vc_i) + \mu^q_{t,i} \le \overline{K}^{q,I} r^{q,I}_{t,i} \qquad \forall t, i \tag{3.21b}$$
$$0 \le c_i - q_{t,i} \le \widetilde{K}^{q,I}(1 - r^{\mu q,I}_{t,i}) \qquad \forall t, i \tag{3.21c}$$
$$0 \le \mu^q_{t,i} \le \widehat{K}^{\mu^q} r^{\mu q,I}_{t,i} \qquad \forall t, i \tag{3.21d}$$
$$0 \le c_i \le K^c(1 - r^c_i) \qquad \forall i \tag{3.21e}$$
$$0 \le fc_i - \sum_{t \in \mathcal{T}} \mu^q_{t,i} + \mu^{cap}_i - \alpha_i \mu^{cm}_i \le \overline{K}^c r^c_i \qquad \forall i \tag{3.21f}$$
$$0 \le \overline{cap}_i - c_i \le \widetilde{K}^{cap}(1 - r^{cap}_i) \qquad \forall i \tag{3.21g}$$
$$0 \le \mu^{cap}_i \le \widehat{K}^{\mu^{cap}} r^{cap}_i \qquad \forall i \tag{3.21h}$$
$$0 \le c^{cm}_i \le \alpha_i \overline{cap}_i(1 - r^{cm,I}_i) \qquad \forall i \tag{3.21i}$$
$$0 \le -\lambda^c_{z(i)} + \mu^{cm}_i \le \overline{K}^{cm} r^{cm,I}_i \qquad \forall i \tag{3.21j}$$
$$0 \le \alpha_i c_i - c^{cm}_i \le \widetilde{K}^{cm,I}(1 - r^{\mu cm,I}_i) \qquad \forall i \tag{3.21k}$$
$$0 \le \mu^{cm}_i \le \widehat{K}^{\mu^{cm}} r^{\mu cm,I}_i \qquad \forall i \tag{3.21l}$$

For legacy generators, the corresponding conditions are

$$0 \le q_{t,j} \le a_{t,j}\overline{cap}_j(1 - r^{q,J}_{t,j}) \qquad \forall t, j \tag{3.22a}$$
$$0 \le -W_t(\lambda^e_t - vc_j) + \mu^q_{t,j} \le \overline{K}^{q,J} r^{q,J}_{t,j} \qquad \forall t, j \tag{3.22b}$$
$$0 \le a_{t,j}\overline{cap}_j - q_{t,j} \le \widetilde{K}^{q,J}(1 - r^{\mu q,J}_{t,j}) \qquad \forall t, j \tag{3.22c}$$
$$0 \le \mu^q_{t,j} \le \widehat{K}^{\mu^q} r^{\mu q,J}_{t,j} \qquad \forall t, j \tag{3.22d}$$
$$0 \le c^{cm}_j \le \alpha_j \overline{cap}_j(1 - r^{cm,J}_j) \qquad \forall j \tag{3.22e}$$
$$0 \le -\lambda^c_{z(j)} + \mu^{cm}_j \le \overline{K}^{cm} r^{cm,J}_j \qquad \forall j \tag{3.22f}$$
$$0 \le \alpha_j \overline{cap}_j - c^{cm}_j \le \widetilde{K}^{cm,J}(1 - r^{\mu cm,J}_j) \qquad \forall j \tag{3.22g}$$
$$0 \le \mu^{cm}_j \le \widehat{K}^{\mu^{cm}} r^{\mu cm,J}_j \qquad \forall j \tag{3.22h}$$

The energy-demand condition becomes

$$0 \le ls^{em}_t \le D^{\max}_t \qquad \forall t \tag{3.23a}$$
$$ls^{em}_t \le K^{ls}(1 - r^{ls}_t) \qquad \forall t \tag{3.23b}$$
$$0 \le W_t(VOLL^{em} - \lambda^e_t) \le \overline{K}^{ls} r^{ls}_t \qquad \forall t \tag{3.23c}$$

For the capacity demand agent, the linearized conditions are

$$
\begin{aligned}
&0 \leq c_z^{dem} \leq K^{dem}(1 - r_z^{dem}) && \forall z && \text{(3.24a)}\\
&0 \leq \lambda_z^c - \nu_z - \lambda^{c,sys} \leq \overline{K}^{dem} r_z^{dem} && \forall z && \text{(3.24b)}\\
&0 \leq c_z^{dem} - d_z^c + \eta_z \leq K^{dem}(1 - r_z^{\nu}) && \forall z && \text{(3.24c)}\\
&0 \leq \nu_z \leq \widehat{K}^{\nu} r_z^{\nu} && \forall z && \text{(3.24d)}\\
&0 \leq \sum_{z \in \mathcal{Z}} c_z^{dem} - d^c \leq K^{sys}(1 - r^{sys}), && && \text{(3.24e)}\\
&0 \leq \lambda^{c,sys} \leq \widehat{K}^{\lambda^{c,sys}} r^{sys}, && && \text{(3.24f)}\\
&0 \leq d_z^c - \eta_z \leq K^{dem}(1 - r_z^{\rho}) && \forall z && \text{(3.24g)}\\
&0 \leq \rho_z \leq \widehat{K}^{\rho} r_z^{\rho} && \forall z && \text{(3.24h)}\\
&0 \leq f_{ab} + \overline{f}_{ab} \leq 2\overline{f}_{ab}(1 - r_{ab}^{lo}) && \forall (a,b) \in \mathcal{P} && \text{(3.24i)}\\
&0 \leq \phi_{ab}^{lo} \leq \widehat{K}^{\phi} r_{ab}^{lo} && \forall (a,b) \in \mathcal{P} && \text{(3.24j)}\\
&0 \leq \overline{f}_{ab} - f_{ab} \leq 2\overline{f}_{ab}(1 - r_{ab}^{hi}) && \forall (a,b) \in \mathcal{P} && \text{(3.24k)}\\
&0 \leq \phi_{ab}^{hi} \leq \widehat{K}^{\phi} r_{ab}^{hi} && \forall (a,b) \in \mathcal{P} && \text{(3.24l)}\\
&-(\nu_a - \rho_a) + (\nu_b - \rho_b) + \phi_{ab}^{hi} - \phi_{ab}^{lo} = 0 && \forall (a,b) \in \mathcal{P} && \text{(3.24m)}
\end{aligned}
$$

All variables $r$ in Equations (3.21)–(3.24) are binary. Together, the first-stage MILP consists of the exploration objective in Equation (3.16), the folded energy balance in Equation (3.19), the capacity market clearing condition in Equation (3.9b), and the linearized optimality conditions in Equations (3.21)–(3.24).

Second-stage redispatch

Once the first-stage MILP has been solved, its dispatch, investment, and energy market load-shedding outcomes are fixed. These values determine $q_{t,g}$, $\overline{q}_{t,g}$, and $d_{n,t}^{served}$ in the redispatch problem.

The second stage is exactly the redispatch-operator problem already defined in Equation (3.8). It is solved as an LP for every first-stage exploration outcome. The formulation is therefore not repeated under another equation number.

### 3.4.4. Choice of solution method

The full primal-dual formulation represents the complete game, including redispatch, but its dense PTDF-related bilinearities make it unsuitable for the case-study network. The sequential primal-dual formulation removes these terms by solving redispatch separately. Its first-stage strong-duality equations nevertheless retain bilinear products between endogenous market prices and quantities, and the model still does not solve within feasible time at case-study scale.

The sequential MILP keeps the same two-stage structure but removes the remaining bilinearities by replacing the first-stage complementarity conditions with the disjunctive formulation in Equation (3.18). The sequential primal-dual and sequential MILP formulations use the same actor problems and pass the same market outcomes to the explicit redispatch LP. Their equivalence is tested in the proof of concept.

The sequential MILP is therefore selected for the case study. It retains the intended market-equilibrium and sequential-redispatch structure while providing the only formulation that can be solved repeatedly across the required PTDF exploration directions.

## 3.5. Proof of concept and verification

The proof of concept is used to test whether the model is implemented correctly and whether its main mechanisms respond as intended under controlled conditions. A small fictional system is used because its inputs and outputs can be traced manually. The section first presents the proof-of-concept setup and then verifies the individual model parts along the model's causal chain: the capacity demand agent determines zonal requirements, the capacity market translates these requirements into investment, the energy market clears without internal network constraints, and the redispatch operator restores network feasibility ex post. The model is then subjected to extreme-condition and numerical robustness tests, followed by a sensitivity analysis of the assumptions that most strongly affect capacity siting, dispatch, and congestion outcomes. The section ends by summarizing what these tests imply for the configuration and interpretation of the later case study.

### 3.5.1. Proof of concept setup

The proof-of-concept system is designed to make each step of the model traceable while still activating the main market and network mechanisms. It consists of three nodes, each of which forms a separate capacity market zone. Every node contains one legacy solar generator with an installed capacity of 200 MW and one investable controllable generator with a maximum capacity of 200 MW. The three nodes are connected through a triangular network. The line capacities are deliberately restrictive relative to system demand. Consequently, the copper-plate energy market outcome is not necessarily feasible on the network, which activates the redispatch stage. The nodal parameters and structure are presented in Table 3.2. These are the default parameters used, only deviating from them to test certain parameters or mechanisms connected to them. Additionally, the mark-up $x$ is 20 €/MWh, $VOLL^{em}$ is 4000 €/MWh, $VOLL^{grid}$ is 300 €/MWh. By default, $\sigma$ is set to 0.5 for the verification, the MEC is therefore half of the line capacity.

| Node | Capacity market zone | Legacy solar capacity | Investable generator FC [€/MW] / VC [€/MWh] | Connected lines and limits | Nodal demand share |
|---|---|---|---|---|---|
| 1 | 1 | 200 MW | 22.50 / 6 | 1 (5 MW), 3 (5 MW) | 3.57% |
| 2 | 2 | 200 MW | 30.00 / 5 | 1 (5 MW), 2 (10 MW) | 42.86% |
| 3 | 3 | 200 MW | 35.50 / 4 | 2 (10 MW), 3 (5 MW) | 53.57% |

**Table 3.2:** Proof-of-concept parameters.

The investable generators differ in both fixed and marginal costs. The fixed-cost differences create a clear order for capacity investment, while the marginal-cost differences create an unambiguous merit order in the energy market. The generator with the lowest fixed cost is located at the node with the smallest demand share. This creates a deliberate spatial mismatch between the economically preferred investment location and the main load centers, allowing the effect of capacity siting on network congestion to be observed.

System demand and the solar capacity factors vary across three time steps, as shown in Table 3.3. The solar profiles differ between nodes so that the location of renewable generation changes over time. Together with the fixed nodal demand shares, this produces different residual-load conditions across the three capacity market zones.

| Time step | Demand [MW] | CF node 0 | CF node 1 | CF node 2 |
|---|---|---|---|---|
| 1 | 200 | 0.50 | 0.25 | 0.00 |
| 2 | 300 | 0.00 | 0.50 | 0.25 |
| 3 | 350 | 0.25 | 0.00 | 0.50 |

**Table 3.3:** Load profiles and solar capacity factors across time steps.

The parameter values are deliberately stylized and are not intended to represent a realistic electricity system. Their purpose is to create transparent investment, dispatch and redispatch decisions that can be calculated and checked manually. The strong differences between the nodes make the baseline suitable for implementation verification, but also restrict the number of alternative equilibria. The effect of more homogeneous cost assumptions is therefore examined separately in subsection 3.5.5.

### 3.5.2. Solution method comparison

The three solution methods are first compared on the small proof-of-concept system, where the redispatch can be traced by hand. At this scale all three methods solve in under a second, so the question here is not solving time but correctness: do the methods agree, and where they do not, why.

All three methods return the same capacity siting: the same investment in the CCGT, nuclear and coal generators, with no difference between methods or runs. The redispatch cost does not agree. The two sequential methods both return a redispatch cost of 2519, while the full primal-dual returns 1703 when minimizing and 252240 when maximizing (Table 3.4).

**Table 3.4:** Proof of concept: solving time and redispatch cost by method. The siting is identical across all methods. The two sequential methods return the same redispatch cost. The full primal-dual does not.

| Method | Solve time [s] | Redispatch cost, min | Redispatch cost, max |
|---|---|---|---|
| Full primal-dual | 0.35–0.87 | 1 703 | 252 240 |
| Sequential primal-dual | 0.11 | 2 519 | 2 519 |
| Sequential MILP | 0.03 | 2 519 | 2 519 |

This needs to be read carefully, because the numbers can be read the wrong way. The full primal-dual returns a wide range, from 1703 to 252240, while the two sequential methods return a single value. At the proof-of-concept scale there is only one equilibrium siting, so there is only one redispatch problem to solve, and its cost is a single number. The two sequential methods return that number, 2519, because they solve the redispatch as its own problem. The range of the full primal-dual is therefore not a range of equilibria. It is the span over which its embedded redispatch can be pushed by the secondary objective without becoming infeasible. The true redispatch cost lies inside it, but the maximizing run overstates it by a factor of 100 and the minimizing run understates it.

The sense checks locate the reason (Table 3.5). The market and capacity blocks satisfy their complementarity conditions in the full primal-dual, with violations at the level of numerical zero. The redispatch block does not: the downward redispatch and the curtailment violate complementarity by up to $1.2 \cdot 10^5$. At the same time the redispatch strong-duality residual is at the level of numerical zero. The formulation therefore reports itself as satisfied, since strong duality holds, while the redispatch it returns is not the optimal one, since complementarity does not. A check on strong duality alone would not catch this.

**Table 3.5:** Proof of concept: maximum complementarity violation by block for the full primal-dual. Market and capacity blocks hold. The redispatch block does not, while the redispatch strong-duality residual is zero.

| Complementarity block | Maximizing run | Minimizing run |
|---|---|---|
| Energy market ($q$) | $4 \cdot 10^{-13}$ | $2 \cdot 10^{-11}$ |
| Investment ($c$) | $0$ | $2 \cdot 10^{-10}$ |
| Capacity demand ($c^{dem}$) | $0$ | $2 \cdot 10^{-11}$ |
| Redispatch up ($r^+$) | $1 \cdot 10^{-14}$ | $2.9 \cdot 10^3$ |
| Redispatch down ($r^-$) | $3.7 \cdot 10^4$ | $1.0 \cdot 10^4$ |
| Curtailment ($ls^{grid}$) | $1.2 \cdot 10^5$ | $2.2 \cdot 10^3$ |
| Redispatch strong-duality residual | $-6 \cdot 10^{-11}$ | $9 \cdot 10^{-10}$ |

The two sequential methods are not in this table, because they solve the redispatch as an explicit linear problem, so its complementarity holds by construction. This is also the positive result of the check: the sequential primal-dual and the sequential MILP reformulate the same equilibrium in two different ways, strong duality and the linearized KKT conditions, and they return the same siting and the same redispatch on a system where the outcome can be followed. The sequential MILP is therefore verified against the strong-duality formulation before it is used at scale.

The full primal-dual could be made correct by enforcing the redispatch complementarity explicitly, instead of through strong duality alone. This was not done. The violations in Table 3.5 are exactly what a correct formulation would have to drive to zero, which requires the redispatch complementarity conditions, and under linearization the binary variables that come with them, on top of the dense network coupling described in subsection 3.4.1. The full primal-dual already does not solve at case study scale (section 4.4), so the corrected version, which is larger, would be harder still. It was therefore not pursued, and the full primal-dual is kept only as the small-scale check reported here.

### 3.5.3. Implementation verification

The verification continues with the chosen sequential MILP, to see if the chosen solution method works correctly.

#### capacity demand agent

Table 3.6 verifies the capacity demand agent. The expected requirement is calculated from the formulation as $req_z = d_z^c - \eta_z$, with $d_z^c$ representing the peak residual load in each zone. The model output matches the expected value in all zones.

At $\sigma = 0.5$, the transfer bounds are 2.50 MW between zones 1 and 2, 2.50 MW between zones 1 and 3, and 5.00 MW between zones 2 and 3. All three transfers reach their bounds and therefore remain within the limits imposed by Equation 3.6e. Following the sign convention of $\eta_z$, this gives

$$\eta_1 = -2.50 - 2.50 = -5.00, \qquad \eta_2 = 2.50 - 5.00 = -2.50, \qquad \eta_3 = 2.50 + 5.00 = 7.50.$$

The direction of the transfers is consistent with the objective of the capacity demand agent. The capacity prices increase from zone 1 to zone 3, so part of the obligation is shifted from zone 3 towards zones 1 and 2. For example, zone 2 receives a contribution of 2.50 MW from zone 1 and provides 5.00 MW to zone 3. Its net contribution is therefore $\eta_2$ = -2.50 MW, increasing its requirement from 150.00 MW to 152.50 MW.

Finally, the sum of $\eta_z$ is zero. The transfer formulation therefore shifts the obligation between zones without changing the aggregate zonal requirement. All resulting requirements also remain non-negative.

**Table 3.6:** Verification of the capacity demand agent for $\sigma = 0.5$.

| Zone | $d_z^c$ [MW] | $\eta_z$ [MW] | Expected $req_z$ [MW] | Model $req_z$ [MW] | Difference [MW] |
|---|---|---|---|---|---|
| 1 | 10.71 | -5.00 | 15.71 | 15.71 | 0.00 |
| 2 | 150.00 | -2.50 | 152.50 | 152.50 | 0.00 |
| 3 | 137.50 | 7.50 | 130.00 | 130.00 | 0.00 |
| Total | 298.21 | 0.00 | 298.21 | 298.21 | 0.00 |

#### Capacity market clearing and investment verification

Table 3.7 verifies that the shifted requirements are translated into capacity market clearing and investment. For each zone, procured capacity demand equals the shifted requirement, indicating that the zonal requirement constraint binds. Local capacity market offers then equal procured capacity demand, confirming the market-clearing constraint. The legacy solar generators do not participate in the capacity market because their de-rating factor is zero.

Available controllable capacity equals the accepted capacity market offers in each zone. This confirms that the capacity offers remain within the available-capacity constraint. The equality is specific to the proof-of-concept setup, in which all available controllable capacity is required and offered to the capacity market. Total procured capacity is 298.21 MW, which exceeds the system-wide requirement of 275 MW by 23.21 MW. The system-wide capacity constraint is therefore also satisfied.

**Table 3.7:** Verification of capacity market clearing and investment for $\sigma = 0.5$.

| Zone | $req_z$ [MW] | $c_z^{dem}$ [MW] | Local CM offers [MW] | Available capacity [MW] | Difference [MW] |
|---|---|---|---|---|---|
| 1 | 15.71 | 15.71 | 15.71 | 15.71 | 0.00 |
| 2 | 152.50 | 152.50 | 152.50 | 152.50 | 0.00 |
| 3 | 130.00 | 130.00 | 130.00 | 130.00 | 0.00 |
| Total | 298.21 | 298.21 | 298.21 | 298.21 | 0.00 |

The investment decision is verified by comparing the market rents of each investable generator with its fixed costs. All three generators invest a positive amount below their maximum installable capacity. Their energy market and capacity market rents should therefore exactly recover their fixed costs. Table 3.8 shows that this condition is satisfied for all three generators. The generator in zone 3 receives part of its revenue from the energy market, which explains why its capacity price of 35.50 €/MW is below its fixed cost of 37.50 €/MW.

**Table 3.8:** Verification of the investment decision for $\sigma = 0.5$.

| Zone | Investment [MW] | Energy rent [€] | CM rent [€] | Fixed cost [€] | Profit [€] |
|---|---|---|---|---|---|
| 1 | 15.71 | 0.00 | 353.57 | 353.57 | 0.00 |
| 2 | 152.50 | 0.00 | 4575.00 | 4575.00 | 0.00 |
| 3 | 130.00 | 260.00 | 4615.00 | 4875.00 | 0.00 |

## Energy market clearing verification

The energy market is modeled as a single copper-plate zone and therefore clears aggregate demand without internal network constraints. For each time step, total generation plus energy market load shedding equals demand. The energy price $\lambda_t^e$ also follows the expected merit order. In timestep 1, demand is covered by the solar power plants and the investable generator in zone 3, which has a marginal cost of 4 €/MWh. At timesteps 2 and 3, the investable generator in zone 2 becomes the marginal generator, resulting in an energy price of 5 €/MWh. Generator-level dispatch remains within the available capacity of each generator. The balance error is zero and no load is shed in the energy market, confirming that the market-clearing and dispatch constraints are satisfied.

**Table 3.9:** Verification of energy market clearing for $\sigma = 0.5$.

| Time step | Demand $D_t$ [MW] | Generation $\sum_g q_{t,g}$ [MW] | Load shedding $ls_t$ [MW] | Balance error [MW] | $\lambda_t^e$ [€/MWh] |
|---|---|---|---|---|---|
| 1 | 200.00 | 200.00 | 0.00 | 0.00 | 4 |
| 2 | 300.00 | 300.00 | 0.00 | 0.00 | 5 |
| 3 | 350.00 | 350.00 | 0.00 | 0.00 | 5 |

The energy market clearing can further be verified by testing if the load shedding works correctly. In the first case $VOLL^{em}$ was higher than the marginal costs of all generators. As the capacity market ensures generation adequacy by covering the peak residual load, energy market prices are set trough the marginal costs of the last generator, not demand. Thus load shedding can never occur. Thus, to check if it does work, runs with $VOLL^{em}$ at 0 €/MWh and 4.5 €/MWh can be compared. As shown in Table 3.10, $VOLL^{em}$ at 0 €/MWh completely stops all generation and the price equals 0. Similarly, $VOLL^{em}$ at 4.5 €/MWh introduces load shedding. As there is only one investable generator with marginal costs below 4.5 €/MWh, every MW of load beyond the capacity of this generator and renewables is shed. The price also sits at the value of $VOLL^{em}$, signaling a shortage where demand sets the price.

**Table 3.10:** Comparison of lower values of $VOLL^{em}$ for $\sigma = 0.5$ at timestep 2.

| $VOLL^{em}$ [€/MWh] | Demand $D_t$ [MW] | Generation $\sum_g q_{t,g}$ [MW] | Load shedding $ls_t$ [MW] | Balance error [MW] | $\lambda_t^e$ [€/MWh] |
|---|---|---|---|---|---|
| 0 | 300.00 | 0.00 | 300.00 | 0.00 | 0.00 |
| 4.5 | 300.00 | 205.00 | 95.00 | 0.00 | 4.5 |

### Redispatch verification

Table 3.11 verifies the redispatch logic for timestep 1 at the generator level. The redispatch model takes the market dispatch as fixed and adjusts generation to restore network feasibility. For each generator, final dispatch satisfies

$q_{t,g}^{final} = q_{t,g}^{mkt} + r_{t,g}^{+} - r_{t,g}^{-}$.

Upward and downward redispatch also remain within the available generator limits. Upward redispatch cannot exceed the difference between available capacity and market dispatch, while downward redispatch cannot exceed the market dispatch. In timestep 1, generation at node 2 is increased by 45.71 MW. This is balanced by downward redispatch of 39.89 MW from the solar generator at node 1 and 5.82 MW from the investable generator at node 3. Total upward and downward redispatch are therefore equal, confirming the redispatch balance for this timestep.

**Table 3.11:** Generator level redispatch outcome in timestep 1.

| Generator | $VC$ [€/MWh] | $q^{mkt}$ [MWh] | $r^{-}$ [MWh] | $r^{+}$ [MWh] | $q^{final}$ [MWh] | $q^{max}$ [MWh] |
|---|---|---|---|---|---|---|
| Node 1 Invest | 6.00 | 0.00 | 0.00 | 0.00 | 0.00 | 15.71 |
| Node 1 solar | 0.01 | 50.00 | 39.89 | 0.00 | 10.11 | 50.00 |
| Node 2 Invest | 5.00 | 0.00 | 0.00 | 45.71 | 45.71 | 152.50 |
| Node 2 solar | 0.01 | 25.00 | 0.00 | 0.00 | 25.00 | 25.00 |
| Node 3 Invest | 4.00 | 125.00 | 5.82 | 0.00 | 119.18 | 130.00 |
| Node 3 solar | 0.01 | 0.00 | 0.00 | 0.00 | 0.00 | 0.00 |
| Total | – | 200.00 | 92.14 | 0.00 | 107.86 | - |

The purpose of redispatch is to restore network feasibility. Table 3.12 therefore compares the line flows resulting from the unconstrained energy market dispatch with the final flows after redispatch. Before redispatch, all three line limits are violated. After redispatch, the flows remain within their respective limits, confirming that the network constraints are enforced.

**Table 3.12:** Verification of network feasibility after redispatch in timestep 1.

| Line | Market flow [MW] | Line limit [MW] | Final flow [MW] | Feasible |
|---|---|---|---|---|
| 1 | 28.82 | $\pm$ 5.00 | 5.00 | Yes |
| 2 | -31.89 | $\pm$ 10.00 | -10.00 | Yes |
| 3 | 14.03 | $\pm$ 5.00 | -2.03 | Yes |

Grid-related load shedding is not required in timestep 1. In timestep 3, no upward redispatch is available in the required location. Downward redispatch of 3.64 MW is therefore balanced by 3.64 MW of grid-related load shedding, confirming that the redispatch balance also holds when congestion cannot be resolved through generation redispatch alone.

Together, the checks confirm that the individual model blocks are connected as intended. The capacity demand agent determines the zonal requirements, the capacity market translates these requirements into investment, and the resulting capacity determines the unconstrained energy market dispatch. The redispatch operator then takes this dispatch as fixed and restores network feasibility.

### 3.5.4. Extreme-condition and numerical robustness

The implementation verification confirms that the individual model components work as intended under the proof-of-concept setup. This section adds two further checks. First, selected model inputs are moved to extreme conditions with a clear expected outcome. For example, transmission limits are temporarily increased to test whether redispatch disappears when the market dispatch is already physically feasible. Second, numerical settings are varied to test whether they influence the solution. These checks focus on the interaction between the redispatch mark-up and the penalty for grid-related load shedding, as well as the bounds used in the first-stage MILP. The aim is to confirm that the model outcomes are caused by the represented system and not by numerical choices.

#### Non-binding transmission constraints

The first extreme-condition test removes congestion from the proof-of-concept network. For this purpose, the thermal limit of each line is increased to 100 MW, which is above the largest absolute market flow of 31.89 MW. The energy- and capacity market outcomes are kept unchanged. The expected result is therefore that the market dispatch is already physically feasible and no redispatch or grid-related load shedding is required.

Table 3.13 compares the baseline proof-of-concept network with the scenario using higher transmission limits. In the baseline, five of the nine line flows violate their thermal limits before redispatch. The redispatch model responds with 50.30 MWh of upward redispatch, 53.95 MWh of downward redispatch, and 3.64 MWh of grid-related load shedding. After increasing the line limits, no market flow violates a network constraint. Upward redispatch, downward redispatch, and grid-related load shedding all fall to zero.

**Table 3.13:** Extreme-condition test with non-binding transmission constraints.

| Scenario | Line limits [MW] | Pre-redispatch violations | Upward redispatch [MWh] | Downward redispatch [MWh] | Grid-related load shedding [MWh] |
|---|---|---|---|---|---|
| Base | 5 / 10 / 5 | 5 | 50.30 | 53.95 | 3.64 |
| Higher limits | 100 / 100 / 100 | 0 | 0.00 | 0.00 | 0.00 |

In the higher-limit scenario, the final line flows are equal to the pre-redispatch market flows. This confirms that the redispatch model does not alter the energy market outcome when it already satisfies the network constraints. Redispatch and grid-related load shedding in the baseline are therefore caused by the binding transmission limits.

#### Redispatch mark-up and $VOLL^{grid}$ interaction

As established previously, the redispatch mark-up is included to prevent interventions that are not necessary to restore network feasibility. Without a mark-up, downward redispatch enters the objective as a negative cost. The model can therefore reduce its objective by redispatching a more expensive generator downward and a cheaper generator upward, even when this additional intervention is not needed to resolve congestion. At the same time, the mark-up cannot be chosen independently from the value of lost load. If the mark-up becomes too high, the model can prefer grid-related load shedding over redispatch. This interaction is tested for the proof-of-concept scenario with $\sigma = 1$ and a fixed $VOLL^{grid}$ of 300 €/MWh. Only the mark-up $x$ in the redispatch objective is varied. The capacity market and energy market outcomes therefore remain unchanged. For a balanced intervention consisting of one MWh of upward and one MWh of downward redispatch, the mark-up contributes $2x$ to the objective. The test consequently compares values below, equal to, and far above the grid-related load-shedding penalty.

**Table 3.14:** Effect of the redispatch mark-up at $VOLL^{grid} = 300$ €/MWh.

| Mark-up $x$ [€/MWh] | Upward redispatch [MWh] | Downward redispatch [MWh] | Grid-related load shedding [MWh] |
|---|---|---|---|
| 0 | 114.92 | 119.92 | 5.00 |
| 20 | 55.38 | 60.38 | 5.00 |
| 150 | 50.96 | 58.68 | 7.72 |
| 2000 | 0.00 | 58.68 | 58.68 |

At $x = 0$, the model uses 114.92 MWh of upward and 119.92 MWh of downward redispatch. Grid-related load shedding remains at 5.00 MWh. Compared to the outcome at $x = 20$, the additional redispatch therefore does not allow more demand to be served. It results from the redispatch cost formulation rather than from the network constraints. This confirms that a positive mark-up is needed to avoid unnecessary interventions. At $x = 20$, redispatch volumes fall substantially, while grid-related load shedding remains unchanged. The mark-up is therefore high enough to remove the unnecessary redispatch observed at $x = 0$, without making load shedding more attractive. This configuration is used as the base value for the proof of concept. At $x = 150$, the mark-up of a balanced upward and downward redispatch pair equals 300 €/MWh before the difference in generator variable costs is considered. Grid-related load shedding consequently increases from 5.00 to 7.72 MWh, while redispatch volumes decrease. Higher tested values of $x = 175$ and $x = 290$ produce the same physical outcome and are therefore not shown separately. Lastly, $x = 2000$ represents an intentionally extreme condition. Upward redispatch falls to zero, while all 58.68 MWh of downward redispatch is balanced by grid-related load shedding. The model thus avoids upward redispatch because its mark-up is far above the value assigned to unserved demand.

Together, the tests confirm the expected interaction between both parameters. The mark-up must be high enough that an additional pair of upward and downward redispatch cannot reduce the objective. Setting $h$ above the highest variable cost provides a simple and conservative lower bound. In the proof of concept, $h = 20$ €/MWh satisfies this condition and removes the unnecessary redispatch observed at $h = 0$.

The upper bound is more difficult to determine and does not follow one strict formula. As shown by the total volumes in Table 3.14, the runs with more grid-related load shedding can still have a lower total intervention volume. The reason lies in the meshed structure of the network. Network feasibility cannot always be restored by only reducing generation at one node and increasing it at another. Both changes affect the flows on several lines at the same time. Resolving one overloaded line can therefore worsen the loading of another line and require further redispatch elsewhere in the network. A higher mark-up places more weight on reducing the total amount of redispatch. At some point, the model therefore prefers simple grid-related load shedding when this avoids a larger set of redispatch interventions to restore network feasibility. It is therefore necessary to choose a value for $x$ that allows for enough headroom compared to $VOLL^{grid}$, allowing the model to restore network feasibility through redispatch if physically possible.

### Robustness of constants for disjunctive constraints

The disjunctive reformulation requires constants that bound the primal variables, dual variables, constraint slacks, and stationarity expressions. These constants must be sufficiently large to include all feasible solutions. At the same time, unnecessarily large values can weaken the MILP formulation. The constants derived in Table C.1 and Table C.1 are therefore tested by multiplying all of them by 100.

The test is performed for the proof-of-concept scenario with $\sigma = 0.5$. All six exploration runs are repeated with the enlarged constants. The resulting market and redispatch outcomes are identical to those obtained with the original bounds. Table 3.15 presents the main outcomes.

**Table 3.15:** Robustness test of the disjunctive constants for $\sigma = 0.5$.

| Configuration | Total capacity [MW] | Market cost [€] | Zonal procurement [MW] | Redispatch volume [MWh] | Average solve time [s] |
|---|---|---|---|---|---|
| Original constants | 298.21 | 12,545.82 | 15.71 / 152.50 / 130.00 | 112.47 | 0.027 |
| Constants x 100 | 298.21 | 12,545.82 | 15.71 / 152.50 / 130.00 | 112.47 | 0.013 |

The enlarged constants produce the same investment, capacity market procurement, energy market dispatch, prices, transfers, and redispatch outcome in every exploration run. This confirms that the original constants do not cut into the relevant solution space.

The average solving time is lower with the enlarged constants. However, both configurations solve within a few hundredths of a second. At this problem size, the difference is therefore considered numerical noise rather than evidence that larger constants improve computational performance. The original, tighter constants are retained following basic logic and experiences from literature (Gabriel & Leuthold, 2010).

### 3.5.5. Sensitivity to model configuration

The previous subsection tested whether selected extreme conditions and numerical parameters influence the model in the expected way, and whether their chosen values unintentionally restrict or distort the solution. This subsection instead changes the cost structure of the proof of concept. The model is run at $\sigma = 0.5$ with equal fixed costs, equal marginal costs, and both cost parameters being equal. The aim is to identify how both parameters influence capacity siting, energy market dispatch, and redispatch.

**Table 3.16:** Sensitivity of capacity siting and redispatch to the cost configuration.

| Configuration | Distinct siting outcomes | Zone 1 capacity [MW] | Zone 2 capacity [MW] | Zone 3 capacity [MW] | Redispatch volume [MWh] |
|---|---|---|---|---|---|
| Baseline | 1 | 15.71 | 152.50 | 130.00 | 112.47 |
| Equal FC | 2 | 5.71–10.71 | 142.50–147.50 | 145.00 | 112.43 |
| Equal VC | 1 | 15.71 | 152.50 | 130.00 | 227.58 |
| Equal FC and VC | 6 | 5.71–15.71 | 142.50–157.50 | 130.00–145.00 | 287.50–333.14 |

Equal fixed costs introduce alternative capacity-siting outcomes. While the baseline produces the same siting in every run, two outcomes are found with equal fixed costs. Zone 3 is preferred in both because its generator earns more in the energy market and therefore requires a lower capacity price. Zones 1 and 2, however, have the same energy market profit and, with equal fixed costs, require the same capacity market revenue. The capacity demand agent is therefore indifferent to the MEC direction between them, which explains the ranges in zonal capacity shown in Table 3.16. This confirms that the PTDF-based objective can recover alternative market-equivalent siting outcomes. In this small network, the resulting shift has almost no effect on total redispatch.

Equal marginal costs do not introduce additional siting degeneracy because the fixed-cost differences still determine the required capacity market revenues and the MEC direction. They do, however, affect the operational layer. Several hourly dispatch patterns can satisfy demand at the same cost. Although these outcomes are equivalent for the energy market, they can create different nodal injections and therefore different redispatch requirements. In the proof of concept, capacity siting remains unchanged, while redispatch increases from 112.47 to 227.58 MWh. This is not the type of degeneracy the solution-space exploration aims to study.

When both fixed and marginal costs are equal, both effects occur together. All six runs produce different capacity-siting outcomes, and the capacity demand agent becomes indifferent to all MEC directions. At the same time, the energy market has multiple equal-cost dispatch outcomes with different consequences for redispatch. Redispatch therefore changes from one value in the baseline to a range of 287.50–333.14 MWh. This range cannot be attributed to capacity siting alone.

The test therefore separates two forms of degeneracy. Alternative capacity siting within a capacity market zone is intended and is explored through the PTDF-based objective. Arbitrary differences in the dispatch of equal-cost generators are not intended, because they add variation to redispatch that is unrelated to the capacity market design.

This issue is expected to be less pronounced in the case study. The larger system contains more legacy generators with different technologies and marginal costs, reducing the number of fully interchangeable dispatch options. Nevertheless, where equal-cost generators remain interchangeable, redispatch outcomes remain non-unique.

# 4

# Case study

This chapter applies the model developed in Chapter 3 to the Dutch electricity system. The main challenge is to represent the system with enough spatial and temporal detail for locational capacity siting and intra-zonal congestion to be meaningful, while keeping the model tractable across the many runs needed for the solution-space exploration.

Two case studies are constructed from the same underlying network and time series. They differ in the amount of legacy controllable generation that remains in the system. The first case removes most legacy controllable capacity and therefore gives the capacity mechanism substantial freedom to determine where new capacity is built. The second retains the existing gas fleet, meaning that a larger part of the spatial generation pattern is already fixed. Together, the cases show both the potential effect of a locational signal and how this effect changes when less of the capacity stock can still respond.

The chapter is divided into three sections. First, the scope and data sources are introduced. The retrieved data are then prepared by constructing the two generation cases, defining the capacity market zones, and reducing the full year to representative days. The final section presents the experimental design, cost assumptions, main run parameters, and implementation workflow.

## 4.1. Scope and data

Chapter 3 developed the model in generic form and verified its mechanics on a small proof-of-concept system. The purpose of the case study is to apply the same two-stage model at a scale where the system-level effects of locational capacity procurement can be observed. This requires a spatially resolved transmission network, nodal generation and demand, and time series for renewable availability. At the same time, the network and time horizon must remain small enough for the equilibrium problem to be solved repeatedly with different exploration objectives.

Public electricity data are often available only at national or bidding-zone level. This is sufficient for a copper-plate energy market representation, but not for the redispatch stage, which requires nodal injections and transmission constraints. The different data sources must also be spatially consistent. Demand, generators, renewable profiles, and transmission lines cannot be clustered independently without creating mismatches between them.

The case study therefore uses PyPSA-Eur (Hörsch et al., 2018). PyPSA-Eur combines several public data sources into a consistent representation of the European transmission network, generation fleet, renewable availability, and electricity demand. Its workflow can be configured by country, time window, temporal resolution, and number of network clusters. The resulting network is then exported and used as input for the model developed in this thesis. PyPSA-Eur is therefore used as a data and network-construction tool, not to optimize the capacity market scenarios.

Using PyPSA-Eur also carries its limitations into the case study. The underlying transmission data partly rely on approximations of line impedances, substation structures, and asset locations (Brown et al., n.d.). Since the PTDF matrix is derived from this network, the resulting line-loading patterns should not be interpreted as an exact representation of Dutch system operation. Demand and generation are also allocated to nodes through spatial approximations rather than actual connection points. This affects nodal injections, local residual demand, and ultimately both the zonal capacity requirements and redispatch outcomes. Renewable profiles and existing capacities contain similar approximations where plant-level information is incomplete. The results are therefore used to compare market designs under a consistent system representation, not as forecasts of individual Dutch grid constraints.

PyPSA-Eur does not provide the fixed investment costs needed for the investable generators in the required form. These are retrieved separately from the Global and National Energy Systems Techno-Economic database (GNESTE), which combines technology-cost data from several sources and allows filtering by technology, region, data type, and reference year (Hatton et al., 2024).

The Dutch transmission system is represented by a meshed network of 34 nodes and 40 transmission lines. Cross-border connections are excluded, so the system boundary covers only the Netherlands. The static network forms the basis for the redispatch model and for the definition of the capacity market zones in subsection 4.2.2. The input time horizon covers one year. Since using all hourly observations would make the repeated equilibrium runs computationally infeasible, the year is reduced to eight representative days as explained in subsection 4.2.3.

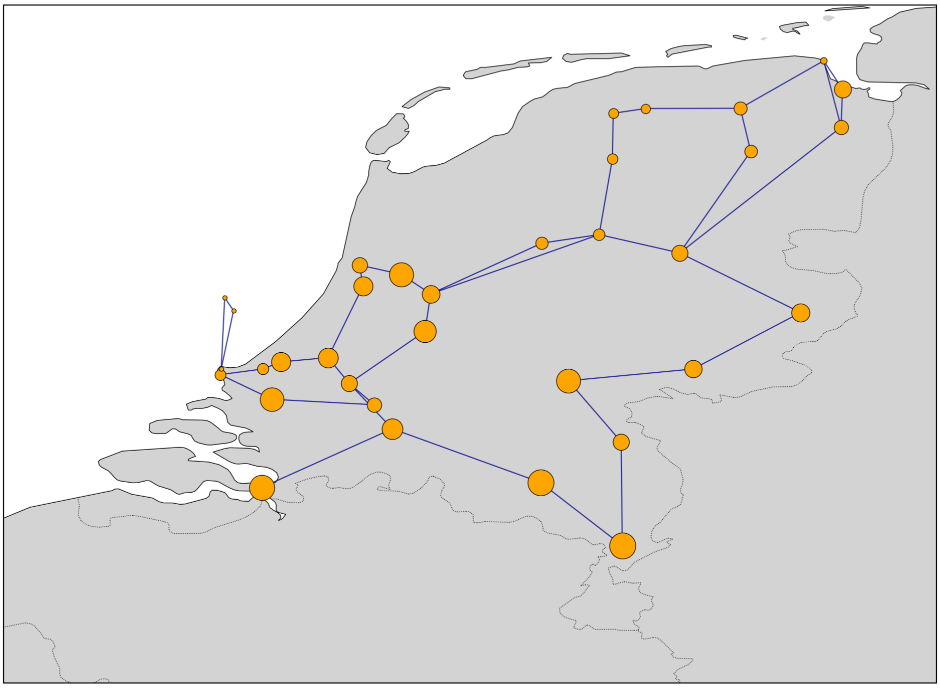

**Figure 4.1:** Dutch transmission grid with nodes sized by their demand share.

## 4.2. Data preparation

Several transformations are required before the retrieved data can enter the model. First, the generation fleet is divided into legacy and investable generators and used to construct two case studies with different amounts of fixed controllable capacity. Second, the transmission network is partitioned into capacity market zones. Finally, the hourly demand and renewable profiles are reduced to eight representative days.

### 4.2.1. Generator data and case-study cases

The generation fleet extracted from PyPSA-Eur contains nuclear, waste, biomass, gas, and coal generation, together with onshore wind, offshore wind, and solar capacity. Renewable generators remain exogenous in both case studies. Their installed capacities and hourly availability profiles are fixed, while controllable generators can participate in the energy and capacity markets.

Coal generation is removed in both cases. Dutch coal-fired power plants are scheduled to close by 2029 and are therefore not included in the future system represented here (Mendelevitch et al., 2024). The two cases differ in their treatment of the existing gas fleet.

**Case study 1: high-mobility capacity system.** In the first case, legacy gas plants are removed together with coal generation. New gas-fired capacity can instead be built at each onshore node. Most of the controllable capacity needed to meet the adequacy requirement must therefore be newly invested.

This setup gives the capacity mechanism substantial influence over the spatial distribution of controllable generation. It is deliberately stylized and should not be interpreted as a forecast in which the complete Dutch gas fleet disappears at once. Its purpose is to isolate the investment-location mechanism and show what a locational capacity market signal can do when a large share of the required capacity is still able to move between nodes.

**Case study 2: legacy-constrained capacity system.** The second case retains the existing gas-fired generation from PyPSA-Eur. Coal generation is still removed, and new gas capacity remains available at all eligible onshore nodes, but investment is only needed to cover the remaining capacity deficit.

A larger part of the spatial generation pattern is consequently fixed before the capacity market design is changed. Some capacity market zones may already contain a substantial amount of eligible legacy capacity, while others may still require new investment. This also creates the possibility that a zone can take on a larger capacity obligation through cross-zonal participation without requiring an equal increase in new construction.

The case is closer to a transition in which a locational signal is introduced into an existing generation system. Locational elements in capacity mechanisms mainly influence new investment (ENTSO-E, 2026). They cannot immediately relocate existing plants, only over a longer period, retirement and replacement decisions can be influenced. Comparing the two cases therefore shows whether the effect of the locational signal remains visible when it only acts on the incremental part of the capacity stock.

**Choice of investable technology.** Combined-cycle gas turbines are used as the only investable controllable technology. Waste generation has limited potential for large-scale expansion, while the future role of biomass remains uncertain (Wu & Pfenninger, 2023). New nuclear projects face long development periods, delays, and cost uncertainty, particularly in Europe (Gilbert et al., 2017). Gas-fired generation is therefore used as a stylized form of controllable capacity, also reflecting the possibility of switching to lower-carbon fuels in the future (IEA, 2021).

Storage, demand response, and other flexible resources could also participate in a capacity mechanism, but are excluded to keep the investment decision traceable. The consequences of this choice are discussed in Chapter 6.

The fixed cost of the investable gas plants is derived from GNESTE. Data for capital costs, fixed operation and maintenance costs, and technical lifetime are selected for gas-fired power plants in the EU with 2030 as the reference year. Annualized capital costs are approximated by dividing capital costs by lifetime and adding fixed operation and maintenance costs. This gives a base fixed cost of 53,935.52 €/MW/year.

### 4.2.2. Capacity market zone definition

In implemented locational capacity mechanisms, constrained areas are normally identified through detailed reliability and deliverability studies. Such studies test how much capacity can be imported into an area during system stress. Applying the same approach here would create a circular dependency. The location of new generators affects congestion and deliverability, while their location is itself determined by the capacity market zones. Defining the zones from one optimized investment outcome would therefore make the later comparison dependent on that initial outcome.

The zones are instead derived from the static transmission network. The aim is to group nodes that have a similar effect on transmission flows. This keeps the zone definition independent of both generation cases and all later investment outcomes.

The PTDF matrix provides the basis for the clustering. Each column describes how an injection at one node affects the flows on all transmission lines. Nodes with similar PTDF columns therefore have a similar effect on the network and are suitable candidates for the same capacity market zone (Kang et al., 2013). The Euclidean distance between the PTDF columns is used as a measure of electrical distance.

Agglomerative hierarchical clustering with Ward linkage is applied to these distances (Blachnik et al., 2021). The method first treats every node as its own cluster and then combines the closest clusters step by step. An advantage is that the number of final zones does not have to be fixed before the clustering is performed. Different partitions can instead be assessed from the resulting dendrogram. The clustering is implemented in Python using SciPy (Virtanen et al., 2020).

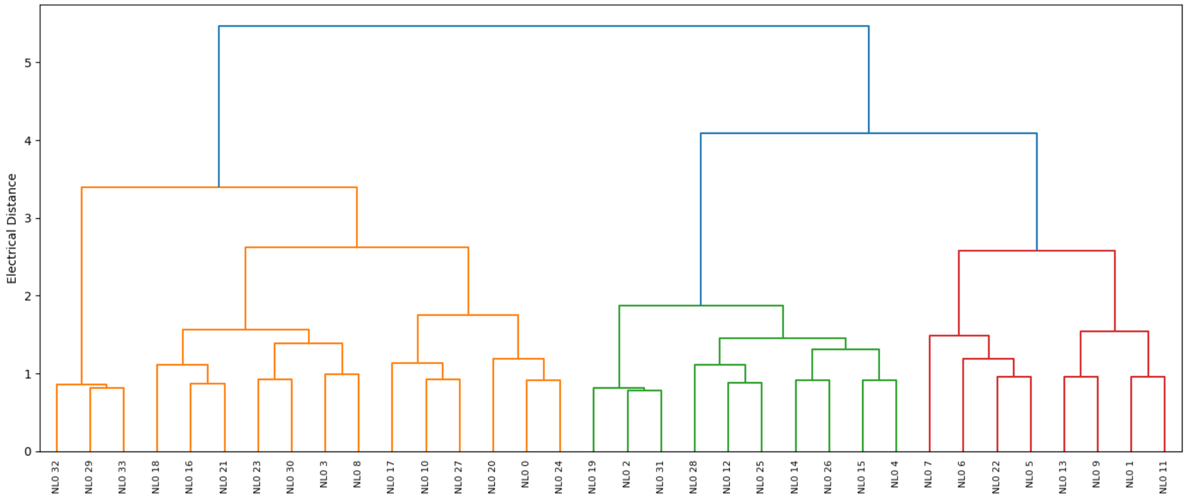


**Figure 4.2:** Dendrogram for the partition of the Dutch electricity network.

The dendrogram in Figure 4.2 supports a partition into three main clusters. A four-zone partition could also be obtained by separating part of the orange cluster. However, two of the three nodes in the resulting small zone would be offshore nodes with almost no demand and no controllable generation. The remaining onshore node would then provide nearly all eligible local capacity. Very small capacity market zones can create market-power concerns and would also make the comparison less informative, even though strategic bidding is not explicitly modeled here. The three-zone partition is therefore used.

The resulting zones are shown in Figure 4.3. Zone 1 (yellow) covers the Randstad and contains the largest concentration of demand and economic activity. Zone 2 (green) covers the northern part of the network and is characterized by its offshore wind connections, while Zone 3 (red) contains the remainder of the network.

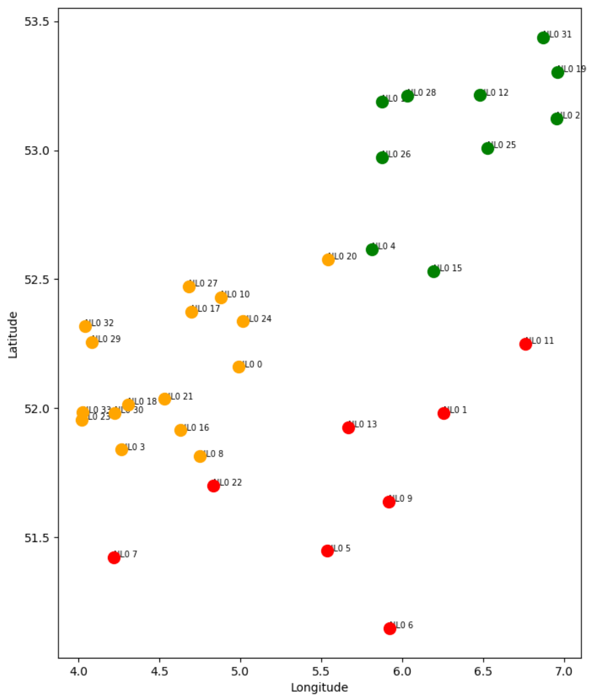


**Figure 4.3:** Nodes Colored according to their capacity market zone.

The maximum entry capacity between two zones is derived from the transmission lines crossing their shared boundary. For each pair of zones (a) and (b), the model sums the nominal capacities of all lines with one endpoint in zone (a) and the other in zone (b):

$\sum_{l\in L:\ n_l^0\in a,;n_l^1\in b \text{ or } n_l^0\in b,;n_l^1\in a} F_l^{\max}$.

In the clustered Dutch network, each pair of capacity market zones is connected by one transmission line. The resulting MEC is therefore equal to the capacity of that line, as shown in Table 3.13.

**Table 4.1:** Transmission lines connecting the capacity market zones and the resulting maximum entry capacities.

| Line index | Zone pair | Connecting buses | Line capacity [MW] | $MEC_{a,b}$ [MW] |
|---|---|---|---|---|
| 20 | 1–2 | NL0 20 – NL0 4 | 2,377.34 | 2,377.34 |
| 9 | 1–3 | NL0 16 – NL0 22 | 2,377.34 | 2,377.34 |
| 36 | 2–3 | NL0 11 – NL0 15 | 2,377.34 | 2,377.34 |

In the capacity market model, the maximum reallocation of capacity obligations between two zones is limited to $\sigma MEC_{a,b}$. At $\sigma = 0$, no obligation can be shifted between zones, while at $\sigma = 1$, the full pairwise MEC can be used.

The MEC remains a simplified, static approximation of cross-zonal deliverability. Summing the capacities of the directly connecting lines does not account for how a transfer is distributed across the full meshed network. It also does not guarantee that transfers between several zone pairs can be delivered simultaneously without creating congestion elsewhere in the system.

### 4.2.3. Representative days

The hourly input year is reduced to eight representative days using the Julia package RepresentativePeriodsFinder.jl (KU Leuven Energy Systems Integration and Modeling group, 2023). The package applies an optimization-based representative-period method following Poncelet et al. (2016).

Including aggregate load, nodal load, and all nodal renewable profiles directly in the selection problem would add substantial computational complexity. In the PyPSA-Eur data, however, each node's demand remains a constant share of total demand over time. The representative-day selection therefore uses aggregate load together with the nodal capacity-factor profiles for solar, onshore wind, and offshore wind. Nodal demand is reconstructed afterwards by multiplying aggregate demand in each selected hour by the fixed nodal demand shares.

The eight selected representative periods and their weights are displayed in Table 4.2. The sum of all weights equals 365, the eight periods therefore cover a whole year.

**Table 4.2:** Selected Decision Periods and Weights

| Period | Weight | Selected |
|---:|---:|:---:|
| 1 | 63.20 | True |
| 151 | 29.46 | True |
| 196 | 45.84 | True |
| 229 | 28.49 | True |
| 249 | 54.64 | True |
| 263 | 26.15 | True |
| 270 | 54.31 | True |
| 348 | 62.91 | True |

Figure 4.4 compares the duration curves of the original time series with those reconstructed from the representative days. The main distributions are preserved reasonably well, particularly for wind generation. Some extremes are nevertheless lost, most visibly in the load and solar profiles. This is an expected consequence of representing a full year through a limited number of days. It is important for the later interpretation because both capacity requirements and congestion outcomes can be driven by combinations of high demand and low renewable production that occur only rarely.

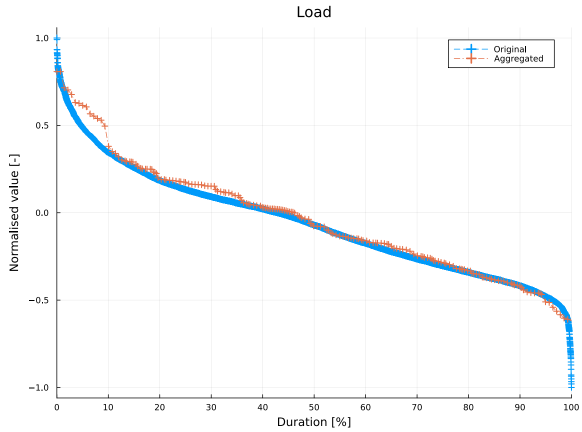


‘‘‘ **(a)** Load

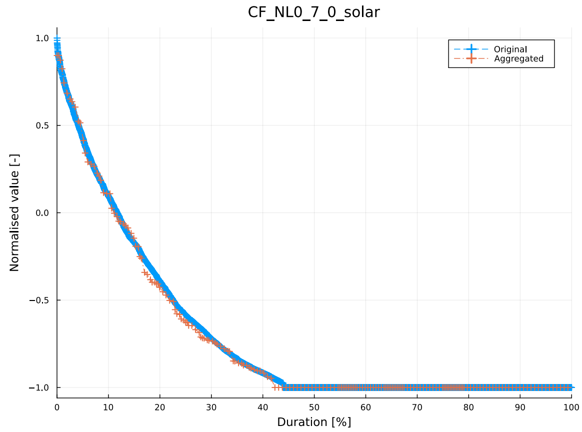


**(b)** Solar

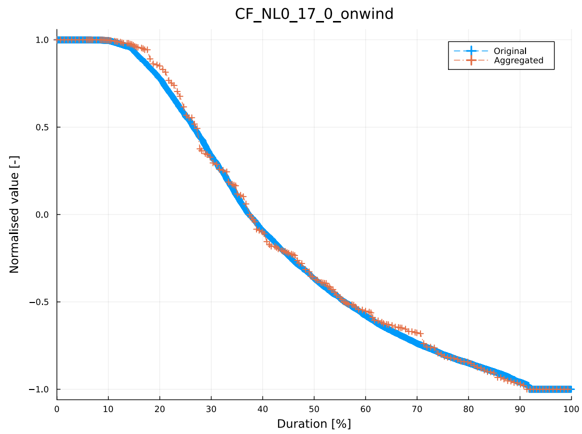


**(c)** Onshore wind

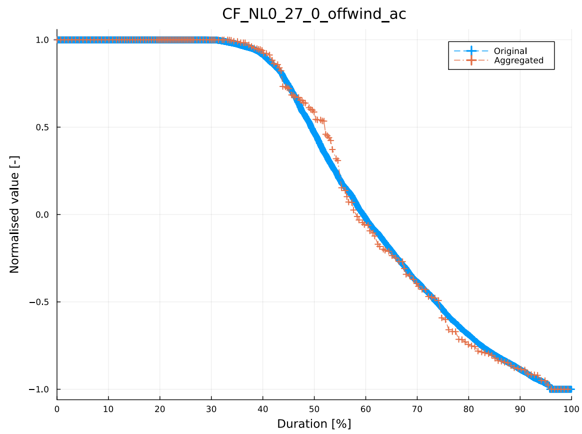


**(d)** Offshore wind

**Figure 4.4:** Comparison of the original and representative-period duration curves for load and selected renewable capacity-factor profiles.
‘‘‘

# 4.3. Experimental design and model implementation

The previous section prepared the network, generator, and time-series data. This section combines them with the model from Chapter 3. The experimental design has two dimensions: the amount of legacy controllable capacity and the spatial structure of the capacity mechanism. The cost configuration is then introduced, followed by the main run parameters and implementation workflow.

## 4.3.1. Scenarios

The two generation cases are each evaluated under the same set of capacity market designs. Within one generation case, the network, demand, renewable availability, generator costs, and all other parameters remain unchanged. Differences between the market-design scenarios can therefore be attributed to the locational structure of the capacity mechanism and the level of cross-zonal participation.

The country-wide capacity market, denoted by (z1), is the non-locational benchmark. A single capacity requirement is calculated from the Dutch system-wide peak residual load. All generators participate in the same capacity market and receive one national capacity price. The mechanism therefore ensures aggregate resource adequacy but does not require capacity to be located in a particular part of the network.

The split capacity market, denoted by (z3), introduces the locational signal. The Netherlands is divided into the three zones from subsection 4.2.2, and each zone receives a capacity requirement based on its own peak residual load. Since the zonal peaks do not necessarily occur at the same time, the sum of the three requirements can exceed the country-wide requirement. The split design may therefore procure more capacity and can require investment in zones where capacity is more expensive.

Cross-zonal participation is varied only within the split design. A signed transfer reallocates capacity obligations between neighboring zones, bounded by the maximum entry capacity multiplied by $\sigma$. The parameter takes the values

$\sigma \in \{0, 0.25, 0.50, 0.75, 1.00\}$.

At $\sigma = 1$, obligations can be transferred up to the full MEC.

The central comparison of the thesis is between (z1) and (z3): whether or not the capacity mechanism contains a locational signal. The variation of $\sigma$ is a secondary comparison within the locational design. It shows how cross-zonal participation modifies the cost and congestion effects after the signal has been introduced.

Each generation case contains six capacity market designs: the country-wide benchmark and five split designs. This results in twelve case-design combinations. For each one, the PTDF-based exploration is carried out in both directions for every transmission line. With 40 lines, this gives 80 exploration runs per design and 960 first-stage runs across the complete experiment.

Each exploration run returns a capacity siting that satisfies the same energy- and capacity market equilibrium conditions but is pushed in a different network direction. The resulting market outcome is then passed to the redispatch model. The observed minimum and maximum redispatch outcomes across the 80 runs form the explored range for that design.

### 4.3.2. Cost parameters

The proof of concept showed that some cost heterogeneity is necessary for interpretable dispatch and investment outcomes. Marginal-cost heterogeneity determines the energy market merit order. If several controllable generators have exactly the same marginal cost, multiple dispatch outcomes can clear the market at the same cost. Redispatch would then partly reflect solver tie-breaking rather than an economically interpretable dispatch order. The legacy fleet already contains several technologies and fuels and therefore provides a spread of marginal costs. The investable gas units use the same underlying technology assumptions in both generation cases.

Fixed costs serve a different role. If every investable generator had a unique fixed cost, investment would be tied to a narrow set of nodes and little siting multiplicity would remain for the exploration objective. If all nodes had identical fixed costs, the different capacity market zones would also have no economic distinction. Fixed costs are therefore heterogeneous between zones but identical within each zone. The zonal difference gives the capacity mechanism an economic reason to favor one zone over another, while equality within a zone preserves the nodal multiplicity that the PTDF objectives explore.

The starting point is the GNESTE-derived EU average of 53,935.52 €/MW/year. A symmetric adjustment of 10% is applied. Zone 1, covering the Randstad, receives the highest fixed cost. Scarce land, higher economic activity, and more difficult siting conditions are represented through an increase to 59,329.07 €/MW/year. Zone 2 receives the lowest fixed cost, reflecting the historical concentration of gas infrastructure in the north, and is set to 48,541.97 €/MW/year. Zone 3 retains the base value of 53,935.52 €/MW/year. These differences are stylized and are not intended as estimates of actual node-specific investment costs. They create a transparent zonal cost ordering through which the capacity market design can affect procurement and siting.

Energy market load shedding and grid-related load shedding are valued separately. $VOLL^{em}$ acts as the energy market price cap. Due to the capacity market implemented at least procuring enough capacity to cover peak residual load, generation is always able to cover demand. Thus, energy prices are always set by the marginal generator, not by demand. Even though a realistic price cap is much higher, $VOLL^{em}$ is set to 100 €/MWh for the model. This does not influence outcomes, 100 €/MWh is higher than variable costs of all generators. But due to $VOLL^{em}$ being present in many bounds for the disjunctive constraints (Table C.2), the lower value allows for quicker solving times. Therefore the value $VOLL^{em}$ is not to be read as an economic parameter, but a bound for quicker solving.

Grid-related load shedding occurs only in the redispatch stage when the market dispatch cannot be made network-feasible through available upward and downward redispatch. It is penalized at $VOLL^{grid}$ = 69,000 €/MWh, following the definition from Ecorys and SEO Economic Research (2022). As $VOLL$ is not paid to any party, but represents lost economic activity, it is an assumption derived from economic analysis rather than an observed price. Since this assumption strongly affects the monetary comparison between designs, its influence is tested separately in the results. A mark-up of $x = 75$ €/MWh is added to both upward and downward redispatch actions. The mark-up prevents cost-neutral redispatch cycles and makes unnecessary simultaneous upward and downward adjustments unattractive.

### 4.3.3. Model implementation

The case study combines preprocessing in Python with representative-period selection and optimization in Julia, as summarized in Figure 4.5. PyPSA-Eur is configured and processed in Python. The same environment is used to classify the generators, construct the PTDF matrix, and cluster the network into capacity market zones. The representative days are selected in Julia. The equilibrium and redispatch models are implemented in JuMP and solved with Gurobi (Gurobi Optimization, LLC, 2024; Lubin et al., 2023).

A fresh first-stage MILP is built for every exploration direction. This prevents information from a previous objective from fixing or unintentionally carrying over the earlier siting outcome. The only difference between the 80 runs of one design is the PTDF weight vector used in the exploration objective. After a feasible first-stage incumbent is obtained, the energy market dispatch and installed capacities are fixed and passed to the second-stage redispatch problem. The redispatch problem is linear and generally solves within seconds.

The standard first-stage runs use a time limit of 220 seconds and a target MIP gap of 0.01. Some PTDF directions are consistently harder to close. The repeatedly difficult directions are rerun with a time limit of 1,500 seconds, using the previous incumbent as a MIP start. This does not change the equilibrium conditions or the exploration objective, but gives the solver more time and a feasible starting point.

All runs returning a feasible incumbent are included in the results, irrespective of the remaining optimality gap. The gap refers to the PTDF-based exploration objective, not to the validity of the market equilibrium. A remaining gap therefore means that a more extreme siting may exist in the same exploration direction. It does not mean that the returned siting violates the energy market, capacity market, or investment conditions. The reported result ranges are consequently observed ranges across the explored equilibria rather than proven global bounds of the complete equilibrium set.

The main case-study and solver parameters are summarized in Table 4.3.

**Table 4.3:** Main parameters of the case-study runs.

| Parameter | Value | Unit / remark |
|---|---|---|
| Geographical scope | Netherlands | – |
| Network resolution | 34 nodes, 40 transmission lines | – |
| Cross-border connections | Excluded | – |
| Input time horizon | One year | – |
| Temporal representation | 8 representative days, 192 hourly time steps | weighted to one year |
| Generation cases | High-mobility; legacy-constrained | – |
| Investable technology | CCGT at each eligible onshore node | – |
| Capacity market designs | Country-wide (z1); three-zone (z3) | – |
| Cross-zonal participation | $\sigma = 0, 0.25, 0.50, 0.75, 1.00$ | (z3) only |
| Maximum entry capacity | 2,377.35 | MW per zone pair |
| Fixed cost, Zone 1 | 59,329.07 | €/MW/year |
| Fixed cost, Zone 2 | 48,541.97 | €/MW/year |
| Fixed cost, Zone 3 | 53,935.52 | €/MW/year |
| Energy market value of lost load $VOLL^{em}$ | 100 | €/MWh |
| Grid-related value of lost load $VOLL^{grid}$ | 69,000 | €/MWh |
| Redispatch mark-up (x) | 75 | €/MWh |
| Exploration runs | 80 per design | 2 per line |
| First-stage target MIP gap | 0.01 | 1% |
| Standard first-stage time limit | 220 | seconds |
| Selected-rerun time limit | 1,500 | seconds |
| First-stage feasibility tolerance | $10^{-3}$ | – |
| Redispatch feasibility tolerance | $10^{-4}$ | – |
| Solver | Gurobi | – |

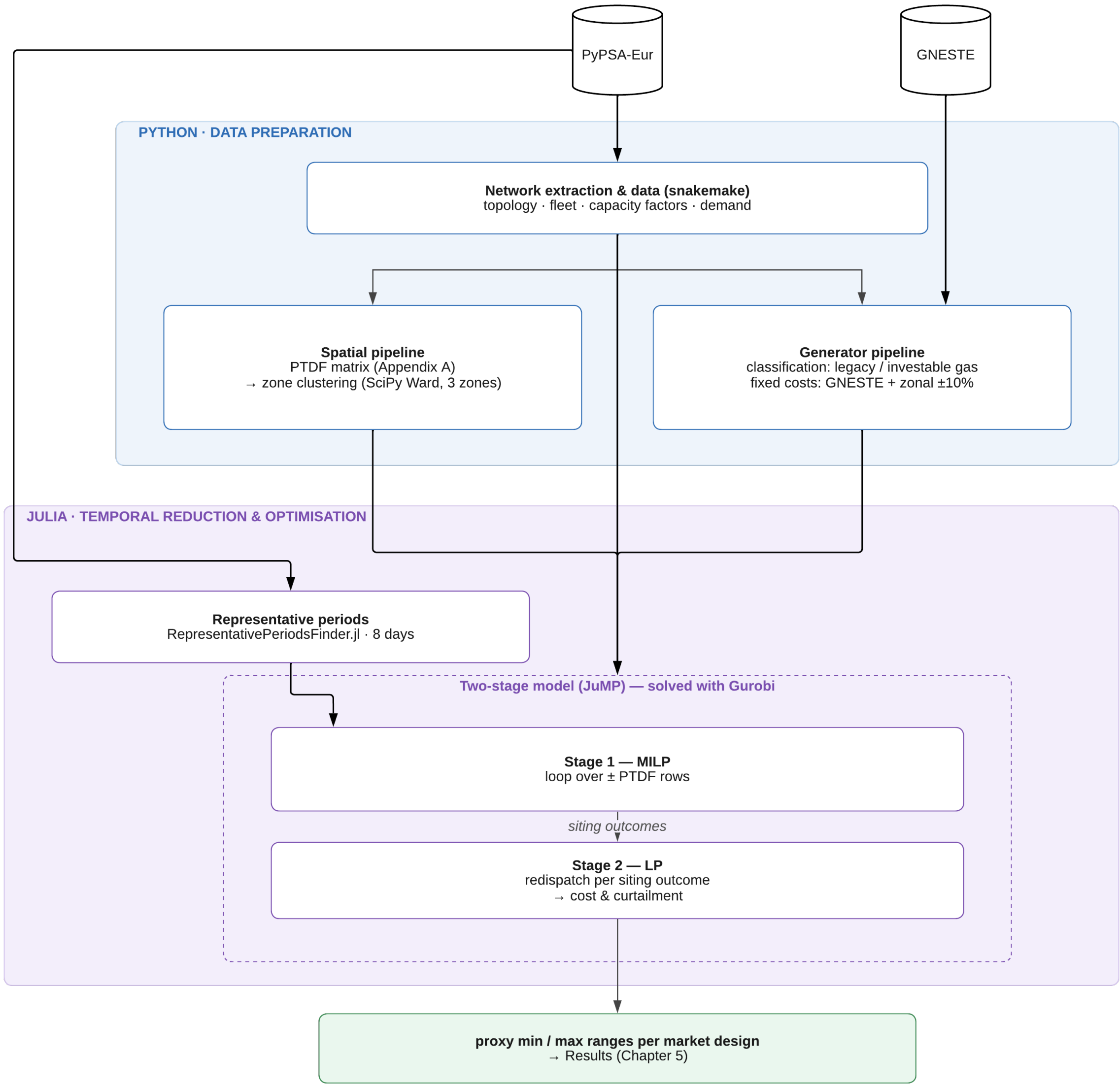


**Figure 4.5:** Workflow of the case-study implementation.

## 4.4. Comparison of solving performance between solution methods

At case study scale the question is which method produces the redispatch range within a usable time. This section reports two benchmarks under identical conditions (same machine, same solver, NonConvex enabled for the strong-duality methods, primal-dual constraints receive bounds K from disjunctive constraints).

### 4.4.1. Comparison of all three methods

At proof-of-concept scale all three methods solve in under a second. At case study scale they do not. Table 4.4 reports the three methods on a single exploration weight with a 3 600 s limit. The full primal-dual reaches the time limit with no feasible incumbent, for both the maximizing and the minimizing objective. The sequential primal-dual also returns no incumbent: none of its weights solved. The sequential MILP returns a usable siting, and the redispatch on it is then solved in 0.42 s, giving a redispatch cost of $3.26 \cdot 10^8$.

**Table 4.4:** Solving performance of the three methods on the case study instance, single exploration weight, 3 600 s limit. The two strong-duality methods return no feasible solution. The sequential MILP returns a usable siting and its redispatch cost.

| Method | Status | Time [s] | Redispatch cost | Bilinear terms | Binaries |
|---|---|---|---|---|---|
| Full primal-dual (max) | no incumbent | 3 600 | — | 951 902 | 0 |
| Full primal-dual (min) | no incumbent | 3 600 | — | 951 902 | 0 |
| Sequential primal-dual | no incumbent | 3 600 | — | 56 442 | 0 |
| Sequential MILP | solved | 3 601 | $3.26 \cdot 10^8$ | 0 | 44 276 |

The bilinear term count in the last columns shows why. The full primal-dual carries 951 902 bilinear terms, the dense PTDF coupling of the embedded redispatch. The sequential split removes the network coupling and brings this down to 56 442, but the price-times-quantity terms of the market clearing remain, and 56 442 is still enough to leave the problem unsolved at 3 600 s. The sequential MILP carries no bilinear terms. The disjunctive reformulation replaces them with 44 276 binary variables, which keeps the problem linear. On this weight the sequential MILP also used most of the time budget, so it is not fast here either. The difference is that it returns a usable result while the two strong-duality methods return nothing, and on most exploration directions it is far faster, as the next benchmark shows.

### 4.4.2. Comparison of the two sequential models

The comparison above leaves one question open. The sequential primal-dual returns no incumbent, but this could depend on the exploration direction. To check this, both sequential methods are run on the same set of PTDF-row directions, chosen across the range of row density. The density of a PTDF row is measured by its $L_1$ norm, $\sum_n |PTDF_{\ell,n}|$, which is the same quantity that drives the bilinear coupling in the full primal-dual: a dense row couples many nodes to one line. The directions span the most radial rows, where a line is influenced by one node, up to the densest rows, where it is influenced by the whole network ($n_{sig}$ counts the nodes with a significant entry in the row). Table 4.5 reports the result of the comparison, Table D.2 shows the density of all rows.

**Table 4.5:** The two sequential methods across PTDF-row directions, ordered by row density. The sequential MILP solves the radial directions to optimality in seconds and reaches the time limit with a gap on the dense ones. The sequential primal-dual returns no incumbent.

| Line | $L_1$ | $n_{sig}$ | Dir | Sequential MILP | | Sequential PD |
|---|---|---|---|---|---|---|
| | | | | time [s] | gap | |
| 29 | 0.82 | 2 | $+$ | 2.8 | $0\%$ | — |
| 29 | 0.82 | 2 | $-$ | 2.7 | $0\%$ | — |
| 32 | 0.92 | 2 | $+$ | 3.1 | $0\%$ | — |
| 32 | 0.92 | 2 | $-$ | 2.5 | $0\%$ | — |
| 23 | 1.00 | 1 | $+$ | 2.8 | $0\%$ | no incumbent (1 081 s)$^\dagger$ |
| 23 | 1.00 | 1 | $-$ | 2.8 | $0\%$ | no incumbent (3 721 s)$^\dagger$ |
| 11 | 3.95 | 10 | $+$ | 220 | $14\%$ | —$^\ddagger$ |
| 11 | 3.95 | 10 | $-$ | 220 | $124\%$ | —$^\ddagger$ |
| 1 | 14.76 | 33 | $+$ | 220 | $21\%$ | —$^\ddagger$ |
| 1 | 14.76 | 33 | $-$ | 220 | $107\%$ | —$^\ddagger$ |
| 2 | 18.24 | 33 | $+$ | 220 | $38\%$ | —$^\ddagger$ |
| 2 | 18.24 | 33 | $-$ | 220 | $77\%$ | —$^\ddagger$ |

$^\dagger$ Run with a 3 600 s limit. $^\ddagger$ The sequential primal-dual was run on the most radial direction (line 23) only. As it returned no incumbent there, and the denser rows only add coupling, they were not run.

The sequential primal-dual returns no feasible incumbent on the most radial direction, where a single node is coupled to the line, even with a 3 600 s limit. Since this is the structurally easiest direction and the formulation does not solve even there, it does not solve on the denser directions, which only add coupling. The intractability of the sequential primal-dual is therefore a property of the formulation, not of a particular direction.

The sequential MILP shows a sharp split. On the radial directions, where the line is coupled to one or two nodes, it solves to optimality in around 3 s. On the denser directions, where ten or more nodes are coupled, it reaches the time limit with a remaining gap. The split sits between these two groups. Difficulty in the sequential MILP therefore grows with the density of the exploration direction, the same density that makes the strong-duality methods intractable.

Two points are needed for an honest reading of this result. First, the gap differs by direction sign: pushing capacity away from a line, the negative weight, is consistently harder to close than pushing it towards the line. Density is the main driver but it is not the only one. Second, the gap is measured on the exploration objective, which has no economic meaning. A run that stops with a gap still returns a valid market equilibrium, since the market clearing is a constraint and not part of the gap. What is lost on the dense directions is the guarantee of having reached the most extreme siting, not the validity of the siting. The redispatch range from these directions is therefore sampled, not proven.

# 5 Results

This chapter presents the results of the Dutch case study. The central comparison is between the country-wide capacity mechanism without a locational signal and the split capacity mechanism with a locational signal. This comparison provides the main empirical basis for answering SQ3. The different values of $\sigma$ are only compared within the split design. They represent different levels of cross-zonal participation and therefore change how strongly the zonal requirements translate into a locational signal. Both designs are evaluated in two case studies. In the first, most controllable capacity has to be newly built, while in the second the existing gas fleet remains in place and limits how much of the capacity stock can still respond.

The chapter first compares the initial capacity position of both case studies before turning to the effect of introducing a locational signal. Afterwards, the role of cross-zonal participation is assessed within the split design. The following sections examine the network mechanisms behind the congestion outcomes and compare capacity market expenditure with the monetary consequences of congestion. The chapter ends by bringing the results of both case studies together. A short account of computational performance is provided first to clarify how the reported outcome ranges should be interpreted.

## 5.1. Computational performance and interpretation of the exploration set

Each capacity market design is solved for 80 PTDF-based exploration directions, consisting of one positive and one negative direction for each of the 40 transmission lines. Across the six designs and two case studies, this results in 960 first-stage runs. All runs returned a feasible incumbent, after which the corresponding redispatch problem could be solved to optimality. All 80 outcomes per scenario are therefore retained in the analysis, including runs that reached the time limit before achieving the requested relative optimality gap of $0.01$.

The reported gaps refer to the PTDF-based exploration objective. This objective has no economic interpretation and may take values close to zero. Very large relative gaps therefore do not imply an equally large uncertainty in capacity market expenditure, investment, or redispatch. They indicate that the solver has not established how close the selected siting outcome is to the optimum of that particular exploration direction.

The two case studies required different computational procedures. Case Study 1 was solved with a time limit of 220 seconds per exploration direction. For Case Study 2, a weight-independent LP was first solved for each design and value of $\sigma$. Its primal solution was used to provide starting values for the complete MILP, which was then solved with an initial time limit of 120 seconds. Runs 29 and 46 were subsequently rerun with a limit of 1,500 seconds. The extended rerun improved run 46 in several scenarios, while run 29 remained difficult.

The warm start does not change the feasible set or equilibrium conditions. It may, however, influence which incumbent is found before the time limit is reached. Together with the remaining solution gaps, this means that the reported minimum–maximum ranges represent the lowest and highest outcomes found by the exploration procedure, not complete bounds on the equilibrium set.

Detailed solving times, gaps, difficult exploration directions, and the relationship between PTDF structure and computational performance are reported in Appendix D. No run is excluded from the subsequent results based on its solving gap.

## 5.2. Starting capacity position and need for new investment

Before comparing the capacity market designs, it is useful to establish how much new capacity can still respond to the locational signal. The residual capacity requirement is identical in both case studies because demand and renewable generation remain unchanged. The difference lies in the amount and location of eligible legacy capacity.

**Table 5.1:** Capacity balance before new investment. A positive balance indicates a legacy surplus, while a negative value indicates a deficit. All values are in MW.

| Case study | Level | Requirement | Legacy contribution | Surplus or deficit | New capacity needed |
|---|---|---|---|---|---|
| Case Study 1 | System | $16,722.7$ | $2,088.2$ | $-14,634.5$ | $14,634.5$ |
| Case Study 1 | Zone 1 | $7,227.7$ | $626.2$ | $-6,601.5$ | $6,601.5$ |
| Case Study 1 | Zone 2 | $2,560.3$ | $139.0$ | $-2,421.3$ | $2,421.3$ |
| Case Study 1 | Zone 3 | $7,001.1$ | $1,323.0$ | $-5,678.1$ | $5,678.1$ |
| Case Study 2 | System | $16,722.7$ | $16,286.7$ | $-436.0$ | $436.0$ |
| Case Study 2 | Zone 1 | $7,227.7$ | $7,266.2$ | $38.5$ | $0.0$ |
| Case Study 2 | Zone 2 | $2,560.3$ | $4,419.5$ | $1,859.2$ | $0.0$ |
| Case Study 2 | Zone 3 | $7,001.1$ | $4,601.0$ | $-2,400.1$ | $2,400.1$ |

In Case Study 1, 14,634.5 MW, or 87.5% of the system-wide requirement, has to be supplied by new capacity. All three zones also start with a deficit. Under strict local procurement, the combined need for new capacity is therefore 14,701.0 MW, slightly above the system-wide deficit because the zonal residual-demand peaks do not fully coincide. The capacity mechanism consequently has considerable freedom to influence where the controllable fleet is built.

Case Study 2 starts from a substantially different position. Legacy capacity already covers 97.4% of the system-wide requirement, leaving a system-level deficit of only 436.0 MW. However, this capacity is unevenly distributed. Zones 1 and 2 have legacy surpluses of 38.5 MW and 1,859.2 MW, while Zone 3 still lacks 2,400.1 MW. With strict local procurement, this deficit has to be filled within Zone 3. Cross-zonal participation can instead make use of the existing surpluses and reduce the need for additional investment. The locational signal therefore acts on most of the controllable fleet in Case Study 1, but only on the remaining marginal investment in Case Study 2.

## 5.3. Effect of introducing a locational capacity market signal

The central comparison is between the country-wide capacity mechanism and the split design at $\sigma = 0$. The country-wide design only enforces the system-wide capacity requirement. The split design additionally requires each zone to cover its own residual capacity requirement. Comparing these two designs therefore isolates the effect of introducing a locational capacity market signal before cross-zonal participation is allowed.

### 5.3.1. Capacity procurement

Table 5.2 compares the capacity requirement, accepted capacity, capacity prices, and capacity market expenditure. Capacity market expenditure includes payments to all accepted capacity, including legacy generators. It is therefore different from the fixed cost of newly built capacity.

**Table 5.2:** Capacity procurement, prices, and capacity market expenditure under the country-wide and split designs. Capacity prices are reported in €/MW and expenditure in million €.

| Case study | Design | Capacity requirement [MW] | Accepted capacity [MW] | System/Zone 1 price | Zone 2 price | Zone 3 price | Capacity market expenditure [million €] |
|---|---|---|---|---|---|---|---|
| Case Study 1 | Country-wide | 16,722.7 | 16,722.7 | 53,935.5 | – | – | 901.9 |
| Case Study 1 | Split | 16,789.2 | 16,789.2 | 59,329.1 | 48,542.0 | 53,935.5 | 930.7 |
| Case Study 2 | Country-wide | 16,722.7 | 16,722.7 | 4,559.1–5,472.6 | – | – | 76.2–91.5 |
| Case Study 2 | Split | 16,789.2 | 16,789.2–18,648.4 | 0.0 | 0.0 | 34,087.4 | 238.6 |

In Case Study 1, the country-wide design procures 16,722.7 MW. The three zonal requirements under the split design sum to 16,789.2 MW, which is 66.5 MW or 0.4% higher. This difference results from the zonal residual-demand peaks not occurring at exactly the same time. The split design therefore requires slightly more capacity even though the underlying demand and renewable generation remain unchanged.

Capacity market expenditure increases from €901.9 million to €930.7 million. Holding the capacity price at the country-wide level, the additional 66.5 MW would increase expenditure by only around €3.6 million. The remaining increase of approximately €25.2 million results from the different zonal clearing prices. The increase is therefore mainly a price effect rather than a volume effect.

New investment is needed in all three zones in Case Study 1. Consequently, all zonal capacity prices remain positive. Zone 1 has the highest price, while Zone 2 has the lowest. The split design therefore not only requires slightly more capacity, but also requires part of the capacity to be procured in a more expensive zone.

The starting position is different in Case Study 2. Under the country-wide design, the legacy fleet supplies 16,286.7 MW of the requirement, leaving only 436.0 MW to new investment. This results in a positive system-wide capacity price and capacity market expenditure between €76.2 million and €91.5 million across the explored equilibria.

Under the split design, legacy capacity is sufficient to meet the requirements of Zones 1 and 2. Their capacity prices are therefore zero. Zone 3 contains 4,601.0 MW of eligible legacy capacity against a requirement of 7,001.1 MW. The remaining 2,400.1 MW has to be supplied by new investment, resulting in a positive price of 34,087.4 €/MW in Zone 3.

The total capacity market expenditure is €238.6 million. Of this amount, approximately €81.8 million is paid to the 2,400.1 MW of new capacity, while approximately €156.8 million is paid to the 4,601.0 MW of accepted legacy capacity in Zone 3. Therefore, the zonal clearing price is also paid to existing capacity located in the deficient zone.

The zonal requirements sum to 16,789.2 MW, which remains the relevant procurement requirement under the split design. However, some explored equilibria report accepted capacity of up to 18,648.4 MW. This variation occurs entirely in Zone 2, where eligible legacy capacity exceeds the local requirement by 1,859.2 MW and the capacity price is zero.

Because the model imposes a minimum procurement requirement rather than an equality, the demand agent is indifferent between accepting only the required 2,560.3 MW and accepting the full 4,419.5 MW of available legacy capacity in Zone 2. The additional accepted capacity therefore does not represent an additional adequacy need. It also does not increase capacity market expenditure because it is accepted at a price of zero. For the comparison between designs, 16,789.2 MW is consequently treated as the relevant capacity requirement.

### 5.3.2. New capacity siting

The main effect of the locational signal is a shift in the zone in which new capacity is built. The zonal allocation under both designs is shown in Figure 5.1. The zones shown for the country-wide design do not represent separate capacity market zones, but the physical locations of the resulting investment mapped to the three-zone definition.

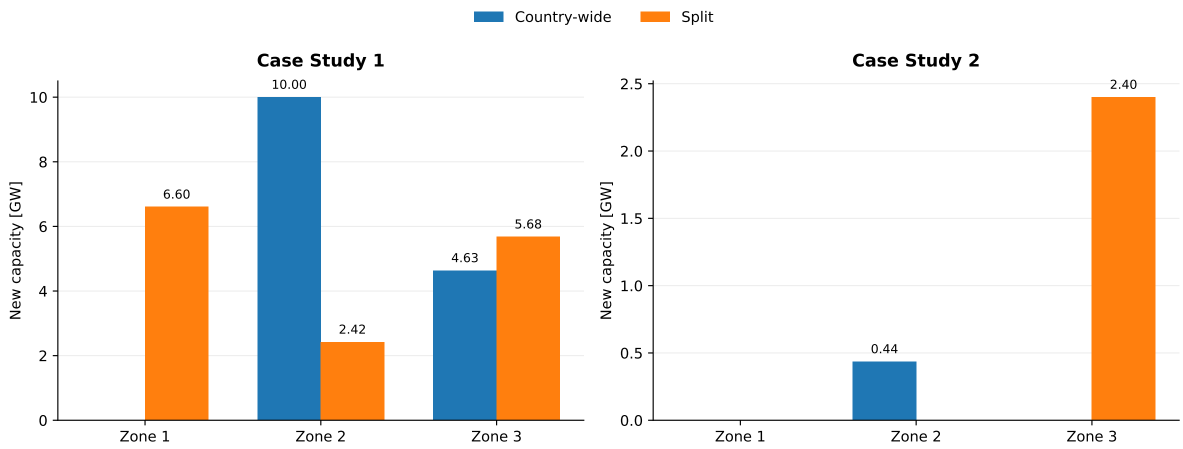


**Figure 5.1:** Zonal allocation of new capacity under the country-wide and split capacity market designs.

In Case Study 1, the country-wide design builds 10,000.0 MW in Zone 2 and 4,634.5 MW in Zone 3, while no new capacity is built in Zone 1. Since the capacity mechanism only enforces aggregate adequacy, it does not prevent investment from concentrating in the zones favoured by the energy market revenues and investment-cost assumptions.

The split design instead builds 6,601.5 MW in Zone 1, 2,421.3 MW in Zone 2, and 5,678.1 MW in Zone 3. Each zone therefore receives the new capacity needed to close its own capacity deficit. The main effect is not the additional 66.5 MW procured overall, but the relocation of a substantial part of the investment from Zone 2 towards Zone 1.

The same mechanism is visible in Case Study 2, although considerably less capacity remains available to respond. Under the country-wide design, the remaining 436.0 MW is built in Zone 2. Under the split design, Zone 3 has to close its local deficit and receives 2,400.1 MW of new capacity instead. The locational signal therefore directs the incremental investment towards the deficient zone, even though most of the controllable fleet is fixed in the legacy capacity.

The zonal investment totals remain effectively unchanged across the explored equilibria. The exact nodal distribution within the zones varies, but is not interpreted further here. The exploration objective has no economic interpretation, and the runs do not represent a probability distribution over possible siting outcomes. The relevant result for this comparison is therefore the shift in investment between zones rather than the detailed distribution within them.

### 5.3.3. Congestion outcomes

The change in capacity siting leads to a clear change in the ex-post congestion outcomes. Table 5.3 reports the observed minimum and maximum across the explored outcomes. These ranges describe the outcomes found by the exploration procedure and should not be interpreted as confidence intervals or probability-weighted distributions.

Redispatch volume includes both upward and downward redispatch. Grid-related load shedding is reported separately because it indicates that the available generation capacity cannot fully restore network feasibility.

**Table 5.3:** Observed congestion-outcome ranges under the country-wide and split designs. Volumes are reported in TWh. Redispatch cost excludes grid-related load-shedding costs.

| Case study | Design | Redispatch volume [TWh] | Upward redispatch [TWh] | Downward redispatch [TWh] | Grid-related load shedding [TWh] | Redispatch cost [million €] |
|---|---|---|---|---|---|---|
| Case Study 1 | Country-wide | 14.13–30.63 | 5.21–12.39 | 8.22–18.24 | 2.30–5.86 | −253.4–−109.0 |
| Case Study 1 | Split | 0.00–2.37 | 0.00–1.14 | 0.00–1.23 | 0.00–0.091 | −4.36–0.74 |
| Case Study 2 | Country-wide | 0.072–0.373 | 0.015–0.131 | 0.056–0.243 | 0.034–0.112 | −7.93–−2.62 |
| Case Study 2 | Split | 0.045–0.205 | 0.023–0.102 | 0.023–0.102 | 0.000 | 0.013–0.118 |

In Case Study 1, the country-wide design results in between 14.13 and 30.63 TWh of redispatch. Under the split design, the observed range falls to between zero and 2.37 TWh. The effect is therefore visible at both ends of the range. The maximum redispatch volume under the split design remains substantially below the minimum observed under the country-wide design.

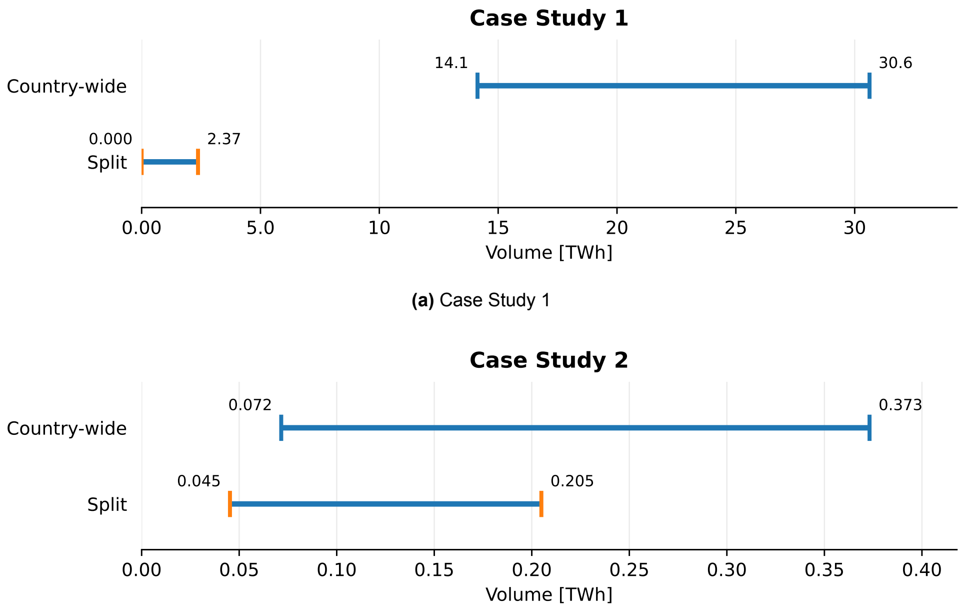


**(a)** Case Study 1

**(b)** Case Study 2

**Figure 5.2:** Observed redispatch-volume ranges under the country-wide and split capacity market designs.

The effect remains visible in Case Study 2, although the absolute redispatch volumes are much smaller. The country-wide design requires between 0.072 and 0.373 TWh of redispatch, compared to between 0.045 and 0.205 TWh under the split design. The two ranges overlap, meaning that the split design does not produce less redispatch in every comparison between the explored outcomes. Nevertheless, both the lower and upper ends of the observed range decrease.

The stronger result concerns grid-related load shedding. Every explored country-wide outcome in Case Study 1 contains between 2.30 and 5.86 TWh of grid-related load shedding. Under the split design, 50 of the 80 explored outcomes require none. The remaining outcomes reach a maximum of 0.091 TWh. The locational signal therefore does not eliminate grid-related load shedding in every explored siting outcome, but it strongly reduces both its occurrence and its maximum magnitude.

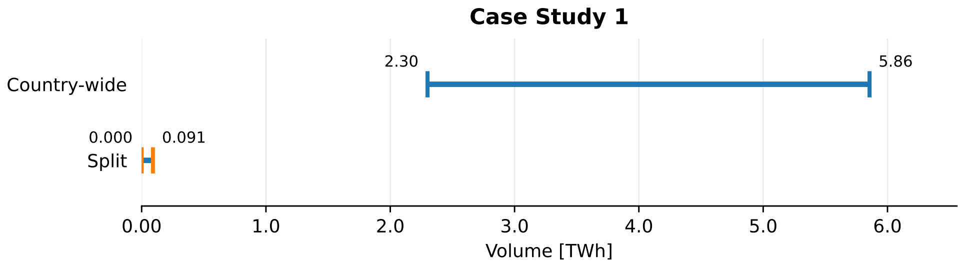


**(a)** Case Study 1

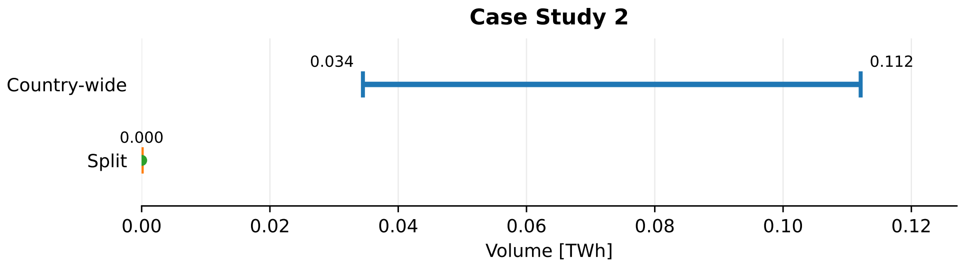


**(b)** Case Study 2

**Figure 5.3:** Observed grid-related load-shedding ranges under the country-wide and split capacity market designs.

In Case Study 2, all country-wide outcomes contain grid-related load shedding, ranging from 0.034 to 0.112 TWh. The split design eliminates it in all 80 explored outcomes. Although only the incremental investment can respond in this case study, directing this capacity towards Zone 3 is sufficient to restore network feasibility throughout the explored set.

A reduction in redispatch volume and a reduction in grid-related load shedding represent different effects. Lower redispatch means that fewer ex-post interventions are required. Lower grid-related load shedding means that sufficient controllable capacity is available in locations from which the network can be returned to a feasible operating point. The latter is therefore more directly connected to capacity deliverability and security of supply.

The redispatch-cost ranges in Table 5.3 exclude grid-related load-shedding costs. Negative redispatch costs occur when the avoided variable costs from downward redispatch exceed the additional costs of upward redispatch. They are therefore incomplete without looking at the costs for grid related load shedding.

Grid-related load-shedding costs are kept separate because they are mechanically determined by the assumed penalty and would otherwise dominate the comparison. At the modeled penalty, they amount to €158.7–404.0 billion under the country-wide design in Case Study 1, compared to €0–6.28 billion under the split design. In Case Study 2, they amount to €2.38–7.73 billion under the country-wide design and zero under the split design. The combined cost implications and their dependence on the assumed penalty are discussed separately in Section 5.6.

### 5.3.4. Interim conclusion on introducing a locational signal

Introducing separate zonal requirements changes where new capacity is built in both case studies. In Case Study 1, several gigawatts move from Zone 2 to Zone 1. Required procurement rises by 0.4% and capacity-market expenditure by roughly 3%, while grid-related load shedding falls from 2.30–5.86 TWh to at most 0.091 TWh. In Case Study 2, the remaining new capacity moves to the deficient Zone 3. Expenditure and new investment increase, the redispatch range falls, and grid-related load shedding disappears from all explored outcomes. The main observed effect is improved deliverability rather than lower redispatch.

## 5.4. How cross-zonal participation modifies the locational signal

Having established the effect of introducing a locational signal, this section examines how allowing neighboring capacity to contribute changes its strength and consequences. Cross-zonal participation is treated as a secondary design choice within the split capacity mechanism. At $\sigma = 0$, each zone remains locally responsible for its full requirement. As $\sigma$ increases, a larger share of this obligation can be covered by capacity located in another zone.

### 5.4.1. Zonal capacity obligations and transfers

Table 5.4 shows the resulting effective requirements. The sum of the three zonal requirements remains 16,789.2 MW for every value of $\sigma$. The transfer formulation is zero-sum: a reduction in the requirement of one zone is matched by an equal increase elsewhere. Cross-zonal participation therefore reallocates procurement obligations rather than reducing the total zonal requirement.

**Table 5.4:** Effective zonal capacity requirements under increasing cross-zonal participation. All values are in MW. Ranges indicate variation across the explored equilibria.

| Case study | $\sigma$ | Zone 1 | Zone 2 | Zone 3 | Total |
|---|---|---|---|---|---|
| Case Study 1 | 0.00 | 7,227.7 | 2,560.3 | 7,001.1 | 16,789.2 |
| Case Study 1 | 0.25 | 6,039.1 | 3,749.0 | 7,001.1 | 16,789.2 |
| Case Study 1 | 0.50 | 4,850.4 | 4,937.7 | 7,001.1 | 16,789.2 |
| Case Study 1 | 0.75 | 3,661.7 | 6,126.3 | 7,001.1 | 16,789.2 |
| Case Study 1 | 1.00 | 2,473.1 | 7,315.0 | 7,001.1 | 16,789.2 |
| Case Study 2 | 0.00 | 7,227.7 | 2,560.3 | 7,001.1 | 16,789.2 |
| Case Study 2 | 0.25 | 7,227.7–7,266.2 | 3,710.5–3,749.0 | 5,812.4 | 16,789.2 |
| Case Study 2 | 0.50 | 7,266.2 | 4,899.2 | 4,623.8 | 16,789.2 |
| Case Study 2 | 0.75 | 7,266.2 | 4,922.0 | 4,601.0 | 16,789.2 |
| Case Study 2 | 1.00 | 7,266.2 | 4,922.0 | 4,601.0 | 16,789.2 |

In Case Study 1, Zone 1 imports capacity contributions from the other zones. Its local procurement obligation consequently falls from 7,227.7 MW at $\sigma = 0$ to 2,473.1 MW at $\sigma = 1$. Zone 2 takes over the corresponding obligation, which increases from 2,560.3 MW to 7,315.0 MW. The net obligation of Zone 3 remains unchanged. At every positive value of $\sigma$, the available transfer envelope is fully used. The mechanism therefore shifts as much of the obligation as permitted from the more expensive Zone 1 towards Zone 2.

The system-wide capacity floor remains non-binding throughout. Its requirement is 16,722.7 MW, while the sum of the effective zonal requirements remains 66.5 MW higher. Allowing cross-zonal participation therefore does not remove the over-procurement caused by non-coincident zonal residual-demand peaks.

In Case Study 2, Zone 3 is the importing zone. Its effective requirement falls from 7,001.1 MW to 5,812.4 MW at $\sigma = 0.25$ and to 4,623.8 MW at $\sigma = 0.50$. At $\sigma = 0.75$, it reaches 4,601.0 MW, which is exactly equal to the eligible legacy capacity already available in the zone. The full initial deficit of 2,400.1 MW has then been transferred to Zones 1 and 2. Increasing $\sigma$ further does not change the effective obligations.

At $\sigma = 0.25$, the exact division of the exporting obligation between Zones 1 and 2 varies slightly. Both zones contain surplus legacy capacity and have a zero capacity price. The model is therefore indifferent between alternative allocations of the same total transfer. The economically relevant outcome is the fixed reduction of 1,188.7 MW in the requirement of Zone 3, rather than the precise division between the two exporting zones.

The distinction between required and accepted capacity remains important. The required procurement is 16,789.2 MW at every value of $\sigma$. At $\sigma = 0$ and $\sigma = 0.25$ in Case Study 2, the reported accepted capacity can exceed this value because additional legacy capacity is accepted in zero-price zones. This does not represent a higher adequacy requirement and does not increase capacity market expenditure. From $\sigma = 0.50$ onward, accepted capacity and required procurement coincide.

### 5.4.2. Capacity market cost

The reallocation of obligations affects capacity market expenditure through several channels. Procurement may move between zones with different prices, less new capacity may be required, and the identity of the marginal unit may change. Table 5.5 reports the zonal prices and expenditure.

**Table 5.5:** Zonal capacity prices and capacity market expenditure under increasing cross-zonal participation. Prices are reported in €/MW and expenditure in million €.

| Case study | $\sigma$ | Zone 1 price | Zone 2 price | Zone 3 price | Zone 1 expenditure | Zone 2 expenditure | Zone 3 expenditure | Total expenditure |
|---|---|---|---|---|---|---|---|---|
| Case Study 1 | 0.00 | 59,329.1 | 48,542.0 | 53,935.5 | 428.8 | 124.3 | 377.6 | 930.7 |
| Case Study 1 | 0.25 | 59,329.1 | 48,542.0 | 53,935.5 | 358.3 | 182.0 | 377.6 | 917.9 |
| Case Study 1 | 0.50 | 59,329.1 | 48,542.0 | 53,935.5 | 287.8 | 239.7 | 377.6 | 905.1 |
| Case Study 1 | 0.75 | 59,329.1 | 48,542.0 | 53,935.5 | 217.2 | 297.4 | 377.6 | 892.2 |
| Case Study 1 | 1.00 | 59,329.1 | 48,542.0 | 53,935.5 | 146.7 | 355.1 | 377.6 | 879.4 |
| Case Study 2 | 0.00 | 0.0 | 0.0 | 34,087.4 | 0.0 | 0.0 | 238.6 | 238.6 |
| Case Study 2 | 0.25 | 0.0 | 0.0 | 18,839.9 | 0.0 | 0.0 | 109.5 | 109.5 |
| Case Study 2 | 0.50 | 5,975.3 | 5,975.3 | 11,368.9 | 43.4 | 29.3 | 52.6 | 125.3 |
| Case Study 2 | 0.75 | 5,975.3 | 5,975.3 | 5,975.3 | 43.4 | 29.4 | 27.5 | 100.3 |
| Case Study 2 | 1.00 | 5,975.3 | 5,975.3 | 5,975.3 | 43.4 | 29.4 | 27.5 | 100.3 |

In Case Study 1, the zonal prices remain unchanged as $\sigma$ increases. Capacity market expenditure nevertheless falls from €930.7 million to €879.4 million. The reduction results from procurement moving from Zone 1, where the capacity price is highest, towards the cheaper Zone 2. Total required procurement and total new capacity remain unchanged. The cost reduction is therefore almost entirely a spatial reallocation effect.

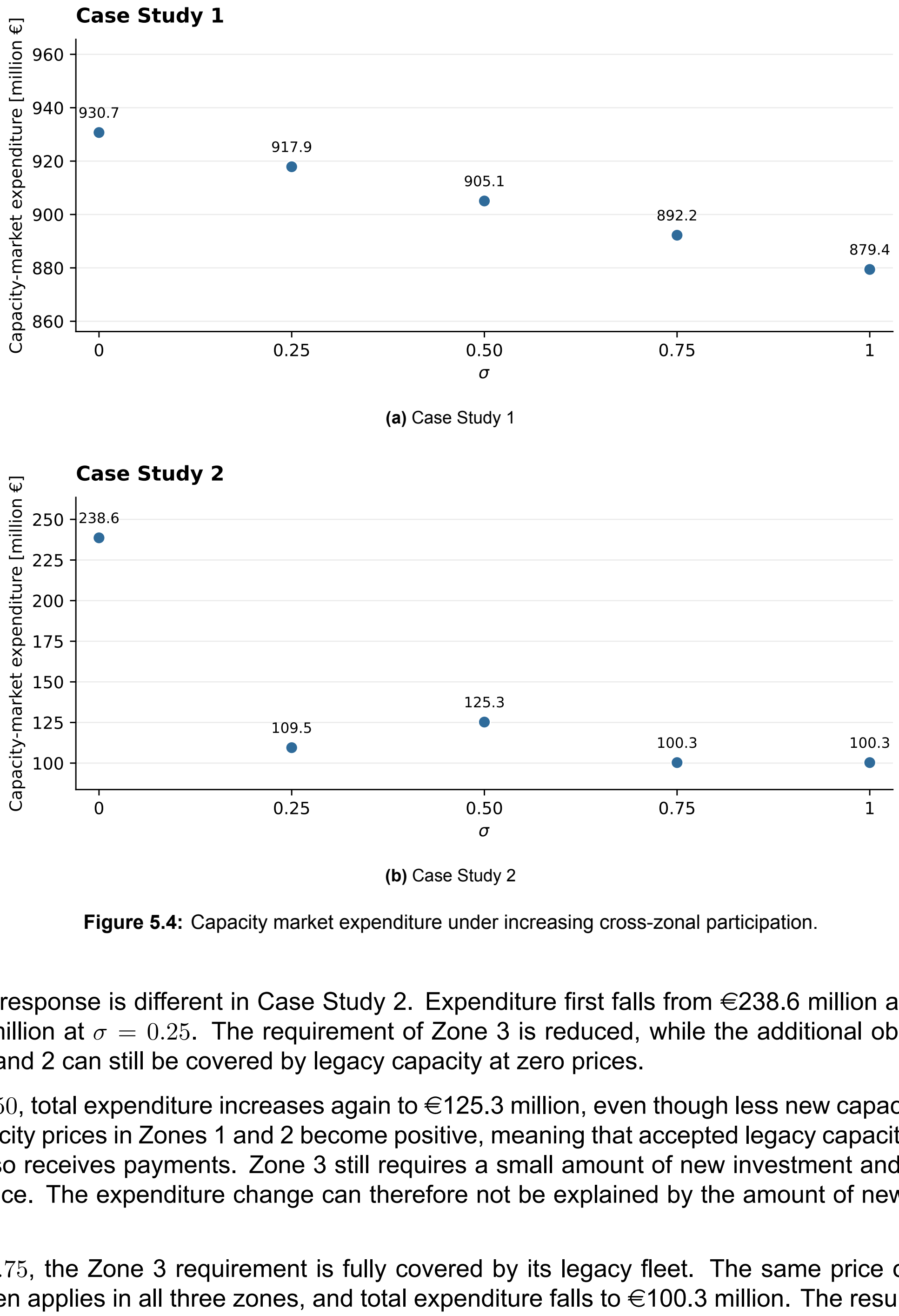


**(a)** Case Study 1



**(b)** Case Study 2

**Figure 5.4:** Capacity market expenditure under increasing cross-zonal participation.

The cost response is different in Case Study 2. Expenditure first falls from €238.6 million at $\sigma = 0$ to €109.5 million at $\sigma = 0.25$. The requirement of Zone 3 is reduced, while the additional obligation in Zones 1 and 2 can still be covered by legacy capacity at zero prices.

At $\sigma = 0.50$, total expenditure increases again to €125.3 million, even though less new capacity is built. The capacity prices in Zones 1 and 2 become positive, meaning that accepted legacy capacity in these zones also receives payments. Zone 3 still requires a small amount of new investment and retains a higher price. The expenditure change can therefore not be explained by the amount of new capacity alone.

At $\sigma = 0.75$, the Zone 3 requirement is fully covered by its legacy fleet. The same price of 5,975.3 €/MW then applies in all three zones, and total expenditure falls to €100.3 million. The result remains unchanged at $\sigma = 1$. Cross-zonal participation can therefore reduce the cost of the locational design, but the cost response is not necessarily monotonic because both new and legacy capacity receive the zonal clearing price.

### 5.4.3. Siting response

The reallocation of capacity obligations weakens the local investment signal. Figure 5.5 shows how new capacity moves between the three zones as $\sigma$ increases.

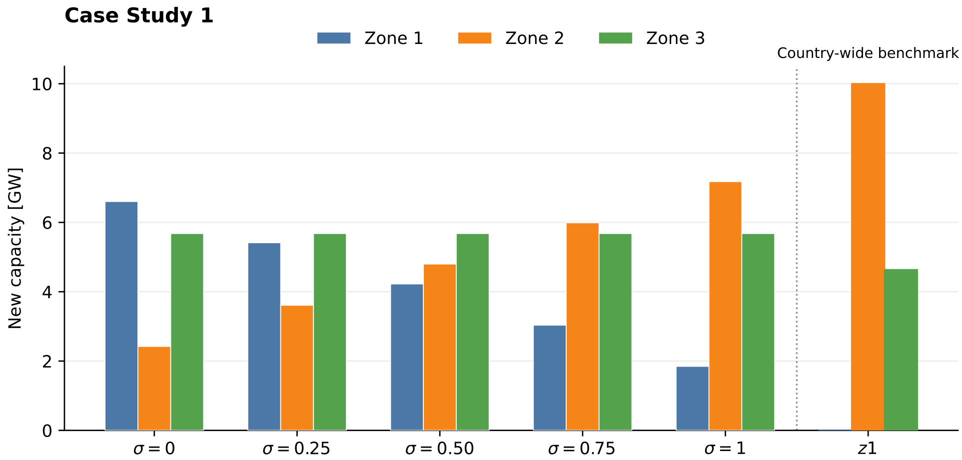


**(a)** Case Study 1

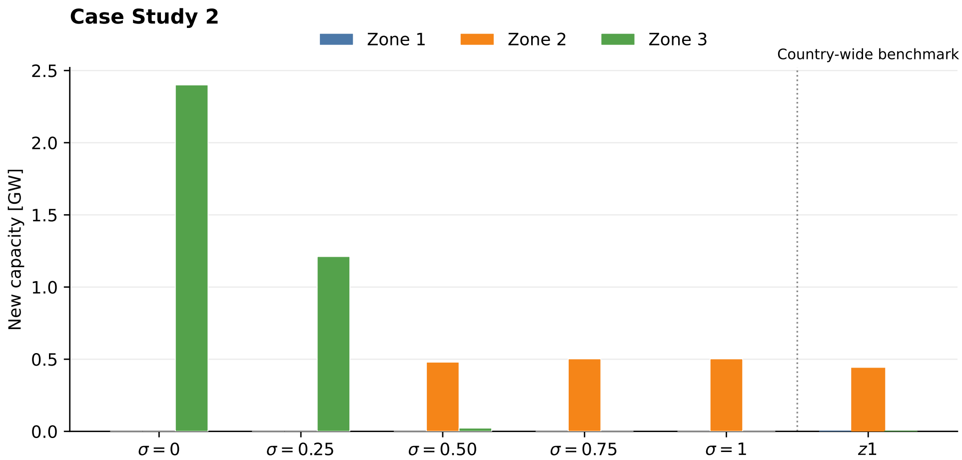


**(b)** Case Study 2

**Figure 5.5:** Zonal allocation of new capacity under increasing cross-zonal participation.

In Case Study 1, total new capacity remains constant at 14,701.0 MW. Its location changes progressively. New capacity in Zone 1 falls from 6,601.5 MW at $\sigma = 0$ to 1,846.9 MW at $\sigma = 1$, while investment in Zone 2 increases from 2,421.3 MW to 7,176.0 MW. Zone 3 remains at 5,678.1 MW.

The siting pattern therefore moves towards the country-wide result as the local requirement is relaxed. It does not fully converge, however. At $\sigma = 1$, 1,846.9 MW is still built in Zone 1, while the country-wide design builds no capacity there. The split design consequently retains a locational effect even at the highest level of participation.

In Case Study 2, cross-zonal participation also reduces the total amount of new capacity. At $\sigma = 0$, 2,400.1 MW is built in Zone 3. This falls to 1,211.4 MW at $\sigma = 0.25$. At $\sigma = 0.50$, only 22.8 MW remains in Zone 3, while 479.7 MW is built in Zone 2. From $\sigma = 0.75$ onward, all 502.5 MW of new capacity is located in Zone 2.

The siting pattern has then almost converged to the country-wide outcome, which also places the remaining investment in Zone 2. The difference of 66.5 MW is the additional capacity still required because the zonal residual-demand peaks do not coincide. In this case, weakening the locational signal reallocates investment by removing most of the additional new capacity initially required in Zone 3.

The response is not linear. In Case Study 1, the transfer limit produces a gradual relocation between Zones 1 and 2. In Case Study 2, the response is threshold-based. Once enough of the Zone 3 obligation can be shifted to zones with existing surplus capacity, the remaining new investment moves almost entirely to Zone 2.

The detailed nodal distribution is not interpreted further. As in the previous section, the exploration runs do not represent a probability distribution and their objective has no economic meaning. The relevant result is the change in zonal siting and total new capacity.

### 5.4.4. Congestion response

Weakening the local investment signal also changes the exposure to ex-post congestion management. Table 5.6 reports the observed minimum–maximum ranges. Grid-related load-shedding costs remain separate from redispatch costs and are not included in this comparison.

**Table 5.6:** Observed congestion-outcome ranges under increasing cross-zonal participation. Volumes are reported in TWh and redispatch costs in million €. Redispatch costs exclude grid-related load-shedding costs.

| Case study | $\sigma$ | Redispatch volume [TWh] | Grid-related load shedding [TWh] | Redispatch cost [million €] |
|---|---|---|---|---|
| Case Study 1 | $0.00$ | $0.00$–$2.37$ | $0.000$–$0.091$ | $-4.36$–$0.74$ |
| Case Study 1 | $0.25$ | $0.00$–$3.56$ | $0.000$–$0.164$ | $-7.88$–$0.84$ |
| Case Study 1 | $0.50$ | $0.19$–$10.69$ | $0.000$–$0.314$ | $-15.08$–$0.15$ |
| Case Study 1 | $0.75$ | $0.47$–$10.83$ | $0.065$–$0.848$ | $-40.78$–$-2.81$ |
| Case Study 1 | $1.00$ | $5.21$–$22.41$ | $0.453$–$2.204$ | $-102.81$–$-21.81$ |
| Case Study 2 | $0.00$ | $0.045$–$0.205$ | $0.000$ | $0.013$–$0.118$ |
| Case Study 2 | $0.25$ | $0.032$–$0.169$ | $0.000$ | $0.013$–$0.155$ |
| Case Study 2 | $0.50$ | $0.072$–$0.332$ | $0.033$–$0.107$ | $-8.84$–$-2.25$ |
| Case Study 2 | $0.75$ | $0.062$–$0.311$ | $0.033$–$0.112$ | $-7.52$–$-2.07$ |
| Case Study 2 | $1.00$ | $0.060$–$0.328$ | $0.033$–$0.112$ | $-9.23$–$-2.07$ |

In Case Study 1, both ends of the redispatch range generally increase as the locational signal is weakened. The upper bound rises from 2.37 TWh at $\sigma = 0$ to 22.41 TWh at $\sigma = 1$. Grid-related load shedding follows the same direction, increasing from a range of zero–0.091 TWh to 0.453–2.204 TWh.

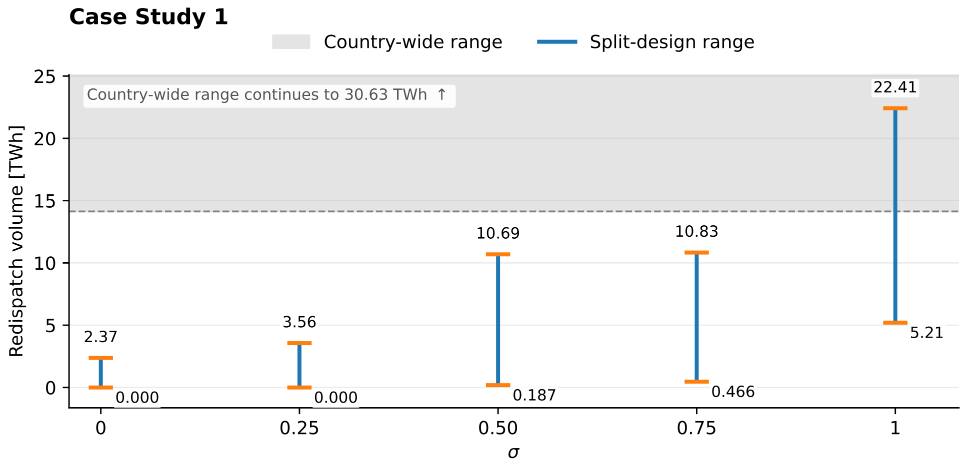


**(a)** Case Study 1

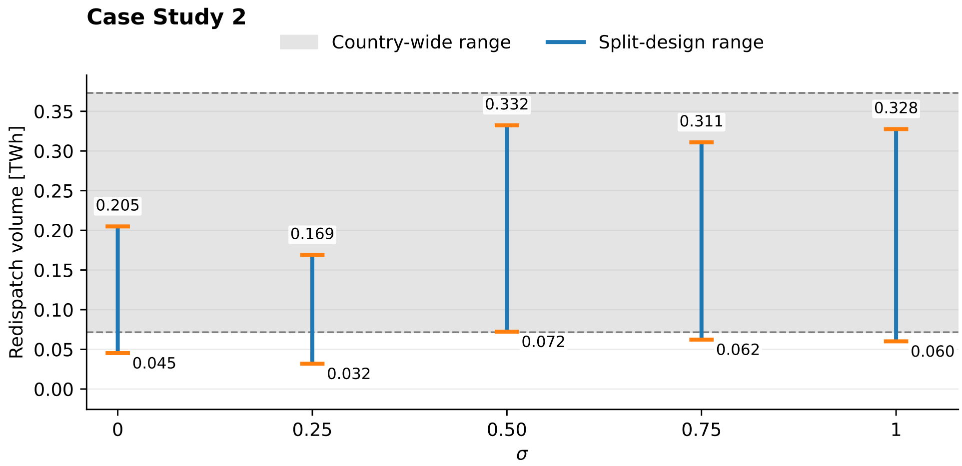


**(b)** Case Study 2

**Figure 5.6:** Observed redispatch-volume ranges under increasing cross-zonal participation.

The deterioration is not uniform between consecutive values of $\sigma$. The largest change occurs between $\sigma = 0.75$ and $\sigma = 1$, when a further reduction of capacity in Zone 1 substantially increases the lower and upper ends of the redispatch range. This indicates that the relationship is affected by network thresholds rather than only by the aggregate amount of capacity moved.

At $\sigma = 1$, the congestion outcomes still remain below the country-wide results. The redispatch range of the country-wide design is 14.13–30.63 TWh, compared to 5.21–22.41 TWh under the split design. Grid-related load shedding is 2.30–5.86 TWh under the country-wide design, compared to 0.453–2.204 TWh at $\sigma = 1$. The split design therefore retains part of its deliverability benefit even at the highest level of cross-zonal participation.

The Case Study 2 response is less monotonic. At $\sigma = 0.25$, the redispatch range falls slightly from 0.045–0.205 TWh to 0.032–0.169 TWh, while grid-related load shedding remains zero. Moderate cross-zonal participation can therefore improve the siting outcome without immediately removing the deliverability benefit.

Once most of the investment moves from Zone 3 to Zone 2 at $\sigma = 0.50$, grid-related load shedding appears and the redispatch range increases to 0.072–0.332 TWh. The outcomes at $\sigma = 0.75$ and $\sigma = 1$ remain close to this level.

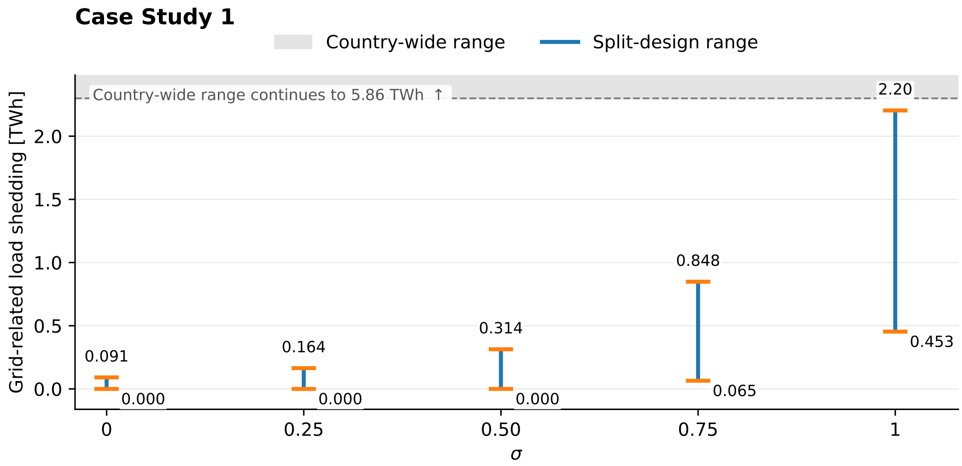


**(a)** Case Study 1

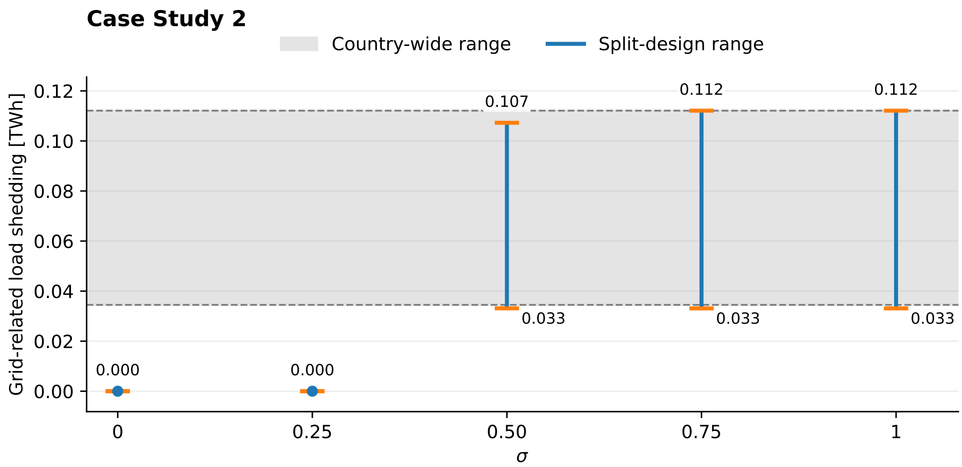


**(b)** Case Study 2

**Figure 5.7:** Observed grid-related load-shedding ranges under increasing cross-zonal participation.

At $\sigma = 1$, the Case Study 2 results almost coincide with the country-wide design. Redispatch reaches 0.060–0.328 TWh, compared to 0.072–0.373 TWh under the country-wide design. Grid-related load shedding reaches 0.033–0.112 TWh, compared to 0.034–0.112 TWh. This corresponds to the near-convergence of the zonal investment pattern.

The remaining non-monotonicity is consistent with the meshed-network structure. Moving capacity from one zone or node can relieve one network constraint while worsening another. Similar aggregate siting outcomes can therefore result in slightly different redispatch ranges depending on the exact nodal distribution and dispatch.

The negative redispatch-cost values again arise when the variable-cost savings from downward redispatch exceed the cost of upward redispatch. They do not include the cost assigned to grid-related load shedding and should not be interpreted as a complete congestion-cost measure.

### 5.4.5. Interim conclusion on cross-zonal participation

Cross-zonal participation lowers the cost of the locational mechanism by letting procurement obligations move between zones. In Case Study 1, investment reallocates from the more expensive Zone 1 toward Zone 2, while total procurement and total new capacity remain unchanged. In Case Study 2, new investment falls from 2,400.1 MW to 502.5 MW because legacy surpluses can cover neighboring requirements, although expenditure does not fall monotonically: changes in zonal prices also affect payments to accepted legacy capacity. In both cases the investment pattern moves back toward the country-wide result as σ increases, gradually in Case Study 1 and threshold-based in Case Study 2.

## 5.5. Network mechanisms behind the congestion outcomes

The previous sections showed that strict zonal procurement substantially reduces redispatch and grid-related load shedding, while increasing cross-zonal participation weakens this effect. This section briefly examines the network mechanism behind these outcomes. The aim is not to provide a complete line-by-line assessment, but to identify whether congestion is concentrated on a small number of constraints and to explain why sufficient aggregate capacity does not always result in feasible redispatch.

### 5.5.1. Dominant bottlenecks and capacity siting

The overload results are strongly concentrated. In Case Study 1, Lines 26, 27, 34, 11, and 14 are the five most important constraints across the different market designs. Together, the five most overloaded lines account for between 68.1 and 90.8% of the total pre-redispatch overload index. All five lines are overloaded under every investigated design. The most severe individual overload occurs on Line 27 and reaches approximately 4.12 GW.

The concentration is even stronger in Case Study 2, where the five most important lines account for between 89.2 and 100% of the overload index. However, the lines with the largest total overload are not necessarily those associated with grid-related load shedding. Lines 5, 20, and 4 dominate the total overload index, while grid-related load shedding is primarily associated with Lines 7, 12, 8, 14, and 23. This distinction matters because a frequently overloaded line does not necessarily make redispatch infeasible.

**Table 5.7:** Dominant transmission constraints across the investigated market designs.

| Case study | Lines with highest total overload | Lines most associated with grid-related load shedding | Share represented by five largest lines |
|---|---|---|---|
| Case Study 1 | 26, 27, 34, 11, 14 | 34, 26, 27, 11, 14 | 68.1–90.8% |
| Case Study 2 | 5, 20, 4, 7, 12 | 7, 12, 8, 14, 23 | 89.2–100% |

The overload index sums the MW exceedance across representative run-hours and exploration runs. It is used to rank the lines and should not be interpreted as annual overload energy.

The change in the dominant lines also reflects the change in capacity siting. Under strict zonal procurement in Case Study 1, the largest overload values occur on Lines 34, 20, 12, 8, and 5, but their combined magnitude remains far below the country-wide outcome. At $\sigma = 1$, Lines 26, 34, 27, 11, and 14 again form the five largest constraints, closely resembling the country-wide design.

The PTDF results support this interpretation. Investment at nodes on the loading side of Lines 26 and 34 is consistently associated with higher overload on these lines. Strict zonal procurement instead places more controllable capacity in areas with a local capacity deficit, thereby reducing the need to transfer energy across the dominant corridors. As cross-zonal participation increases, this siting effect weakens and the original bottlenecks gradually reappear.

### 5.5.2. Redispatch feasibility and local headroom

The remaining question is why congestion sometimes results in grid-related load shedding rather than additional upward redispatch. Figure 5.8 compares the selected highest-shedding event for the country-wide design, strict zonal procurement, and $\sigma = 1$ in Case Study 1. All three selected events occur at model timestep $t = 177$, corresponding to the first hour of the eighth representative day. This representative day corresponds to original day 348 of the input year.

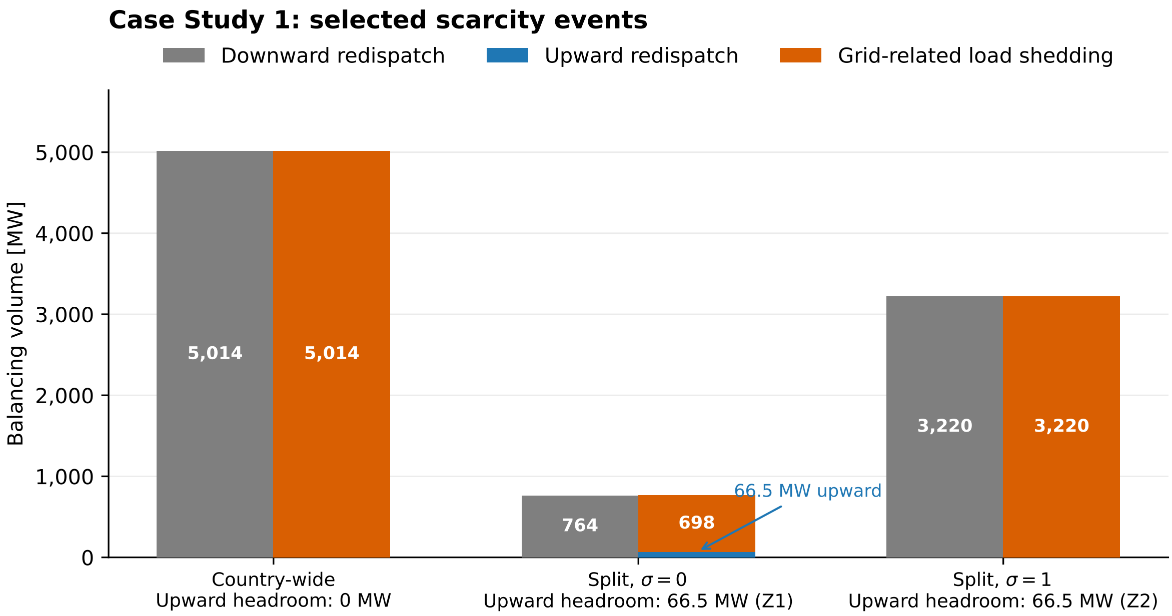


**Figure 5.8:** Downward redispatch and the corresponding balancing response in the selected Case Study 1 scarcity events. The right-hand bar combines upward redispatch and grid-related load shedding. The upward headroom reported below each design refers to the market dispatch before redispatch.

Under country-wide procurement, all controllable capacity is already fully dispatched before redispatch. The TSO redispatches 5,013.5 MW downward in Zone 2, but no upward headroom is available elsewhere. The same volume must therefore be shed in Zone 1.

Strict zonal procurement changes this outcome. It retains 66.5 MW of upward headroom in Zone 1, which is fully used. Downward redispatch falls to 764.0 MW and grid-related load shedding to 697.5 MW. The remaining shedding occurs because Line 8 is binding after redispatch.

At $\sigma = 1$, only 66.5 MW of nominal upward headroom remains, now located in Zone 2. This headroom is not used because it cannot relieve the constrained area without violating another network constraint. Lines 11, 12, 14, 26, and 34 are binding after redispatch, and 3,219.8 MW is shed in Zone 1.

Case Study 2 shows the same mechanism at a smaller scale. In the selected strict-zonal event, 395.0 MW of upward redispatch is available and no grid-related load shedding occurs. In the selected country-wide and $\sigma = 1$ events, no upward redispatch is possible and both outcomes require 875.2 MW of grid-related load shedding.

The network benefit of the locational signal therefore does not follow from an increase in aggregate capacity. It follows from placing controllable capacity on the electrically useful side of the important constraints and preserving local upward redispatch capability. Increasing cross-zonal participation weakens this effect. Capacity again shifts towards locations that are attractive for procurement but less useful during network scarcity, causing the dominant bottlenecks and grid-related load shedding to reappear.

## 5.6. Combined capacity market and congestion-cost comparison

The previous sections considered capacity market expenditure and congestion outcomes separately. This section combines them in one accounting measure to compare the additional ex-ante expenditure of a locational mechanism with its effect on ex-post congestion. The measure is defined as

$$C^{\text{combined}} = C^{\text{CM}} + C^{\text{RD}} + VOLL^{\text{grid}} E^{\text{grid-LS}}, \tag{5.1}$$

where $C^{\text{RD}}$ excludes grid-related load shedding. This is not a complete social-cost measure. Capacity market payments are transfers to generators, while redispatch costs represent changes in generation cost. The calculation is used only to compare capacity market expenditure with the monetary consequences assigned to congestion.

The physical redispatch and load-shedding outcomes remain unchanged. Only the ex-post value assigned to grid-related load shedding is varied. All complete exploration runs are included after rerun replacement, without applying a solving-gap threshold. The results are again reported as observed minimum–maximum ranges rather than probability-weighted outcomes.

### 5.6.1. Observed combined-cost comparison

Figure 5.9 compares capacity market expenditure, capacity market expenditure plus net redispatch cost, and the combined cost at the modeled value of $VOLL^{\mathrm{grid}} = 69{,}000$ €/MWh. A logarithmic scale is used because the valuation of grid-related load shedding increases the combined cost by several orders of magnitude in some outcomes.

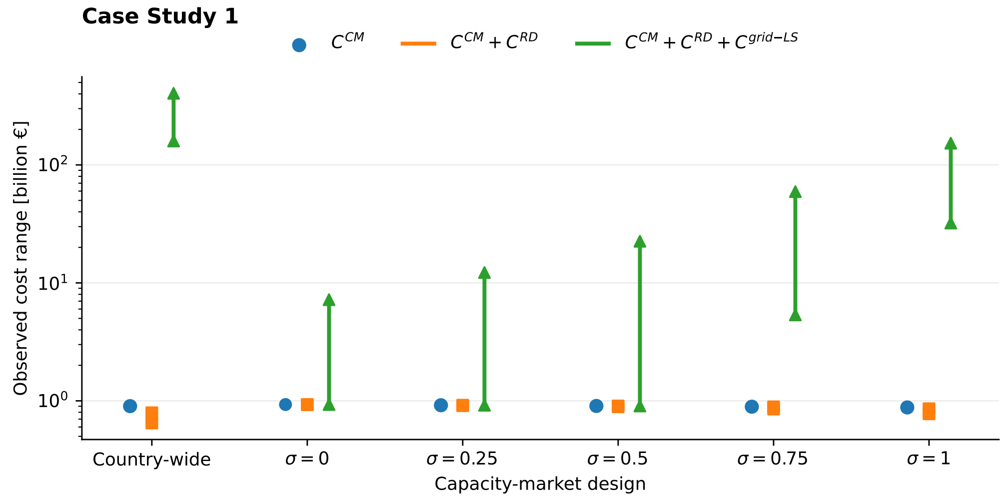


**(a)** Case Study 1.

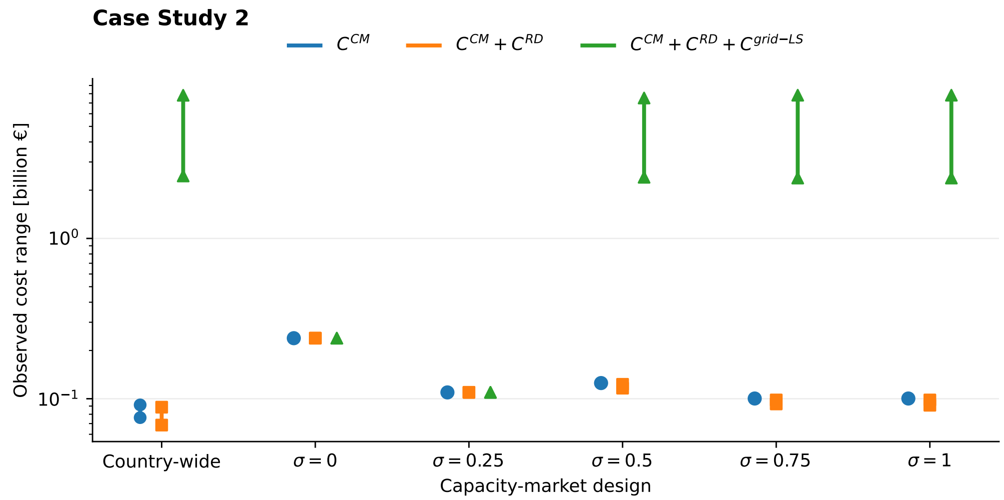


**(b)** Case Study 2.

**Figure 5.9:** Observed ranges of capacity market expenditure, capacity market expenditure plus net redispatch cost, and combined cost after valuing grid-related load shedding at $69{,}000$ €/MWh.

In Case Study 1, the capacity market cost difference remains small compared with the congestion exposure. Country-wide procurement costs approximately 901.9 million €, while strict zonal procurement increases this to 930.7 million €. As cross-zonal participation increases, expenditure falls and reaches 879.4 million € at $\sigma = 1$. As discussed in Sections 5.3 and 5.4, this development is mainly caused by the changing zonal prices and the reallocation of procurement between Zones 1 and 2.

Net redispatch cost is considerably smaller than either capacity market expenditure or the cost of grid-related load shedding. It is negative in several runs because the variable-cost reduction from downward redispatch exceeds the cost of upward redispatch under the model's redispatch accounting. This reduces the combined value of $C^{\mathrm{CM}} + C^{\mathrm{RD}}$, but does not change the overall comparison.

Once grid-related load shedding is included, the country-wide combined cost in Case Study 1 ranges from 159.48 to 404.69 billion €, of which grid-related load shedding accounts for nearly the entire amount. Under strict zonal procurement, the range falls to 0.93–7.21 billion €. The range then increases with $\sigma$, reaching 32.15–152.83 billion € at $\sigma = 1$. Even at this level of cross-zonal participation, the observed maximum remains below the minimum country-wide outcome.

Case Study 2 shows the same mechanism, but the difference between designs is smaller. The country-wide combined cost ranges from 2.45 to 7.82 billion €. Strict zonal procurement has a higher capacity market expenditure of 238.6 million €, but eliminates grid-related load shedding in all explored runs. Its combined cost therefore remains between 238.7 and 238.8 million €. At $\sigma = 0.25$, the combined cost falls further to approximately 109.5–109.7 million € because the locational benefit is maintained while capacity market expenditure is substantially lower.

From $\sigma = 0.5$ onwards, grid-related load shedding reappears and the combined-cost ranges approach the country-wide outcome. At $\sigma = 0.75$ and $\sigma = 1$, the combined cost ranges from approximately 2.38 to 7.83 billion €. The higher values of $\sigma$ therefore no longer provide a clear combined-cost advantage in every explored equilibrium.

### 5.6.2. Break-even valuation of grid-related load shedding

The combined-cost comparison depends strongly on the value assigned to grid-related load shedding. To test this dependence without changing the physical model outcomes, a break-even value is calculated for every matched country-wide and split-design run:

$$VOLL^{\mathrm{grid},*} = \frac{\left(C_{\mathrm{L}}^{\mathrm{CM}} - C_{\mathrm{CW}}^{\mathrm{CM}}\right) + \left(C_{\mathrm{L}}^{\mathrm{RD}} - C_{\mathrm{CW}}^{\mathrm{RD}}\right)}{E_{\mathrm{CW}}^{\text{grid-LS}} - E_{\mathrm{L}}^{\text{grid-LS}}}, \tag{5.2}$$

where $\mathrm{L}$ denotes the respective locational design and $\mathrm{CW}$ the country-wide design. The break-even value indicates the minimum value that must be assigned to each MWh of grid-related load shedding avoided by the locational design for its higher capacity market and redispatch costs to be recovered. At this value, both designs have the same combined cost. Above it, the avoided grid-related load shedding gives the locational design the lower combined cost. Below it, the reduction in load shedding is not valued highly enough to compensate for its additional cost.

**Table 5.8:** Observed break-even values relative to country-wide procurement.

| Case study | $\sigma$ | Break-even range [€/MWh] | Locational design has lower combined cost at 69,000 €/MWh |
|---|---|---|---|
| Case Study 1 | 0 | 47.2–60.7 | 80/80 |
| Case Study 1 | 0.25 | 45.0–55.1 | 80/80 |
| Case Study 1 | 0.50 | 42.7–49.8 | 80/80 |
| Case Study 1 | 0.75 | 39.5–43.4 | 80/80 |
| Case Study 1 | 1 | 23.8–37.6 | 80/80 |
| Case Study 2 | 0 | 1,357–4,784 | 80/80 |
| Case Study 2 | 0.25 | 204–1,044 | 80/80 |
| Case Study 2 | 0.50 | 615–38,335 | 76/80 |
| Case Study 2 | 0.75 | 186–62,347 | 69/80 |
| Case Study 2 | 1 | 186–1,354,921 | 70/80 |

Break-even ranges are calculated only for matched runs in which the locational design reduces grid-related load shedding. The final column compares combined cost directly across all 80 matched runs at the modeled value of $VOLL^{\mathrm{grid}}$.

In Case Study 1, all break-even values remain below 61 €/MWh. They are therefore far below the value used in the model, and every locational design has a lower combined cost than country-wide procurement in all 80 matched runs. Increasing $\sigma$ reduces the amount of avoided grid-related load shedding, but it also lowers the difference in capacity market and net redispatch cost. The resulting break-even ranges therefore remain low.

For Case Study 2, strict zonal procurement has a higher break-even range of approximately 1,357–4,784 €/MWh because the additional capacity market expenditure is larger and the country-wide load-shedding volume is much lower than in Case Study 1. The range falls to 204–1,044 €/MWh at $\sigma = 0.25$, giving this design the lower combined cost in all matched runs at the modeled value.

The higher values of $\sigma$ no longer produce a uniform result. In several matched runs, the locational design avoids little, no, or even less grid-related load shedding than the country-wide design. Where the difference in physical shedding becomes very small, the break-even value can become extremely large, as visible for $\sigma = 1$. This does not indicate a proportionally larger economic benefit. It instead reflects that almost no avoided load shedding remains over which the cost difference can be spread.

Overall, capacity market expenditure changes relatively predictably, while the combined-cost ranges are mainly driven by grid-related load shedding. Under the selected valuation, strict zonal procurement and limited cross-zonal participation have a lower combined cost mainly because they avoid high-impact load-shedding outcomes, not because of redispatch-cost savings alone. At higher participation levels, this difference becomes less consistent across the explored equilibria.

## 5.7. Synthesis across both case studies

The results show that a locational capacity-market signal changes more than the cost of capacity procurement: it changes where controllable capacity is located and, with that, how useful this capacity is once network constraints bind. Two factors explain most of the difference between the explored outcomes. The inherited generation fleet determines how much capacity can still respond to the signal, and cross-zonal participation determines how strongly that signal is maintained. This section synthesizes what only the comparison across the two case studies shows. The per-case results are summarized in subsections 5.3.4 and 5.4.5.

### 5.7.1. What changes when a locational signal is introduced?

Across both case studies, separate zonal requirements shift controllable capacity toward deficit zones and reduce reliance on transfers across the dominant constraints. The comparison adds two observations that neither case shows alone.

First, the size of the response scales with the open investment margin, but the effectiveness does not. In Case Study 1 the signal can still shape most of the final fleet, and congestion outcomes respond strongly. In Case Study 2 the same mechanism acts on a small residual deficit, yet closing that deficit is sufficient to eliminate grid-related load shedding. The signal works through different margins in the two systems: it reshapes the fleet in one and completes it in the other.

Second, the consistent result is not a simple increase in capacity-market expenditure. Zonal procurement raises expenditure in both cases, for different reasons: non-coincident zonal residual-demand peaks in Case Study 1 and zonal prices paid to eligible legacy capacity in Case Study 2. What is consistent is the improvement in deliverability. The risk that aggregate adequacy cannot be translated into feasible supply falls in both systems, and the monetary weight of this improvement depends on the value assigned to grid-related load shedding.

### 5.7.2. How does cross-zonal participation modify that effect?

In both case studies, participation moves the capacity distribution back toward the country-wide outcome, but the path differs. In Case Study 1 the return is gradual: each increase in σ shifts investment further toward Zone 2, and the dominant bottlenecks reappear step by step, although the outcome at $\sigma = 0$ still remains better than fully country-wide procurement. In Case Study 2 the response is threshold-based: up to $\sigma = 0.25$ most of the locational benefit is preserved at substantially lower procurement cost, and from $\sigma = 0.5$ onward grid-related load shedding reappears.

The comparison also shows why the cost saving differs. Participation only avoids new investment where the exporting zone holds surplus legacy capacity. Where it does not, as in Case Study 1, participation reallocates procurement rather than reducing it. The value of cross-zonal participation is therefore not a design constant. It depends on the starting system, and no single value of $\sigma$ is optimal across both cases.

# 6 Discussion

Chapter 5 showed how the capacity market design affects procurement, investment siting, redispatch, and grid-related load shedding. This chapter interprets these findings and discusses how far they can be generalized. The limitations are addressed first, followed by the main findings on deliverability, cross-zonal participation, and the inherited generation fleet. The chapter then turns to the wider design and institutional implications.

## 6.1. Limitations and interpretation boundaries

Before interpreting the results, it is important to distinguish between limitations that affect the exact numerical outcomes and those that limit what the model represents more generally. The first group mainly concerns the exploration of alternative equilibria and the remaining solution gaps. The second concerns the simplified investment, temporal, and network representation. A final limitation lies in the monetary valuation of congestion outcomes.

### 6.1.1. Equilibrium exploration and computational limitations

The market model can produce several capacity-siting outcomes with the same primary objective value. The PTDF-based exploration objective was introduced to recover spatially different points from this solution space. It has no economic interpretation, and the exploration directions do not form a probability distribution. The frequency with which an outcome occurs across the runs therefore says nothing about how likely that outcome would be in practice.

For this reason, the reported minimum–maximum ranges should be read as systematically identified outcomes rather than distributions. Their main value is to show that market-equivalent siting decisions can have very different network consequences. They do not establish complete bounds on the solution space. Additional exploration directions could still identify outcomes outside the observed ranges.

The warm-start procedure and the time limit add another restriction. The warm start is needed to find feasible incumbents for a difficult mixed-integer problem, but it may influence which part of the solution space is reached when the time limit binds. Several exploration directions remain associated with larger gaps, including after the reruns. Since the same directions are difficult across several capacity market designs, this appears to be partly a structural feature of the formulation rather than a problem of one scenario alone.

These issues matter most for the exact width of the ranges and for the reported minima and maxima. They matter less for the comparison between the designs. Across both case studies, country-wide procurement, strict zonal procurement, and increasing cross-zonal participation lead to consistently different capacity distributions and congestion outcomes. The direction of the design effect is therefore more robust than the precise extrema of the observed ranges.

### 6.1.2. Simplified investment and system representation

New CCGT capacity has substantial spatial freedom in the model. It can be built at every candidate node without restrictions related to land availability, permits, gas infrastructure, cooling, labor, or grid-connection lead times. Case Study 1 consequently represents a system in which most of the future controllable fleet can respond directly to the capacity market signal. This is useful for identifying the mechanism, but it likely overstates how quickly a real capacity market could reshape the full generation fleet.

Case Study 2 provides a more conservative comparison because most controllable capacity is inherited and fixed. Only the remaining investment requirement can react. Even this case remains stylized, since retirement and replacement are not modeled dynamically. In practice, the locational signal would gain influence gradually as existing plants retire and new capacity becomes necessary.

The cost differences between otherwise similar generators are also stylized. Fixed-cost differences are needed to avoid investment degeneracy, while variable-cost differences prevent the energy market dispatch from being determined by solver tie-breaking alone. They should not be interpreted as forecasts of the exact costs at individual locations. Real differences would arise from connection charges, land prices, gas access, financing conditions, and local permitting, among other factors. The precise investment nodes and capacity prices are therefore less robust than the broader finding that local requirements change where investment occurs.

Temporal aggregation introduces a different uncertainty. The representative days preserve recurring combinations of demand and renewable availability, but they may omit rare conditions in which high demand, low renewable output, and severe congestion occur together. These are precisely the conditions that can determine adequacy and redispatch feasibility. The model may therefore understate some extreme scarcity outcomes. A different selection of representative periods could also change which zones and lines emerge as most critical.

The transmission network is based on a clustered PyPSA-Eur representation and not on a complete operational model of the Dutch grid. Line capacities, nodal demand, generator connections, and the capacity market zones are approximations. Individual overloaded lines and exact node-level outcomes should therefore not be read as operational forecasts. The relevant finding is more general: different spatial distributions of controllable capacity interact differently with a meshed and constrained network.

Cross-border trade with other countries, storage, demand response, and other flexible technologies are excluded. Imports could reduce domestic investment needs. Storage and demand response could provide local capacity and upward redispatch headroom, which would reduce the role of new CCGT and potentially lower grid-related load shedding. Their exclusion makes thermal investment more important in the model. It does not, however, remove the underlying question of where flexible capacity must be available.

### 6.1.3. Interpretation of congestion and total costs

Cross-zonal participation is represented through pairwise maximum entry capacity values. These limits control how much capacity in a neighboring zone can contribute to the local requirement, but they do not verify whether several transfers can take place simultaneously. In a meshed network, different zonal contributions may rely on the same physical lines. The capacity mechanism can therefore credit a combination of transfers that would not be jointly deliverable during scarcity.

This becomes more important as $\sigma$ increases. At high participation levels, the local obligation may be relaxed further than a full network assessment would permit. The resulting congestion and grid-related load shedding should therefore be interpreted as the effect of relaxing local procurement under the chosen MEC formulation. They are not a prediction of what a more detailed flow-based design would produce.

The monetary comparison is also sensitive to the value assigned to grid-related load shedding. The physical redispatch and load-shedding volumes do not change with the ex-post valuation, while the total-cost ranking does. A comparison at one value of $VOLL^{\text{grid}}$ can therefore give a false sense of precision. The break-even analysis is more useful because it shows how highly avoided load shedding must be valued before the additional procurement and redispatch costs of a locational design are recovered.

The model thus provides stronger evidence on physical outcomes than on exact monetary differences. Capacity siting, local headroom, dominant bottlenecks, and grid-related load shedding can be compared directly across the designs. The total-cost ranking remains conditional on assumptions that are more difficult to justify precisely.

For case study 1, the redispatch and load shedding volumes are very high, also in comparison to case study 2. The freedom offered by the first case study's small legacy system allows for more extreme siting outcomes. In some cases, grid related load shedding volumes equal several percent of overall energy traded on the energy market. Hence, the high $VOLL^{\text{grid}}$ plus high grid related load shedding volumes in case study 1 make the costs almost entirely driven by grid related load shedding.

## 6.2. Interpretation of the main findings

Despite these limitations, a clear mechanism emerges from the results. Locational procurement changes where controllable capacity is built and, through this, whether it remains useful once the network becomes constrained. The following subsections discuss this effect, the trade-off created by cross-zonal participation, and the importance of the inherited generation fleet and the selected spatial resolution.

### 6.2.1. Locational capacity as a deliverability mechanism

The central result is that sufficient aggregate capacity does not guarantee that demand can be served during scarcity. The country-wide mechanism meets the system-wide capacity requirement, but it leaves the location of new investment open. If too much capacity is built on the wrong side of an important constraint, the system can be resource adequate while the network-constrained dispatch still requires load shedding.

The split mechanism adds a spatial condition. Capacity must be procured within each zone unless a neighboring contribution is explicitly credited. This changes where new generators can recover their fixed costs and counteracts the concentration of investment in the lowest-cost locations. The signal works through the local capacity obligation and the resulting capacity revenue. Redispatch compensation does not provide the same incentive because generators are neutral towards cost-based redispatch.

This distinction is relevant for the literature. Existing studies mainly evaluate locational capacity mechanisms through reductions in redispatch volumes and costs (Hladik et al., 2020; Thomassen & Fuhrmanek, 2025). The results support that direction, but they also show why redispatch alone is an incomplete measure. Redispatch remains non-zero under several locational designs, and its ranges do not change monotonically with the strength of the signal. The clearer result concerns whether redispatch remains feasible at all.

Under country-wide procurement, some scarcity events cannot be resolved because controllable generators in the affected area are already fully dispatched, while remaining capacity elsewhere cannot reach the load without violating another constraint. Strict zonal procurement greatly reduces these cases in Case Study 1 and eliminates grid-related load shedding in all explored outcomes of Case Study 2. The locational signal is therefore more consistent in improving deliverability than in removing the need for redispatch.

This gives further substance to the distinction between resource adequacy and transmission adequacy discussed in Chapter 2. A country-wide requirement asks whether sufficient capacity exists in total. The zonal requirement adds the question whether enough of this capacity is located where it can contribute under network constraints. Resource adequacy remains necessary, but it is not always sufficient.

The improvement is not free. Separate zonal requirements can increase total procurement when zonal residual-demand peaks are not coincident. They can also create higher clearing prices in deficit zones. This additional expenditure is not automatically inefficient. Part of it pays for capacity that remains useful in a constrained network, which is a quality that the country-wide auction does not value.

The same physical correction can have a very different procurement cost depending on how much existing capacity already sits in the constrained zone. Subsection 6.2.3 returns to this dependence on the inherited fleet.

A locational capacity mechanism nevertheless remains a limited instrument. It does not coordinate hourly dispatch, and it cannot remove congestion caused by renewable output, load patterns, or the existing fleet. This is similar to the role of locational measures described by Lété et al. (2026): they can mitigate a problem created by the wider market design without removing its source. The mechanism should therefore be judged by whether it improves the location and availability of controllable capacity, not by whether redispatch disappears.

### 6.2.2. The trade-off introduced by cross-zonal participation

Strict zonal procurement provides the strongest local signal, but complete local self-sufficiency can be unnecessarily expensive. Capacity in a neighboring zone may contribute during scarcity if sufficient transfer capability exists. Recognizing this contribution can lower local procurement, avoid new investment, and reduce capacity market expenditure.

At the same time, participation weakens the reason to invest in the deficit zone. Once part of the local requirement can be covered from elsewhere, investment can return to locations that are cheaper from the capacity market perspective but more dependent on the transmission grid. The cost saving and the loss of the locational signal are therefore two sides of the same design choice.

The same tension appears in the wider debate on fragmented capacity mechanisms. Separate national mechanisms protect local security of supply but tend to procure too much capacity when neighboring resources are ignored. Integration reduces this inefficiency, although only if the foreign contribution is reliable (Adekola et al., 2026; Höschle, Le Cadre, & Belmans, 2018). In this thesis, the same problem occurs within one national bidding zone. Increasing participation reduces the separation between the internal capacity market zones, but it also brings back part of the siting pattern that the split design was introduced to correct.

The two case studies show why the effect depends on the neighboring fleet. In Case Study 1, higher $\sigma$ mainly moves investment from Zone 1 to Zone 2. Procurement expenditure falls, while the dominant bottlenecks from the country-wide design gradually reappear. Grid-related load shedding increases as more of the deficit zone depends on imports.

Case Study 2 behaves differently. At $\sigma = 0.25$, the mechanism can make use of existing surplus legacy capacity outside the deficit zone. New investment and capacity market expenditure fall substantially, while grid-related load shedding remains absent across the explored outcomes. Once participation increases further, however, the remaining investment moves closer to the country-wide pattern and load shedding returns. Limited participation is therefore useful in this case, but the benefit does not extend indefinitely.

The effect of increasing $\sigma$ is not fully monotonic because capacity shifts in a meshed network alter several line flows at once. A relocation may relieve one constraint while worsening another, and nodes within the same zone can have materially different effects on congestion. $\sigma$ should therefore not be interpreted as a parameter that produces a smooth increase in network stress at every step.

Nor is there one value that can be labeled universally optimal. In this model, $\sigma$ is used to expose the trade-off between local procurement and reliance on neighboring capacity. A practical mechanism would instead need to determine how much foreign or neighboring capacity remains simultaneously deliverable under the relevant scarcity conditions.

### 6.2.3. Dependence on the inherited generation fleet

The difference between the two case studies is mainly explained by how much capacity is still able to respond. In Case Study 1, most controllable capacity must be newly built. The locational requirement can therefore reshape a large part of the final fleet, and the consequences for siting, redispatch, and grid-related load shedding are substantial.

Most capacity in Case Study 2 is already installed and fixed. The mechanism cannot relocate this fleet. It can only influence the remaining investment requirement. The overall siting response is consequently smaller. Still, the incremental investment matters because it is placed exactly in the zone where local headroom is missing.

The inherited fleet also changes how cross-zonal participation reduces costs. If the exporting zone has no surplus, taking on additional obligation may require new investment there. Participation then mainly reallocates procurement. If surplus legacy capacity is already present, it can cover part of the neighboring requirement without an equivalent new build. The cost saving in Case Study 2 follows from this second mechanism.

This finding is consistent with the ENTSO-E position on locational elements in capacity mechanisms and other support schemes. Such instruments mainly influence new assets and have little direct effect on the location of existing capacity (ENTSO-E, 2026). Their contribution is therefore mostly long term. A mechanism introduced into a legacy-heavy system may have only a limited immediate effect, but its influence grows as replacement and retirement decisions arise.

A small short-term response should consequently not be interpreted as a failure of the locational signal. It shows that implementation timing matters. The signal is strongest where major investment decisions are still open and weakest once the spatial structure of the controllable fleet has already been determined.

### 6.2.4. Spatial resolution and dominant constraints

The results also show that the network problem is concentrated. A limited number of lines repeatedly appear as dominant bottlenecks, while some investment nodes create much worse outcomes than others, even when they belong to the same capacity market zone.

This is a limitation of using broad zonal requirements. Capacity procured anywhere within the zone counts equally, although its actual contribution to a scarcity event may depend strongly on the node. The zonal obligation can therefore be met while some capacity remains poorly located relative to the constraint that matters. This helps explain why strict zonal procurement in Case Study 1 improves deliverability substantially without eliminating grid-related load shedding in every explored outcome.

One response would be to define the capacity market zones more closely around the dominant structural constraints. Another would be to keep broader zones but restrict how much capacity at particular locations can count towards the zonal requirement. Eligibility criteria or local volume limits, which are also discussed by ENTSO-E (2026), could provide such a distinction.

More granular intervention also creates costs. Smaller zones and node-specific restrictions reduce competition and increase the risk of local market power. They can also make the mechanism sensitive to changes in network conditions. Since the signal affects long-term investment, the design needs a degree of stability. The relevant balance is therefore between enough spatial detail to capture persistent deliverability problems and enough aggregation to preserve competition and predictability.

## 6.3. Implications for capacity market design

The results do not point to one capacity market design that should be applied in every system. They instead show which physical and institutional questions need to be answered before introducing a locational element. The first concerns the design itself: how local requirements, participation, and spatial granularity should be combined. The second concerns whether such a mechanism can be fitted into the current European regulatory framework.

### 6.3.1. Design implications

Internal deliverability should be considered where transmission constraints can prevent procured capacity from serving demand during scarcity. In such systems, a country-wide requirement may meet the aggregate adequacy target while leaving the TSO without sufficient local options. A zonal requirement can address this by placing an additional condition on the capacity that counts towards adequacy.

This does not imply that every zone must be self-sufficient. Case Study 2 shows that neighboring surplus capacity can be valuable and can reduce unnecessary investment. The important question is how much of that capacity can be credited without removing the local headroom that is needed when the grid becomes constrained.

Pairwise transfer limits provide only a partial answer. Several zones may rely on the same bottleneck, and one transfer can change the feasibility of another. Cross-zonal contributions should therefore be assessed jointly and under the scarcity conditions for which the capacity is procured. A flow-based representation would be better suited to this than independently scaled MEC values.

The spatial definition of the requirement is equally important. Broad zones are easier to implement and maintain competition, but they may hide decisive internal constraints. Finer zones or targeted qualification rules can strengthen the signal, although they also increase complexity and the possibility of local market power. The results do not determine the correct level of granularity, but they show that the choice cannot be separated from the lines and nodes that drive scarcity-state infeasibility.

A locational capacity mechanism should still be treated as one instrument within a wider set of measures. ENTSO-E similarly places locational elements in capacity mechanisms alongside grid development, bidding-zone reform, connection rules, and congestion management tools (ENTSO-E, 2026). The mechanism influences long-term capacity siting. It does not remove the network constraints or coordinate short-term dispatch.

Assessment should therefore not rely on capacity market expenditure alone. A cheaper auction can produce capacity that is less useful during scarcity, while a more expensive local requirement may preserve redispatch headroom and avoid grid-related load shedding. Procurement volume, capacity expenditure, redispatch, local headroom, and load shedding need to be considered together. Looking at only one of these outcomes would miss the main trade-off identified in the results.

### 6.3.2. Institutional and regulatory implications

The current European regulatory framework creates a tension for the design studied here. As discussed in Chapter 1, EU regulation treats capacity mechanisms as instruments for resource adequacy and excludes congestion-management measures from their scope (European Union, n.d.). A locational capacity mechanism could therefore not be justified only as a way to reduce routine redispatch costs.

The findings provide a different rationale. Capacity that cannot reach demand during scarcity does not make the same contribution to security of supply as capacity located on the useful side of the constraint. The local requirement can thus be understood as a deliverability condition within the adequacy assessment. Lower redispatch costs may follow, but they are not the only or necessarily the main reason for the intervention.

Whether this interpretation is compatible with the present legal framework cannot be answered by the model. It would require a separate legal assessment. ENTSO-E also notes that locational elements in capacity mechanisms may require regulatory reform and must remain consistent with state-aid and internal market principles (ENTSO-E, 2026). The thesis therefore provides an engineering and economic argument for including deliverability, but not a complete legal basis for doing so.

Implementation would also require a clear method for defining zones, local requirements, and cross-zonal contributions. These parameters may be technical, but they influence investment locations and capacity payments. They would therefore require regulatory oversight and periodic review.

The same applies to $\sigma$. It is an experimental parameter in this thesis and should not be interpreted as a policy value that can simply be selected. In practice, the contribution of neighboring capacity would have to follow from an assessment of scarcity-state deliverability. The institutional requirement is therefore relatively narrow but important: the mechanism needs a clear legal objective and a transparent method for translating network constraints into local requirements and transfer credits.

## 6.4. Areas for further research

A first extension concerns the representation of the network inside the capacity mechanism. The pairwise MEC limits used here could be replaced by a flow-based formulation. Adekola et al. (2026) apply this logic to coupled national capacity markets by embedding network constraints and scarcity scenarios directly in the market clearing. Applying the same approach to internal capacity market zones would account for simultaneous contributions, intra-zonal bottlenecks, and loop flows. The resulting flow-based outcome would provide a network-feasible benchmark for the degree and direction of cross-zonal participation, rather than relying on one common value of $\sigma$.

The definition of the capacity market zones also deserves further attention. The results show that a small number of lines and investment nodes can dominate deliverability, while the current requirements do not distinguish between nodes within one zone. Alternative boundaries could therefore be tested against the dominant structural constraints. A less granular option would be to retain the broader zones but limit how much capacity at particular locations can count towards the requirement. This would show whether most of the deliverability benefit can be retained without creating a highly fragmented capacity market.

A second extension is a dynamic and technology-neutral investment model. Storage, demand response, interconnectors, and other flexible resources may provide local capacity and redispatch capability differently from CCGT. Multiple investment years and endogenous retirement would also allow the gradual interaction between the locational signal and the inherited fleet to be studied. The comparison between the two case studies suggests that this transition over time is central to the practical relevance of the mechanism.

The timing of procurement could be varied as well. Resource adequacy may be secured several years ahead, while the local deliverability assessment is updated closer to delivery. Flexible technologies could be particularly relevant in such a layered design because they can respond more quickly than large conventional units (Gill et al., 2025).

A third extension concerns the temporal and computational representation. Full-year chronology, additional weather years, or targeted extreme-event sampling would provide a stronger test of scarcity and deliverability. The equilibrium exploration could be extended through additional or adaptive search directions, while tighter formulations could reduce the remaining solution gaps. This would help establish whether the observed ranges already cover the main relevant siting patterns or whether materially different outcomes remain unexplored.

Finally, the legal and institutional design requires separate research. This should examine whether internal deliverability can be included in the European resource-adequacy framework, how the technical methodology should be governed, and how the resulting costs should be allocated. Without this step, the mechanism remains a technically motivated design rather than an implementable policy proposal.

# 7 Conclusion

As the last chapter of this thesis, the conclusion wraps up the study by providing the answers to the sub- and research questions. This is followed by a personal reflection on the academic work conducted in this study. At last, the thesis and its results are connected to their societal relevance, as well as its connection to the CoSEM program.

## 7.1. Answering the research questions

SQ1: Which actors, decisions, and interactions must be represented in a zonal energy market with cost-based redispatch and a capacity mechanism?
The system consists of generators, two demand agents, and a market operator. The generators are divided into renewable, legacy controllable, and investable controllable generators. Renewable generators offer their available output at zero marginal cost and do not participate in the capacity market. Legacy controllable generators participate in both the energy and capacity markets, but their installed capacity and location are fixed. Investable controllable generators make the same operational decisions, while also deciding how much new capacity to build. They are therefore the only actors that can change the spatial distribution of controllable capacity in response to the locational signal.

The demand side is represented by separate energy and capacity demand agents. The energy demand agent serves demand up to the value of lost load, which also acts as the energy market price cap. The capacity demand agent procures sufficient capacity to meet the system-wide and zonal requirements and determines the cross-zonal allocation of capacity obligations within the defined transfer limits. The market operator acts after both markets have cleared. It takes the market dispatch as given and minimizes the cost of restoring network feasibility through upward redispatch, downward redispatch, and, where necessary, grid-related load shedding.

The energy and capacity markets are interdependent rather than strictly sequential. The expected revenues from both markets influence the investment decision, while installed capacity limits how much a generator can offer in the energy and capacity markets. Redispatch is the only genuinely sequential stage. Since it is cost-based and not anticipated by generators, it does not provide an additional investment incentive. The main channel through which the capacity market design influences congestion is therefore the siting of new controllable capacity. This siting determines the market dispatch, the available local redispatch headroom, and ultimately whether the network can remain feasible during scarcity.

SQ2: Which forms of locational signals exist in capacity mechanisms, and how do they function?
Locational signals in capacity mechanisms are mainly introduced to ensure that procured capacity is deliverable during scarcity. Aggregate resource adequacy only establishes that sufficient capacity exists in total. It does not establish that this capacity can reach load when transmission constraints become binding. Reducing congestion-management needs and supporting the co-development of generation and transmission are additional rationales. In this thesis, the locational signal is primarily

interpreted as a way to improve the deliverability of procured capacity. Lower redispatch volumes and costs may follow from better capacity siting, but they are treated as resulting benefits rather than the defining purpose of the mechanism.

The form of the signal depends on its spatial relationship with the energy market. The review distinguishes three archetypes. Archetype A uses the same spatial resolution for the energy and capacity markets, as in Chile and Italy. Archetype B aggregates the nodes of a nodal energy market into larger capacity market zones, as found in several US markets. Archetype C makes the capacity mechanism more spatially granular than the underlying energy market, as seen in targeted European mechanisms.

The key difference is that US capacity mechanisms operate on top of nodal energy markets, where the short-term value of location is already reflected in energy prices. Their capacity market zones add a coarser deliverability test to the system-wide resource-adequacy requirement. European zonal energy markets do not reflect internal transmission constraints in the market price. A locational capacity mechanism must therefore be more granular than the energy market if it is to influence internal siting.

Based on this, the design studied in this thesis adapts the nested US structure to a European zonal energy market. A system-wide capacity requirement provides resource adequacy, while three zonal requirements add a spatial condition for deliverability. Cross-zonal participation then relaxes this local condition. Capacity obligations can be shifted between connected zones up to the maximum entry capacity multiplied by $\sigma$. The transfer is zero-sum: a reduction in the obligation of one zone is matched by an increase elsewhere. At $\sigma = 0$, every zone remains responsible for its full local requirement. At $\sigma = 1$, obligations can be shifted up to the full pairwise transfer bound.

SQ3: How do locational signals affect capacity procurement, capacity siting, and congestion outcomes across the investigated scenarios?
The results show that the main effect of the locational signal is not a large change in aggregate capacity procurement. It is a change in where new controllable capacity is built and, consequently, how useful that capacity is once the network becomes constrained.

This effect is strongest in Case Study 1, where $87.5\%$ of the system-wide requirement has to be supplied by new capacity. The country-wide mechanism procures $16{,}722.7$ MW, while the split mechanism procures $16{,}789.2$ MW. The difference of $66.5$ MW, or $0.4\%$, results from the zonal residual-demand peaks not occurring at the same time. Capacity market expenditure increases from €$901.9$ million to €$930.7$ million. Most of this increase is caused by the different zonal prices rather than the additional procurement volume.

The change in siting is much larger. Under country-wide procurement, no new capacity is built in Zone 1, while $10.0$ GW is built in Zone 2. Strict zonal procurement instead directs $6.60$ GW towards Zone 1 and reduces investment in Zone 2 to $2.42$ GW. This relocation substantially changes the congestion outcomes. The observed redispatch range falls from $14.13$–$30.63$ TWh under country-wide procurement to zero–$2.37$ TWh under the split design. Grid-related load shedding falls from $2.30$–$5.86$ TWh to zero–$0.091$ TWh. Of the 80 explored strict-zonal outcomes, 50 require no grid-related load shedding at all.

Case Study 2 shows the same mechanism under a more constrained starting position. Legacy capacity already covers $97.4\%$ of the system-wide requirement, leaving only $436.0$ MW of new investment under country-wide procurement. This investment is built in Zone 2, even though the remaining local capacity deficit is located in Zone 3. Strict zonal procurement instead requires $2{,}400.1$ MW of new capacity in Zone 3. Capacity market expenditure consequently increases from €$76.2$–$91.5$ million to €$238.6$ million, partly because the positive zonal price is also paid to existing capacity in Zone 3.

Despite the higher expenditure, the spatial correction improves the network outcome. The observed redispatch range falls from $0.072$–$0.373$ TWh to $0.045$–$0.205$ TWh. More importantly, grid-related load shedding falls from $0.034$–$0.112$ TWh to zero in all 80 explored outcomes. Even when only the incremental investment can respond, placing it in the deficient zone is therefore sufficient to restore network feasibility throughout the explored set.

Cross-zonal participation weakens these effects. In Case Study 1, the total capacity requirement and total new investment remain unchanged, but obligations and investment progressively move from the more expensive Zone 1 towards Zone 2. Capacity market expenditure falls from €$930.7$ million at

$\sigma = 0$ to €$879.4$ million at $\sigma = 1$. At the same time, the redispatch range rises to $5.21$–$22.41$ TWh and grid-related load shedding to $0.453$–$2.204$ TWh. The outcome moves towards the country-wide design, although the locational signal is not fully removed.

In Case Study 2, cross-zonal participation can make use of existing legacy surpluses in Zones 1 and 2. It therefore reduces the need for new investment rather than only moving it between zones. At $\sigma = 0.25$, capacity market expenditure falls to €$109.5$ million while grid-related load shedding remains at zero. From $\sigma = 0.5$ onward, however, load shedding reappears as the remaining investment increasingly returns towards the country-wide siting pattern. The effect of participation is therefore not simply lower procurement cost. It depends on whether another zone already contains surplus capacity and on how far the local investment signal is relaxed.

Across the investigated scenarios, the locational signal consistently changes capacity siting and improves deliverability. Its effect on capacity market expenditure is less uniform and depends strongly on the inherited generation fleet. The physical results are therefore clearer than a comparison based only on capacity market or redispatch costs.

SQ4: What trade-offs and design implications for locational signaling in capacity markets follow from the model results?

The central trade-off is between lower and more flexible capacity procurement on one side, and protection against adverse capacity siting on the other. A strict zonal requirement can increase capacity market expenditure because capacity has to be procured in more expensive or locally deficient zones. However, it also ensures that controllable capacity is available on the useful side of important transmission constraints. The resulting benefit is not limited to lower redispatch volume. More importantly, the system retains local upward redispatch headroom and is less likely to require grid-related load shedding.

Cross-zonal participation can reduce the additional cost of the locational design. In Case Study 1, it shifts procurement towards a cheaper zone. In Case Study 2, limited participation allows existing surplus capacity to contribute to a neighboring deficit and reduces the need for new investment. However, the same relaxation weakens the locational investment signal and increases reliance on the transmission grid. Once participation becomes sufficiently large, the dominant bottlenecks and grid-related load shedding return.

There is therefore no value of $\sigma$ that is generally preferable. In Case Study 2, $\sigma = 0.25$ preserves the full observed deliverability benefit while substantially reducing capacity market expenditure. The same balance does not automatically apply to Case Study 1 or to another network. The suitable level of participation depends on the available transfer capability, the location of existing capacity, and whether the credited contribution remains simultaneously deliverable during scarcity.

The monetary comparison also depends on the value assigned to grid-related load shedding. In Case Study 1, the break-even values remain below €$61$/MWh, meaning that the reduction in load shedding compensates for the additional procurement cost even at a low valuation. In Case Study 2, strict zonal procurement requires a higher valuation of approximately €$1{,}357$–$4{,}784$/MWh. Limited participation lowers this range, while higher participation produces no uniform cost advantage across the explored outcomes. The exact total-cost ranking is therefore conditional on the assumed value of lost load. The physical finding that locational procurement improves deliverability is more robust.

Several design implications follow. First, internal deliverability should be considered where transmission constraints can prevent aggregate capacity from serving load during scarcity. Second, cross-zonal contributions should be based on simultaneous physical deliverability rather than nominal pairwise transfer capability alone. Third, the timing of implementation matters. A locational signal has the largest effect while substantial investment and replacement decisions are still open. Once most of the generation fleet is fixed, it can only correct the remaining shortages at the margin.

Lastly, a locational capacity mechanism should not be treated as a replacement for grid expansion, bidding-zone reform, nodal pricing, or operational congestion management. It does not remove transmission constraints or coordinate hourly dispatch. Its role is more limited but still relevant: it influences the long-term spatial availability of controllable capacity and reduces the risk that resource adequacy cannot be translated into feasible supply during scarcity.

**To what extent do locational signals in capacity markets shape the trade-off between capacity procurement costs and congestion outcomes in a zonal energy market?**

Within the investigated Dutch case studies, locational signals materially shape this trade-off. The trade-off is asymmetric. The signal reshapes where capacity sits, and therefore its deliverability, far more than it changes total procurement cost. The cost arm moves only a few percent in Case Study 1, while feasibility changes substantially. Separate zonal requirements increase or reallocate capacity market expenditure, but they also redirect new controllable capacity towards locally deficient parts of the system. This reduces redispatch exposure and, more importantly, improves the ability of the system to restore network feasibility during scarcity.

The strength of the result is conditional. Cross-zonal participation determines how much of the local signal is retained, while the inherited generation fleet determines how much capacity can still respond. Where most controllable capacity has to be built, the mechanism can substantially reshape the system. Where most capacity already exists, its influence is smaller but can still be decisive for the remaining local deficit.

The locational signal therefore does not provide one universally optimal capacity market design. It shifts part of the cost from ex-post congestion management towards ex-ante procurement of more deliverable capacity. Limited cross-zonal participation can reduce this additional cost without removing the benefit, particularly where surplus legacy capacity is available. Too much participation, however, can undermine the deliverability condition and move the result back towards country-wide procurement. The relevant policy question is consequently more than how much capacity should be procured, but how much local capacity is needed to ensure that the procured capacity remains useful when the network is constrained.

## 7.2. Contribution and academic reflection

This thesis contributes a model that separates the capacity market cost of a locational signal from its congestion outcomes. Existing studies generally evaluate locational capacity mechanisms as part of a combined system-cost assessment or focus mainly on redispatch volumes (Hladik et al., 2020; Thomassen & Fuhrmanek, 2025). That framing makes it difficult to observe the precise capacity market costs and, more importantly, how deliverability is affected. Separating these outcomes, and reporting grid-related load shedding as its own outcome, is the central conceptual step of this work.

The second contribution is methodological. The results are treated as a space rather than a point: sweeping PTDF-based exploration weights shows that several siting patterns can clear the same market at identical cost, each with different redispatch consequences. This makes it possible to identify deliverability, rather than capacity market or redispatch costs, as the outcome that responds most consistently to a locational signal.

Keeping this model solvable was itself an exercise in the complexity management that motivated the research approach in Section 1.3. The measures taken map onto the categories reviewed by Kotzur et al. (2021). Scope reduction avoids complexity: storage, demand response, and risk aversion are excluded because they are not central to isolating the investigated mechanism. Temporal aggregation reduces the year to eight representative days. However, due to the nature of the study, both temporal and spatial aggregation were limited. Missing extreme conditions through temporal aggregation or hiding internal congestion through spatial aggregation would weaken the analysis. The main computational choice was therefore the solution method. Reformulating the complementarity conditions through disjunctive constraints makes the first stage solvable as a MILP. The sequential structure then separates the market-equilibrium stage from redispatch, while a warm start helps provide a feasible incumbent for the more difficult Case Study 2 runs. The model therefore remained solvable through deliberate choices along every complexity dimension, while aiming to affect the resulting solutions as little as possible.

The main result should therefore not be read as an estimate of the optimal capacity market design for the Netherlands. What the model shows is that locational procurement can improve deliverability even when its effect on redispatch costs is unclear, and that this benefit weakens as more cross-zonal participation is allowed. The exact magnitudes depend on the modeled network, generation fleet, and explored equilibria. A direct next step is therefore to replace the current MEC-based representation of cross-zonal participation with a flow-based one. This would show whether the deliverability benefit remains when simultaneous contributions between zones are limited by the same network constraints that later determine redispatch.

## 7.3. Personal reflection

The first challenge I encountered was learning a new programming language in Julia. The first weeks were slow. Getting used to it took time. But after a few weeks it started to become easier, especially with the support of AI. I think that is also a good learning for myself in terms of AI use: learning a new programming language can be much easier with it. While this is less so in writing code, where it can also help accelerate the learning curve, it was especially helpful in diagnosing errors. With a new programming language, errors are frequent in the beginning, and AI proved helpful in identifying them and explaining what exactly the issue was, helping to prevent similar issues in the future (see Appendix E for details on AI use).

For the modeling, I knew going in that high spatial resolution comes with longer computing times, but I did not expect it to the extent I encountered, and because of this I underestimated how long the model development would take. On top of that, I didn't really have a blueprint for how to model my problem. The main challenge here was the exploration of the solution space, and many of these decisions didn't have one right answer. It was less about finding the correct solution and more about choosing an approach and being able to justify it, weighing things like tractability and what the model actually needed to capture. It was also the amount of small decisions at every step that I underestimated. While they are small in isolation, they added up quickly, especially when considered in the context of how they influence and are influenced by other decisions. Overall, CoSEM provided me with the foundational skills for building this model, but what I had to learn in the end clearly exceeded that.

The literature was a challenge in a different way. European perspectives on my specific topic were rare, and much of the relevant US material came from technical reports rather than academic papers. Finding a structure for the literature review was therefore difficult. There was no obvious way to organize it, and it took several attempts before it worked.

If I were to do one thing differently, I would keep the precise research goal in mind more often. Some things, like the model formulation, I simply had to learn first, and I can't really fault myself for that. But I sometimes lost myself in details and small decisions that had to be made, yet honestly had very little impact on my actual research question. Keeping the bigger picture in mind, especially in the middle part of my thesis, would have helped.

# References


Adekola, K., de Vries, L., & Bruninx, K. (2026). Coupling europe's capacity markets. https://doi.org/10.48550/arXiv.2603.08248

Askeland, M., Jaehnert, S., & Korpås, M. (2019). Equilibrium assessment of storage technologies in a power market with capacity remuneration. *Sustainable Energy Technologies and Assessments*, *31*, 228–235. https://doi.org/10.1016/j.seta.2018.12.012

Aurora Energy Research. (2025, January). Capacity remuneration mechanisms report [Aurora BFF, January 2025]. Retrieved May 25, 2025, from https://auroraer.com/wp-content/uploads/2025/01/Capacity-Remuneration-Mechanisms-Report-Aurora-BFF-January-2025.pdf

BDEW. (2023). *Fakten: Redispatch in Deutschland – Auswertung der Transparenzdaten April 2013 bis einschließlich Dezember 2022*. BDEW – Bundesverband der Energie- und Wasserwirtschaft. Retrieved November 19, 2025, from https://www.bdew.de/service/anwendungshilfen/fakten-redispatch-in-deutschland/

Benedettini, S. (2013). PJM and ISO-NE forward capacity markets: A critical assessment. *Research Report Series*. https://scholar.google.com/scholar_lookup?title=PJM%20and%20ISO-NE%20Forward%20Capacity%20Markets%3A%20a%20Critical%20Assessment&author=S.%20Benedettini&publication_year=2013

Blachnik, M., Wawrzyniak, K., & Jakubek, M. (2021). Partitioning Power Grid for the Design of the Zonal Energy Market While Preserving Control Area Constraints. *Electronics*, *10*(5), 610. https://doi.org/10.3390/electronics10050610

Brown, T., Victoria, M., Zeyen, E., Hofmann, F., Neumann, F., Frysztacki, M., Hampp, J., Schlachtberger, D., Hörsch, J., Schledorn, A., Schauß, C., van Greevenbroek, K., Millinger, M., Glaum, P., Xiong, B., & Seibold, T. (n.d.). *PyPSA-Eur: An open sector-coupled optimisation model of the European energy system* (Version v2026.02.0). Retrieved June 4, 2026, from https://github.com/PyPSA/pypsa-eur/blob/master/doc/limitations.md

Bucksteeg, M., Spiecker, S., & Weber, C. (2019). Impact of coordinated capacity mechanisms on the european power market. *The Energy Journal*, *40*(2), 221–264. https://doi.org/10.5547/01956574.40.2.mbuc

CAISO. (2026). *Final 2027 Local Capacity Technical Study Report* (Rulemaking 25-10-003). https://www.caiso.com/documents/may-1-2026-final-2027-local-capacity-technical-report-and-update-regarding-2027-flexible-capacity-needs-assessment-resource-adequacy-program-r-25-10-003.pdf

Cepeda, M. (2018). Assessing cross-border integration of capacity mechanisms in coupled electricity markets. *Energy Policy*, *119*, 28–40. https://doi.org/https://doi.org/10.1016/j.enpol.2018.04.016

Chappin, E. (2021). *TU Delft - Bathtub model* [YouTube, 546 views (as of retrieval date)]. TU Delft. Retrieved December 15, 2025, from https://www.youtube.com/watch?v=HoWSnQbxscc

Cruickshank, A., Dervieux, C., Barroso, L., Mastropietro, P., Batlle, C., Keech, A., & de Vries, L. J. (2016, February). *Capacity mechanisms: Needs, solutions and state of affairs Working Group C5.17*. CIGRÉ. https://www.researchgate.net/publication/356064023_Capacity_mechanisms_needs_solutions_and_state_of_affairs_Working_Group_C517

de Vries, L., & Heijnen, P. (2008). The impact of electricity market design upon investment under uncertainty: The effectiveness of capacity mechanisms. *Utilities Policy*, *16*(3), 215–227. https://doi.org/10.1016/j.jup.2007.12.002

Dimanchev, E., Gabriel, S. A., Reichenberg, L., & Korpås, M. (2024). Consequences of the missing risk market problem for power system emissions. *Energy Economics*, *136*, 107639. https://doi.org/10.1016/j.eneco.2024.107639

Draghi, Z., DiLorenzo, A., Cohen, E., Chow, L., Gannon, J. R., & Barcic, N. (2025). *2023 Resource Adequacy Report*. California Pubilc Utilities Comission. https://www.cpuc.ca.gov/-/media/cpuc-website/divisions/energy-division/documents/resource-adequacy-homepage/2023-resource-adequacy-reportv2.pdf

Duan, J., van Kooten, G. C., & Liu, X. (2020). Renewable electricity grids, battery storage and missing money. *Resources, Conservation and Recycling*, *161*, 105001. https://doi.org/10.1016/j.resconrec.2020.105001

ECCO International. (2024). *Design of a Bid-based Wholesale Energy Market, Ancillary Services and Capacity Market in Chile*. Coordinador Electrico Nacional. https://www.coordinador.cl/wp-content/uploads/2024/07/ECCO_CEN_ENERGY_MARKET_DESIGN_ENG_2024.pdf

Ecorys & SEO Economic Research. (2022). *The value of lost load for electricity in the netherlands* (tech. rep.). Netherlands Authority for Consumers and Markets.

Ehrenmann, A., & Smeers, Y. (2011). Generation capacity expansion in a risky environment: A stochastic equilibrium analysis. *Operations Research*, *59*(6), 1332–1346. Retrieved December 3, 2025, from http://www.jstor.org/stable/41316039

Eicke, A., Khanna, T., & Hirth, L. (2020). Locational investment signals: How to steer the siting of new generation capacity in power systems? *The Energy Journal*, *41*. https://doi.org/10.5547/01956574.41.6.aeic

Eicke, A., & Schittekatte, T. (2022). Fighting the wrong battle? a critical assessment of arguments against nodal electricity prices in the European debate. *Energy Policy*, *170*, 113220. https://doi.org/https://doi.org/10.1016/j.enpol.2022.113220

ENTSO-E. (n.d.). Grid Map. Retrieved May 24, 2026, from https://www.entsoe.eu/data/map/

ENTSO-E. (2025). *The role of capacity mechanisms to enable a secure and competitive energy transition*. Retrieved November 20, 2025, from https://www.entsoe.eu/2025/04/16/entso-e-paper-on-the-role-of-capacity-mechanisms-to-enable-a-secure-and-competitive-energy-transition/

ENTSO-E. (2026). *Market Design Options for Congestion Management*. https://eepublicdownloads.blob.core.windows.net/public-cdn-container/clean-documents/Publications/Position%20papers%20and%20reports/2026/ENTSO-E_Market_Design_Options_CM_260611.pdf

European Commission. (2025). Energy. Retrieved November 19, 2025, from https://commission.europa.eu/topics/energy_en

European Union. (n.d.). Regulation (eu) 2019/943 of the european parliament and of the council of 5 june 2019 on the internal market for electricity (recast). https://eur-lex.europa.eu/legal-content/EN/TXT/?uri=CELEX:02019R0943-20240716

Fabra, N. (2018). A primer on capacity mechanisms. *Energy Economics*, *75*, 323–335. https://doi.org/10.1016/j.eneco.2018.08.003

Finon, D., & Roques, F. (2013). European electricity market reforms: The “visible hand” of public coordination. *Economics of Energy & Environmental Policy*, *2*(2), 107–124. Retrieved May 24, 2025, from http://www.jstor.org/stable/26189459

Fraunholz, C., Hladik, D., Keles, D., MÃ¶st, D., & Fichtner, W. (2020). *On the long-term efficiency of market splitting in germany* (Working Paper Series in Production and Energy No. 38). Karlsruhe Institute of Technology (KIT), Institute for Industrial Production (IIP). https://doi.org/10.5445/IR/1000105902

Fraunholz, C., Miskiw, K. K., Kraft, E., Fichtner, W., & Weber, C. (2023). On the role of risk aversion and market design in capacity expansion planning. *The Energy Journal*, *44*(3), 111–138. https://doi.org/10.5547/01956574.44.2.cfra

Gabriel, S. A., Conejo, A. J., Fuller, J. D., Hobbs, B. F., & Ruiz, C. (2013). *Complementarity Modeling in Energy Markets* (Vol. 180). Springer. https://doi.org/10.1007/978-1-4419-6123-5

Gabriel, S. A., & Leuthold, F. U. (2010). Solving discretely-constrained MPEC problems with applications in electric power markets. *Energy Economics*, *32*(1), 3–14. https://doi.org/10.1016/j.eneco.2009.03.008

Gilbert, A., Sovacool, B. K., Johnstone, P., & Stirling, A. (2017). Cost overruns and financial risk in the construction of nuclear power reactors: A critical appraisal. *Energy Policy*, *102*, 644–649. https://doi.org/10.1016/j.enpol.2016.04.001

Gill, S., Maclever, C., Gross, R., & Bell, K. (2025). *Locational Signals in a Reformed National Market: A review of options*. UK Energy Research Centre. Retrieved March 9, 2026, from https://ukerc.ac.uk/publications/locational-signals-in-a-reformed-national-market-a-review-of-options/

Gomez, T., Herrero, I., Rodilla, P., Escobar, R., Lanza, S., de la Fuente, I., Llorens, M. L., & Junco, P. (2019). European Union Electricity Markets: Current Practice and Future View. *IEEE Power and Energy Magazine*, *17*(1), 20–31. https://doi.org/10.1109/MPE.2018.2871739

Grimm, V., Martin, A., Sölch, C., Weibelzahl, M., & Zöttl, G. (2022). Market-Based Redispatch May Result in Inefficient Dispatch [Num Pages: 205-230]. *The Energy Journal*, *43*(5), 205–230. https://doi.org/10.5547/01956574.43.5.csol

Gurobi Optimization, LLC. (2024). Gurobi Optimizer Reference Manual. https://www.gurobi.com

Hatton, L., Johnson, N., Dixon, L., Mosongo, B., De Kock, S., Marquard, A., Howells, M., & Staffell, I. (2024). The global and national energy systems techno-economic (gneste) database: Cost and performance data for electricity generation and storage technologies. *Data in Brief*, *55*, 110669. https://doi.org/https://doi.org/10.1016/j.dib.2024.110669

Hickey, C., Bunn, D., Deane, P., McInerney, C., & Ó Gallachoir, B. (2021). The variation in capacity remunerations requirements in european electricity markets. *The Energy Journal*, *42*(2), 135–164. https://doi.org/10.5547/01956574.42.2.chic

Hirth, L., & Schlecht, I. (2020). *Market-Based Redispatch in Zonal Electricity Markets: The Preconditions for and Consequence of Inc-Dec Gaming* (Working Paper). Kiel, Hamburg: ZBW – Leibniz Information Centre for Economics. Retrieved May 18, 2026, from https://www.econstor.eu/handle/10419/222925

Hladik, D., Fraunholz, C., Kühnbach, M., Manz, P., & Kunze, R. (2020). Insights on Germany's future congestion management from a multi-model approach. *Energies*, *13*(16), 4176. https://doi.org/10.3390/en13164176

Hörsch, J., Hofmann, F., Schlachtberger, D., & Brown, T. (2018). Pypsa-eur: An open optimisation model of the european transmission system. *Energy Strategy Reviews*, *22*, 207–215. https://doi.org/10.1016/j.esr.2018.08.012

Höschle, H., Le Cadre, H., & Belmans, R. (2018). Inefficiencies caused by non-harmonized capacity mechanisms in an interconnected electricity market. *Sustainable Energy, Grids and Networks*, *13*, 29–41. https://doi.org/10.1016/j.segan.2017.11.002

Höschle, H., Le Cadre, H., Smeers, Y., Papavasiliou, A., & Belmans, R. (2018). An admm-based method for computing risk-averse equilibrium in capacity markets. *IEEE Transactions on Power Systems*, *33*(5), 4819–4830. https://doi.org/10.1109/tpwrs.2018.2807738

IEA. (2016). *Re-powering markets: Market design and regulation during the transition to low-carbon power systems* (Licence: CC BY 4.0). International Energy Agency. Paris. https://www.iea.org/reports/re-powering-markets

IEA. (2021). *Net Zero by 2050 – Net Zero by 2050 - A Roadmap for the Global Energy Sector*. Retrieved June 5, 2026, from https://www.iea.org/reports/net-zero-by-2050

IEA. (2025). *Electricity Market Design*. IEA. Paris.

IRENA. (2025). Renewable capacity statistics 2025. Retrieved November 19, 2025, from https://www.irena.org/-/media/Files/IRENA/Agency/Publication/2025/Mar/IRENA_DAT_RE_Capacity_Statistics_2025.pdf

ISO New England. (2026). *Market Rule 1*. https://www.iso-ne.com/participate/rules-procedures/tariff/market-rule-1

Janda, K., Málek, J., & Rečka, L. (2017). Influence of renewable energy sources on transmission networks in central Europe. *Energy Policy*, *108*, 524–537. https://doi.org/https://doi.org/10.1016/j.enpol.2017.06.021

Kang, C. Q., Chen, Q. X., Lin, W. M., Hong, Y. R., Xia, Q., Chen, Z. X., Wu, Y., & Xin, J. B. (2013). Zonal marginal pricing approach based on sequential network partition and congestion contribution identification. *International Journal of Electrical Power & Energy Systems*, *51*, 321–328. https://doi.org/10.1016/j.ijepes.2013.02.033

Kenis, M., Dvorkin, V., Schittekatte, T., Bruninx, K., Delarue, E., & Botterud, A. (2024). Evaluating Offshore Electricity Market Design Considering Endogenous Infrastructure Investments: Zonal or Nodal? *Policy and Regulation IEEE Transactions on Energy Markets*, *2*(4), 476–487. https://doi.org/10.1109/TEMPR.2024.3399611

Kotzur, L., Nolting, L., Hoffmann, M., Groß, T., Smolenko, A., Priesmann, J., Büsing, H., Beer, R., Kullmann, F., Singh, B., Praktiknjo, A., Stolten, D., & Robinius, M. (2021). A modeler's guide to handle complexity in energy systems optimization. *Advances in Applied Energy*, *4*, 100063. https://doi.org/10.1016/j.adapen.2021.100063

KU Leuven Energy Systems Integration and Modeling group. (2023). RepresentativePeriodsFinder.jl [Julia package documentation]. Retrieved June 5, 2026, from https://ucm.pages.gitlab.kuleuven.be/representativeperiodsfinder.jl/

Kunz, F., & Zerrahn, A. (2015). Benefits of coordinating congestion management in electricity transmission networks: Theory and application to Germany. *Utilities Policy*, *37*, 34–45. https://doi.org/10.1016/j.jup.2015.09.009

Kwon, C. (2019). *Operations research: Julia programming for operations research* (2nd ed.). Changhyun Kwon. https://www.chkwon.net/julia/

Lawson, A. J. (2025). *PJM's Electric Capacity Market: Background and Current Issues*. Congressional Research Service. Retrieved March 16, 2026, from https://www.congress.gov/crs-product/R48553

Legat, B., Garcia, J. D., & contributors. (2026). *Dualization.jl* (Version v0.7.6). GitHub. https://github.com/jump-dev/Dualization.jl

Lété, Q., Smeers, Y., & Papavasiliou, A. (2022). An analysis of zonal electricity pricing from a long-term perspective. *Energy Economics*, *107*, 105853. https://doi.org/10.1016/j.eneco.2022.105853

Lété, Q., Smeers, Y., & Papavasiliou, A. (2026). Power Generation Investment Under Zonal Electricity Pricing with Market-Based Re-dispatch. *The Energy Journal*, *47*(1), 131–164. https://doi.org/10.1177/01956574251367717

Leuthold, F. U., Weigt, H., & von Hirschhausen, C. (2012). A Large-Scale Spatial Optimization Model of the European Electricity Market. *Networks and Spatial Economics*, *12*(1), 75–107. https://doi.org/10.1007/s11067-010-9148-1

Lorenczik, S. (2019). Interaction effects of market failure and crms in interconnected electricity markets. *Energy Policy*, *135*, 110961. https://doi.org/10.1016/j.enpol.2019.110961

Lubin, M., Dowson, O., Garcia, J. D., Huchette, J., Legat, B., & Vielma, J. P. (2023). Jump 1.0: Recent improvements to a modeling language for mathematical optimization. *Mathematical Programming Computation*, *15*(3), 581–589. https://doi.org/10.1007/s12532-023-00239-3

Martin, P., Christine, B., Gert, B., & Marius, B. (2022). Strategic behavior in market-based redispatch: International experience. *The Electricity Journal*, *35*(3), 107095. https://doi.org/10.1016/j.tej.2022.107095

McCullough, R., Weisdorf, M., Ende, J.-C., & Absar, A. (2020). Exactly how inefficient is the PJM capacity Market? *The Electricity Journal*, *33*(8), 106819. https://doi.org/10.1016/j.tej.2020.106819

Mendelevitch, R., Gores, S., Ritter, D., Dünzen, K., & Cook, V. (2024). *EU 2040 Climate Target: Contributions of the Energy Supply Sector* (tech. rep.). Oeko-Institut. Retrieved June 5, 2026, from https://www.oeko.de/fileadmin/oekodoc/Sector_Papers-Energy_7.pdf?utm_source=chatgpt.com

Menegatti, E. S., & Meeus, L. (2024). *Cross-border participation: A false hope for fixing capacity market externalities?* (RSC Working Paper No. 2024/53). European University Institute, Robert Schuman Centre for Advanced Studies. Retrieved December 17, 2025, from https://hdl.handle.net/1814/77489

Middlemiss, L., Mulder, P., Hesselman, M., Feenstra, M., Tirado Herrero, S., & Straver, K. (2020). *Energy poverty and the energy transition: Towards improved energy poverty monitoring, measuring and policy action*. TNO. https://publications.tno.nl/publication/34637565/tst4jN/TNO-2020-energy.pdf

Miro. (n.d.). Diagram maker | create a diagram. Retrieved December 17, 2025, from https://miro.com/diagramming/

MISO. (2026). *Business Practices Manual: Resource Adequacy* (BPM-011-r34). https://www.misoenergy.org/legal/rules-manuals-and-agreements/business-practice-manuals/

Nieto, A. D., & Fraser, H. (2007). Locational Electricity Capacity Markets: Alternatives to Restore the Missing Signals. *The Electricity Journal*, *20*(2), 10–26. https://doi.org/10.1016/j.tej.2006.12.006

NYISO. (2023). *Locational Minimum Installed Capacity Requirements Determination Process*. https://www.nysrc.org/wp-content/uploads/2023/04/LCR-determination-process.pdf

NYISO. (2026). *Installed Capacity Manual* (Version: 17.0). https://www.nyiso.com/documents/20142/2923301/M-04-ICAP-v17.0-Final.pdf/234db95c-9a91-66fe-7306-2900ef905338

Papavasiliou, A. (2021). *Overview of EU Capacity Remuneration Mechanisms*. Greek Regulatory Authority for Energy (RAE). https://www.raaey.gr/energeia/wp-content/uploads/2021/05/Report-I-CRM-final.pdf?_rt=N3wxfHJlY29ydGFyIGltYWdlbiBhIGZvcm1hfDE3NDk0MzIyMjQ&_rt_nonce=d356c588b8

Pfenninger, S., Hawkes, A., & Keirstead, J. (2014). Energy systems modeling for twenty-first century energy challenges. *Renewable and Sustainable Energy Reviews*, *33*, 74–86. https://doi.org/10.1016/j.rser.2014.02.003

Pfenninger, S., Hirth, L., Schlecht, I., Schmid, E., Wiese, F., Brown, T., Davis, C., Gidden, M., Heinrichs, H., Heuberger, C., Hilpert, S., Krien, U., Matke, C., Nebel, A., Morrison, R., Müller, B., Pleßmann, G., Reeg, M., Richstein, J. C., … Wingenbach, C. (2018). Opening the black box of energy modelling: Strategies and lessons learned. *Energy Strategy Reviews*, *19*, 63–71. https://doi.org/10.1016/j.esr.2017.12.002

PJM. (2025). *PJM Manual 18: PJM Capacity Market* (Revision 62). Retrieved May 15, 2026, from https://www.miso-pjm.com/-/media/DotCom/documents/manuals/m18-redline.ashx

Poncelet, K., Höschle, H., Delarue, E., Virag, A., & D'haeseleer, W. (2016). Selecting representative days for capturing the implications of integrating intermittent renewables in generation expansion planning problems. *IEEE Transactions on Power Systems*, *32*(3), 1936–1948. https://doi.org/10.1109/TPWRS.2016.2596803

Poplavskaya, K., Joos, M., Krakowski, V., Knorr, K., & de Vries, L. (2020). Redispatch and balancing: Same but different. Links, conflicts and solutions. https://doi.org/10.1109/eem49802.2020.9221963

Purchala, K., Meeus, L., Van Dommelen, D., & Belmans, R. (2005). Usefulness of DC power flow for active power flow analysis [ISSN: 1932-5517]. *IEEE Power Engineering Society General Meeting, 2005*, 454–459 Vol. 1. https://doi.org/10.1109/PES.2005.1489581

Roques, F. (2019). Counting on the neighbours: Challenges and practical approaches for cross-border participation in capacity mechanisms. *Oxford Review of Economic Policy*, *35*(2), 332–349. https://doi.org/10.1093/oxrep/grz008

S. Oliveira, F., William-Rioux, B., & Pierru, A. (2023). Capacity expansion in liberalized electricity markets with locational pricing and renewable energy investments. *Energy Economics*, *127*, 106958. https://doi.org/10.1016/j.eneco.2023.106958

Serra, P. (2022). Chile's electricity markets: Four decades on from their original design. *Energy Strategy Reviews*, *39*, 100798. https://doi.org/10.1016/j.esr.2021.100798

Siemer, J. (2026, March). Kernpunkte zum EEG-Entwurf vom Bundeswirtschaftsministerium bestätigt. Retrieved April 21, 2026, from https://www.pv-magazine.de/2026/03/23/kernpunkte-zum-eeg-entwurf-vom-bundeswirtschaftsministerium-bestaetigt/

Spees, K., Newell, S. A., & Pfeifenberger, J. P. (2013). Capacity Markets - Lessons Learned from the First Decade. *Economics of Energy & Environmental Policy*, *2*(2). https://doi.org/10.5547/2160-5890.2.2.1

Subramanian, A. S. R., Gundersen, T., & Adams, T. A. (2018). Modeling and simulation of energy systems: A review. *Processes*, *6*(12), 238. https://doi.org/10.3390/pr6120238

Thomaßen, G., & Fuhrmanek, A. (2025). Where to build renewables in Europe? The benefits of locational auction design. *Energy Economics*, *147*. https://doi.org/10.1016/j.eneco.2025.108579

Thomassen, G., & Fuhrmanek, A. (2025). *Locational price signals in Europe: Future-proofing the European power market* (JRC142047). Publications Office of the European Union. Luxembourg (Luxembourg). https://doi.org/10.2760/7466842

Thomassen, G., Fuhrmanek, A., Cadenovic, R., Pozo, C. D., & Vitiello, S. (2024). *Redispatch and Congestion Management* (ISBN: 9789268154137 9789268160213 ISSN: 1831-9424, 1831-9424). Publications Office of the European Union. https://doi.org/10.2760/853898

Trepper, K., Bucksteeg, M., & Weber, C. (2015). Market splitting in Germany – new evidence from a three-stage numerical model of europe. *Energy Policy*, *87*, 199–215. https://doi.org/https://doi.org/10.1016/j.enpol.2015.08.016

Van den Bergh, K., Delarue, E., & D'haeseleer, W. (2014). DC power flow in unit commitment models. *WP EN2014-12*. https://www.mech.kuleuven.be/en/tme/research/energy_environment/pdf/wpen2014-12.pdf

Virtanen, P., Gommers, R., Oliphant, T. E., Haberland, M., Reddy, T., Cournapeau, D., Burovski, E., Peterson, P., Weckesser, W., Bright, J., van der Walt, S. J., Brett, M., Wilson, J., Millman, K. J., Mayorov, N., Nelson, A. R. J., Jones, E., Kern, R., Larson, E., … SciPy 1.0 Contributors. (2020). SciPy 1.0: Fundamental Algorithms for Scientific Computing in Python. *Nature Methods*, *17*, 261–272. https://doi.org/10.1038/s41592-019-0686-2

Wu, F., & Pfenninger, S. (2023). Challenges and opportunities for bioenergy in Europe: National deployment, policy support, and possible future roles. *Bioresource Technology Reports*, *22*, 101430. https://doi.org/10.1016/j.biteb.2023.101430

# A

# Design options for locational signals in capacity mechanisms

Table A.1 synthesises the design options across all markets discussed in Section 2.2. The terms it uses to classify them (local requirements, constraint tests, and feasibility checks) are defined and illustrated per market in the notes that follow the table.

**Table A.1:** Synthesis of locational signal design options in capacity mechanisms.

| Category | Design option | Markets |
|---|---|---|
| Zone definition | Nodal (matching energy market) | Chile |
| | Energy market bidding zones | Italy |
| | Transmission-test-based | PJM, ISO-NE, NYISO, MISO, CAISO |
| | Targeted (single location tender) | France, Germany |
| | Not applicable (no zonal representation in auction) | Ireland |
| Zone structure | Nested (zones within zones) | PJM |
| | Flat (constrained zones vs. rest-of-system) | ISO-NE, CAISO |
| | Hybrid (mostly flat with nested or sub-regional element) | NYISO, MISO |
| | Not applicable (nodal, single zone, or no zonal representation) | Chile, Italy, France, Germany, Ireland |
| Zone stability | Dynamic (re-evaluated per auction) | PJM, ISO-NE |
| | Fixed (multi-year or permanent) | NYISO, MISO, CAISO, Italy |
| | One-off intervention | France, Germany |
| | Not applicable (nodal or no zonal representation) | Chile, Ireland |
| Constraint direction | Import only | PJM, NYISO, CAISO |
| | Import and export | ISO-NE, MISO |
| | Not applicable (nodal, single zone, or targeted tender) | Chile, Italy, France, Germany, Ireland |

*continued on next page*

Table A.1 – continued from previous page

| Category | Design option | Markets |
|---|---|---|
| Local requirement expression | MW volume | PJM, ISO-NE, MISO, CAISO |
| | Percentage of total obligation | NYISO |
| | Not applicable (nodal administrative pricing) | Chile |
| | Not applicable (capacity-market zones follow energy-market zones) | Italy |
| | Selective acceptance of additional capacity | Ireland |
| | Tender volume for a targeted area | France, Germany |
| Procurement mechanism | Centralised forward auction | PJM, ISO-NE, Italy |
| | Residual auction (mostly bilateral) | NYISO, MISO |
| | Purely bilateral | CAISO |
| | Administrative price-based payment | Chile |
| | Targeted tender | France, Germany |
| | Centralised auction (selective acceptance) | Ireland |
| Locational price signal | Zonal clearing price differentiation | PJM, ISO-NE, Italy |
| | Local procurement obligation (quantity signal) | NYISO, MISO, CAISO |
| | Nodal administrative price | Chile |
| | Tender price (targeted location) | France, Germany |
| | Selective TSO acceptance at the bid price | Ireland |
| Granularity vs. energy market | Equal (CM = energy market) | Chile, Italy |
| | Coarser (CM aggregates energy nodes) | PJM, ISO-NE, NYISO, MISO, CAISO |
| | More local (targeted procurement beneath an aggregate market) | France, Germany, Ireland |

## Per market mechanics in the US

**PJM.** An LDA is only modeled separately, with its own reliability requirement, once it is identified as constrained: if PJM identifies a reliability concern in the area, if it carried a locational price adder in one of the three preceding rounds, or through the Load Deliverability Analysis (PJM, 2025). Beyond the main forward auction, which clears three to four years ahead of an annual delivery period (Spees et al., 2013), PJM runs a Conditional Incremental Auction to procure additional capacity in an LDA when a backbone transmission line is delayed (Benedettini, 2013; PJM, 2025), giving the locational element a faster reaction path when transmission assumptions move.

**ISO-NE.** Constrained zones are determined dynamically for each auction: the most recent transmission transfer capability assessment identifies potentially constrained zones, which are then tested to confirm they are actually constrained (ISO New England, 2026). An import-constrained zone receives a Local Sourcing Requirement (LSR), the minimum capacity that must clear inside it. An export-constrained zone receives a Maximum Capacity Limit (MCL), which caps how much capacity may clear in it (ISO New England, 2026). The auction is a descending clock auction run simultaneously for the main and constrained zones, stopping when bid volume meets the requirement. Like PJM it clears three to four years ahead (Spees et al., 2013).[1]

[1] ISO-NE's final Forward Capacity Auction was held in February 2024 for the 2027–2028 Capacity Commitment Period; no further FCAs will be held (ISO New England, 2026).

**CAISO.** CAISO identifies import-constrained areas through an annual Local Capacity Technical Analysis based on reliability standards (Draghi et al., 2025; Spees et al., 2013). Ten such areas currently exist. Each load serving entity must cover 115% of its historic peak load (ECCO International, 2024). For the constrained areas, the local requirement is set by CAISO's annual Local Capacity Technical Study (CAISO, 2026), which determines how much local generation is needed to return the system to a safe operating state within 30 minutes of a contingency without firm load shedding. The resulting MW requirement per area is allocated to each load serving entity by its load ratio in the relevant Transmission Access Charge area during the month of highest forecast peak load (Draghi et al., 2025).

**NYISO.** Zones are mostly flat, the exception being Zone J (New York City), which is embedded in the larger G-J Locality (NYISO, 2023). A load serving entity in one of the three import-constrained zones receives a Locational Capacity Requirement (LCR) based on the import capability of that zone, a percentage of its obligation that must be procured locally (NYISO, 2023, 2026). Auctions are planned and regular, run closer to delivery, and price only the volume not already procured bilaterally (NYISO, 2026).

**MISO.** MISO uses ten Local Resource Zones (LRZs), defined by six criteria including electrical and state boundaries, transmission interconnection strength, and previous LOLE-study results (MISO, 2026). Above the LRZs sit two Sub-Regional Resource Zones, MISO Midwest (LRZs 1–7) and MISO South (LRZs 8–10), whose mutual transfers are capped at a fixed Regional Directional Transfer Limit (MISO, 2026). Each LRZ has a Local Reliability Requirement (LRR) based on its coincident peak demand. The Local Clearing Requirement, the volume that must be met by sources inside the zone, is the LRR minus the zone's import ability. After procurement, a Simultaneous Feasibility Test checks that the result is physically deliverable, and if it is not, the import and export limits are adjusted and the auction re-cleared (MISO, 2026).

# B

# PTDF matrix construction

In meshed AC grids, nodal injections and withdrawals affect the whole network on multiple lines, as flows cannot be directed through specific lines. Hence, network-wide flow effects are needed instead of simple path assumptions (Kunz & Zerrahn, 2015). Because AC load flows are complex to model, DC load flow can be used to linearize AC power flows for electricity network models, reducing complexity while achieving acceptable accuracy (Van den Bergh et al., 2014). Especially for questions on market design, congestion management, and investment decisions, DC load flow is a useful approximation for including transmission network constraints (Leuthold et al., 2012). DC load flow makes use of three assumptions according to (Purchala et al., 2005):

1. Small voltage angle difference
2. Line resistance is negligible and lines therefore lossless
3. Flat voltage profile

Those assumptions usually result in minor average error margins (< 5%), even though error margins for individual lines can be significantly higher (Purchala et al., 2005).

To model the DC power flow for this model, a power transfer distribution factor (PTDF) matrix is constructed. Through a PTDF, voltage angles can be left out from the optimization problem, further reducing complexity (Leuthold et al., 2012). The following construction of the PTDF matrix follows the steps laid out in Van den Bergh et al., 2014: First, the network topology is represented by the incidence matrix $IM$. $im_{l,n} = 1$ if line $l$ starts at node $n$, $im_{l,n} = -1$ if line $l$ ends at node $n$, and $im_{l,n} = 0$ if line $l$ is not connected to node $n$. The line orientation is arbitrary, but the sign convention must be consistent. Then, the result of the DC approximation given negligible resistance is calculated: The line susceptance $B_l$, and the diagonal matrix thereof $B_d$, is obtained by taking the reciprocal of line reactance $X_l$:

$$B_l = \frac{1}{X_l}$$

The DC power flow equation at time $t$ is represented by multiplying nodal injection $p^{inj}_{n,t}$ with the $PTDF$ matrix:

$$p^{flow}_{l,t} = \sum_n PTDF_{l,n}\, p^{inj}_{n,t}$$

With

$$PTDF = (B_d\, IM)\,(IM^T\, B_d\, IM)^{-1}$$

$$p^{inj}_{n,t} = \sum_{g \in \mathcal{G}_n} \left(q_{t,g} + r^{+}_{t,g} - r^{-}_{t,g}\right) - d^{served}_{n,t} + ls^{grid}_{n,t}.$$

Finally, a reference node has to be defined. As he DC nodal-balance equations are linearly dependent, $IM^T\, B_d\, IM$ is singular and at least one node has to be designated as a reference node and removed from the equations: For $B_d\,IM$ the column of the corresponding node is removed, and for $IM^T\,B_d\,IM$ the row and column for the corresponding node. In pure AC grids, one reference node is enough, while additional reference nodes are only needed in certain special cases.

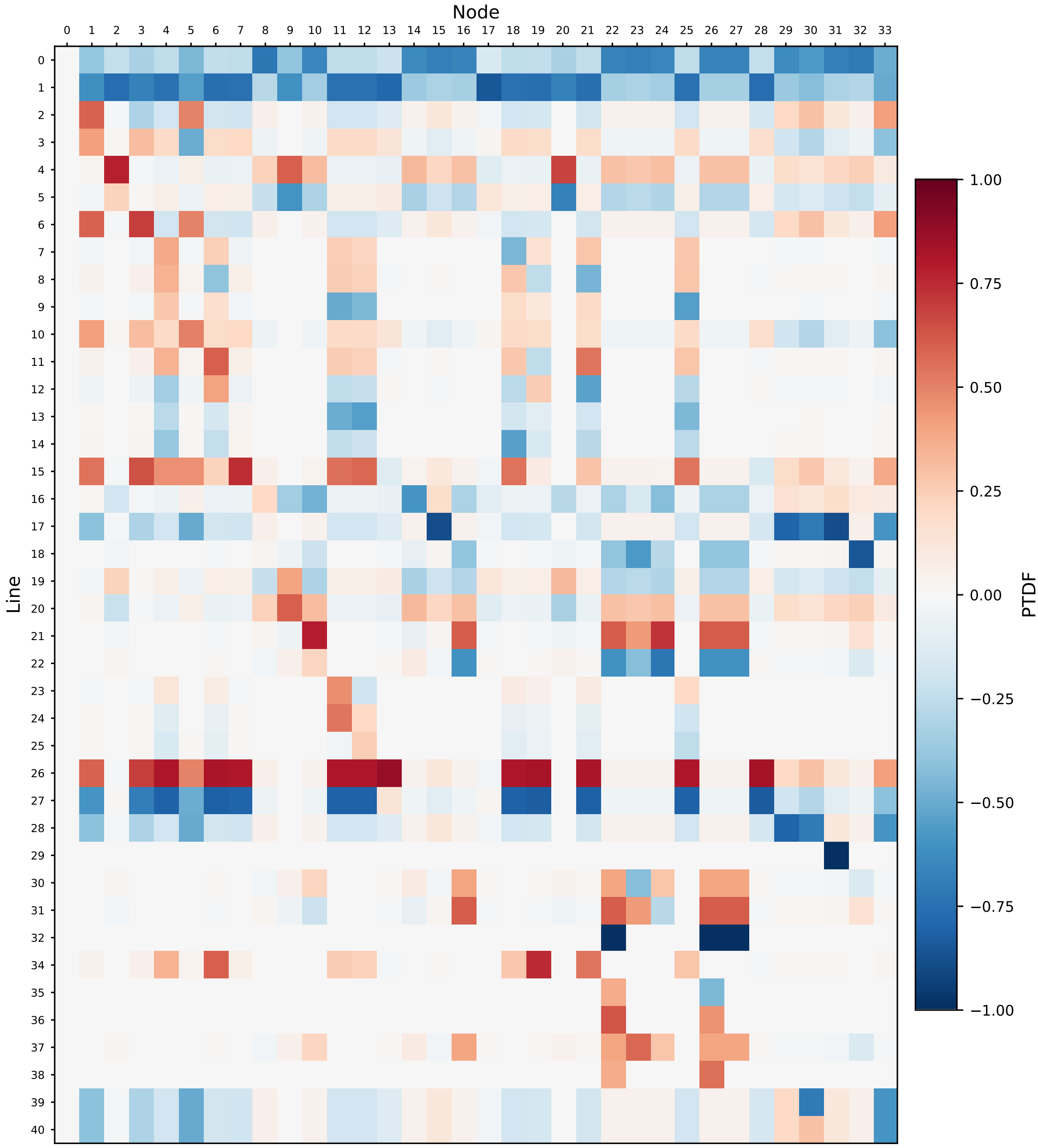


**Figure B.1:** PTDF matrix for the 34-node reduced Dutch network. Color encodes each line's sensitivity to injection at each node; red positive, blue negative, white near zero. Node 0 is the slack bus, so its column is zero by construction. Full numerical values are available in the project repository.

# C
# Methodology appendix

This appendix contains the mathematical derivations referenced in Chapter 3. It first states the general construction of a Mixed Complementarity Problem, then gives the actor-specific optimality and primal-dual equations, and finally documents the bounds used in the sequential MILP.

## C.1. General construction of a Mixed Complementarity Problem

For a convex optimization problem of the form

$$\min_{\boldsymbol{x}} \quad f(\boldsymbol{x}) \tag{C.1a}$$
$$\text{s.t.} \quad h(\boldsymbol{x}) = 0 \tag{C.1b}$$
$$g(\boldsymbol{x}) \geq 0. \tag{C.1c}$$

the Lagrangian is

$$\mathcal{L}(\boldsymbol{x}, \lambda, \mu) = f(\boldsymbol{x}) + \lambda^T h(\boldsymbol{x}) - \mu^T g(\boldsymbol{x}), \qquad \mu \geq 0. \tag{C.2}$$

The KKT conditions are

$$\nabla_{\boldsymbol{x}} \mathcal{L}(\boldsymbol{x}, \lambda, \mu) = 0, \tag{C.3a}$$
$$h(\boldsymbol{x}) = 0, \tag{C.3b}$$
$$g(\boldsymbol{x}) \geq 0, \tag{C.3c}$$
$$\mu \geq 0, \tag{C.3d}$$
$$\mu^T g(\boldsymbol{x}) = 0. \tag{C.3e}$$

For a non-negative scalar component $u$ of $\boldsymbol{x}$,, stationarity and complementary slackness can be written compactly as

$$0 \leq u \perp \frac{\partial \mathcal{L}}{\partial u} \geq 0 \tag{C.4}$$

For a free variable, the corresponding stationarity condition remains an equality. Combining the KKT systems of all actors with the market-clearing conditions gives the MCP used in this study.

## C.2. Strong duality and primal-dual reformulation

For each linear actor problem, the complementarity conditions can equivalently be replaced by primal feasibility, dual feasibility, and equality of the primal and dual objective values:

$$P_\omega(\boldsymbol{x}_\omega) = D_\omega(\mu_\omega) \qquad \forall \omega \in \mathcal{A}. \tag{C.5}$$

The actor-specific strong-duality equations are stated together with the corresponding KKT conditions in the next section.

## C.3. Actor optimality conditions and primal-dual equations

### C.3.1. Investable generator

Primal feasibility is given by Equations (3.1b)–(3.1d). Writing the maximizatio problem as the minimization of negative profit gives

$$\begin{aligned}\mathcal{L}_i = & -\sum_{t\in\mathcal{T}} W_t(\lambda_t^e - vc_i)q_{t,i} + fc_i c_i - \lambda_{z(i)}^c c_i^{cm} \\ & -\sum_{t\in\mathcal{T}} \mu_{t,i}^q (c_i - q_{t,i}) - \mu_i^{cap}(\overline{cap}_i - c_i) - \mu_i^{cm}(\alpha_i c_i - c_i^{cm})\end{aligned} \tag{C.6}$$

The KKT conditions are

$$0 \le q_{t,i} \perp -W_t(\lambda_t^e - vc_i) + \mu_{t,i}^q \ge 0 \qquad \forall t, i, \tag{C.7a}$$

$$0 \le c_i \perp fc_i - \sum_{t\in\mathcal{T}} \mu_{t,i}^q + \mu_i^{cap} - \alpha_i \mu_i^{cm} \ge 0 \qquad \forall i \tag{C.7b}$$

$$0 \le c_i^{cm} \perp -\lambda_{z(i)}^c + \mu_i^{cm} \ge 0 \qquad \forall i \tag{C.7c}$$

$$0 \le \mu_{t,i}^q \perp c_i - q_{t,i} \ge 0 \qquad \forall t, i \tag{C.7d}$$

$$0 \le \mu_i^{cap} \perp \overline{cap}_i - c_i \ge 0 \qquad \forall i \tag{C.7e}$$

$$0 \le \mu_i^{cm} \perp \alpha_i c_i - c_i^{cm} \ge 0 \qquad \forall i \tag{C.7f}$$

Strong duality requires

$$\begin{aligned}&\sum_{t\in\mathcal{T}} W_t(\lambda_t^e - vc_i)q_{t,i} - fc_i c_i + \lambda_{z(i)}^c c_i^{cm} \\ &\qquad = \overline{cap}_i \mu_i^{cap} \qquad \forall i\end{aligned} \tag{C.8}$$

### C.3.2. Legacy generator

Primal feasibility is given by Equations (3.2b) and (3.2c). The Lagrangian is

$$\begin{aligned}\mathcal{L}_j = & -\sum_{t\in\mathcal{T}} W_t(\lambda_t^e - vc_j)q_{t,j} - \lambda_{z(j)}^c c_j^{cm} \\ & -\sum_{t\in\mathcal{T}} \mu_{t,j}^q (a_{t,j}\overline{cap}_j - q_{t,j}) - \mu_j^{cm}(\alpha_j \overline{cap}_j - c_j^{cm})\end{aligned} \tag{C.9}$$

The KKT conditions are

$$
\begin{aligned}
&0 \le q_{t,j} \perp -W_t(\lambda_t^e - vc_j) + \mu_{t,j}^q \ge 0 && \forall t,j && \text{(C.10a)}\\
&0 \le c_j^{cm} \perp -\lambda_{z(j)}^c + \mu_j^{cm} \ge 0 && \forall j && \text{(C.10b)}\\
&0 \le \mu_{t,j}^q \perp a_{t,j}\overline{cap}_j - q_{t,j} \ge 0 && \forall t,j && \text{(C.10c)}\\
&0 \le \mu_j^{cm} \perp \alpha_j \overline{cap}_j - c_j^{cm} \ge 0 && \forall j && \text{(C.10d)}
\end{aligned}
$$

Strong duality requires

$$
\begin{aligned}
&\sum_{t\in\mathcal{T}} W_t(\lambda_t^e - vc_j)q_{t,j} + \lambda_{z(j)}^c c_j^{cm}\\
&\quad = \sum_{t\in\mathcal{T}} a_{t,j}\overline{cap}_j \mu_{t,j}^q + \alpha_j \overline{cap}_j \mu_j^{cm} \qquad \forall j
\end{aligned}
\tag{C.11}
$$

## C.3.3. Energy-demand agent

Using Equation (3.4b) to substitute $D_t = D_t^{\max} - ls_t^{em}$, the remaining optimality condition is

$$
0 \le ls_t^{em} \perp W_t(VOLL^{em} - \lambda_t^e) \ge 0 \qquad \forall t \tag{C.12}
$$

Together with market clearing, the corresponding folded balance is

$$
\sum_{g\in\mathcal{G}} q_{t,g} + ls_t^{em} = D_t^{\max} \qquad \forall t \tag{C.13}
$$

## C.3.4. Capacity-demand agent

Primal feasibility is given by Equations (3.6b)–(3.6e). Let $\overline{f}_{ab} = \sigma MEC_{ab}$. The Lagrangian is

$$
\begin{aligned}
\mathcal{L}^{CD} = &\sum_{z\in\mathcal{Z}} \lambda_z^c c_z^{dem} - \sum_{z\in\mathcal{Z}} \nu_z(c_z^{dem} - d_z^c + \eta_z)\\
&- \lambda^{c,sys}\left(\sum_{z\in\mathcal{Z}} c_z^{dem} - d^c\right) - \sum_{z\in\mathcal{Z}} \rho_z(d_z^c - \eta_z)\\
&- \sum_{(a,b)\in\mathcal{P}} \phi_{ab}^{lo}(f_{ab} + \overline{f}_{ab}) - \sum_{(a,b)\in\mathcal{P}} \phi_{ab}^{hi}(\overline{f}_{ab} - f_{ab})
\end{aligned}
\tag{C.14}
$$

The KKT conditions are

$$
\begin{aligned}
&0 \le c_z^{dem} \perp \lambda_z^c - \nu_z - \lambda^{c,sys} \ge 0 && \forall z && \text{(C.15a)}\\
&-(\nu_a - \rho_a) + (\nu_b - \rho_b) + \phi_{ab}^{hi} - \phi_{ab}^{lo} = 0 && \forall (a,b)\in\mathcal{P} && \text{(C.15b)}\\
&0 \le \nu_z \perp c_z^{dem} - d_z^c + \eta_z \ge 0 && \forall z && \text{(C.15c)}\\
&0 \le \lambda^{c,sys} \perp \sum_{z\in\mathcal{Z}} c_z^{dem} - d^c \ge 0 && && \text{(C.15d)}\\
&0 \le \rho_z \perp d_z^c - \eta_z \ge 0 && \forall z && \text{(C.15e)}\\
&0 \le \phi_{ab}^{lo} \perp f_{ab} + \overline{f}_{ab} \ge 0 && \forall (a,b)\in\mathcal{P} && \text{(C.15f)}\\
&0 \le \phi_{ab}^{hi} \perp \overline{f}_{ab} - f_{ab} \ge 0 && \forall (a,b)\in\mathcal{P} && \text{(C.15g)}
\end{aligned}
$$

Strong duality requires

$$
\begin{aligned}
\sum_{z\in\mathcal{Z}} \lambda_z^c c_z^{dem} = & \sum_{z\in\mathcal{Z}} d_z^c \nu_z - \sum_{z\in\mathcal{Z}} d_z^c \rho_z + d^c \lambda^{c,sys} \\
& - \sum_{(a,b)\in\mathcal{P}} \overline{f}_{ab} \left(\phi_{ab}^{lo} + \phi_{ab}^{hi}\right)
\end{aligned} \tag{C.16}
$$

### C.3.5. Redispatch operator

Primal feasibility is given by Equations (3.8b)–(3.8h). The Lagrangian is

$$
\begin{aligned}
\mathcal{L}^{RD} = & \sum_{t\in\mathcal{T}} W_t \left[\sum_{g\in\mathcal{G}} \left((vc_g + x) r_{t,g}^{+} + (-vc_g + x) r_{t,g}^{-}\right) + VOLL^{grid} \sum_{n\in\mathcal{N}} ls_{n,t}^{grid}\right] \\
& - \sum_{t\in\mathcal{T}} \sum_{g\in\mathcal{G}} \overline{\beta}_{t,g}^{q} (\overline{q}_{t,g} - q_{t,g} - r_{t,g}^{+}) \\
& - \sum_{t\in\mathcal{T}} \sum_{g\in\mathcal{G}} \overline{\beta}_{t,g}^{-} (q_{t,g} - r_{t,g}^{-}) \\
& - \sum_{t\in\mathcal{T}} \sum_{n\in\mathcal{N}} \overline{\gamma}_{n,t} (d_{n,t}^{served} - ls_{n,t}^{grid}) \\
& + \sum_{t\in\mathcal{T}} \lambda_t^{RD} \left(\sum_{g\in\mathcal{G}} r_{t,g}^{+} - \sum_{g\in\mathcal{G}} r_{t,g}^{-} + \sum_{n\in\mathcal{N}} ls_{n,t}^{grid}\right) \\
& - \sum_{t\in\mathcal{T}} \sum_{l\in\mathcal{L}} \underline{\rho}_{l,t} (F_l + p_{l,t}^{flow}) - \sum_{t\in\mathcal{T}} \sum_{l\in\mathcal{L}} \overline{\rho}_{l,t} (F_l - p_{l,t}^{flow}) \\
& + \sum_{t\in\mathcal{T}} \sum_{l\in\mathcal{L}} \phi_{l,t} \left[p_{l,t}^{flow} - \sum_{n\in\mathcal{N}} PTDF_{l,n} p_{n,t}^{inj}\right].
\end{aligned} \tag{C.17}
$$

The KKT conditions are

$$
\begin{aligned}
& 0 \le r_{t,g}^{+} \perp W_t(vc_g + x) + \overline{\beta}_{t,g}^{q} + \lambda_t^{RD} - \sum_{l\in\mathcal{L}} PTDF_{l,n(g)} \phi_{l,t} \ge 0 && \forall t, g && \text{(C.18a)} \\
& 0 \le r_{t,g}^{-} \perp W_t(-vc_g + x) + \overline{\beta}_{t,g}^{-} - \lambda_t^{RD} + \sum_{l\in\mathcal{L}} PTDF_{l,n(g)} \phi_{l,t} \ge 0 && \forall t, g && \text{(C.18b)} \\
& 0 \le ls_{n,t}^{grid} \perp W_t VOLL^{grid} + \overline{\gamma}_{n,t} + \lambda_t^{RD} - \sum_{l\in\mathcal{L}} PTDF_{l,n} \phi_{l,t} \ge 0 && \forall t, n && \text{(C.18c)} \\
& \phi_{l,t} + \overline{\rho}_{l,t} - \underline{\rho}_{l,t} = 0 && \forall t, l && \text{(C.18d)} \\
& 0 \le \overline{\beta}_{t,g}^{q} \perp \overline{q}_{t,g} - q_{t,g} - r_{t,g}^{+} \ge 0 && \forall t, g && \text{(C.18e)} \\
& 0 \le \overline{\beta}_{t,g}^{-} \perp q_{t,g} - r_{t,g}^{-} \ge 0 && \forall t, g && \text{(C.18f)} \\
& 0 \le \overline{\gamma}_{n,t} \perp d_{n,t}^{served} - ls_{n,t}^{grid} \ge 0 && \forall t, n && \text{(C.18g)} \\
& 0 \le \underline{\rho}_{l,t} \perp F_l + p_{l,t}^{flow} \ge 0 && \forall t, l && \text{(C.18h)} \\
& 0 \le \overline{\rho}_{l,t} \perp F_l - p_{l,t}^{flow} \ge 0 && \forall t, l && \text{(C.18i)}
\end{aligned}
$$

Strong duality requires

$$\begin{aligned}&\sum_{t\in\mathcal{T}} W_t \left[\sum_{g\in\mathcal{G}} \left((vc_g + x)r^+_{t,g} + (-vc_g + x)r^-_{t,g}\right) + VOLL^{grid} \sum_{n\in\mathcal{N}} ls^{grid}_{n,t}\right] \\ &= -\sum_{t\in\mathcal{T}} \left[\sum_{g\in\mathcal{G}} (\overline{q}_{t,g} - q_{t,g})\overline{\beta}^q_{t,g} + \sum_{g\in\mathcal{G}} q_{t,g}\overline{\beta}^-_{t,g} \right. \\ &\qquad \left. + \sum_{n\in\mathcal{N}} d^{served}_{n,t}\overline{\gamma}_{n,t} + \sum_{l\in\mathcal{L}} F_l \left(\underline{\rho}_{l,t} + \overline{\rho}_{l,t}\right) + \sum_{l\in\mathcal{L}} f^{mkt}_{l,t}\phi_{l,t}\right]\end{aligned} \tag{C.19}$$

where $f^{mkt}_{l,t}$ is defined in Equation (3.12).

# C.4. Bounds used in the sequential MILP

The disjunctive reformulation in subsection 3.4.3 uses the following definitions:

$$\overline{f}_{ab} = \sigma MEC_{ab} \tag{C.20}$$

$$W^{\max} = \max_{t\in\mathcal{T}} W_t, \qquad W^{tot} = \sum_{t\in\mathcal{T}} W_t, \qquad \overline{\lambda^c} = \max_{i\in\mathcal{I}} fc_i \tag{C.21}$$

**Table C.1:** Bounds on primal variables and constraint slacks used in the disjunctive reformulation.

| Constant | Value | Reasoning |
|---|---|---|
| $K^q$ | $\max_{g\in\mathcal{G}} \overline{cap}_g$ | Dispatch cannot exceed the installed or installable capacity of the largest generator. |
| $K^{ls}$ | $\max_{t\in\mathcal{T}} D^{\max}_t$ | Energy market load shedding cannot exceed total demand in the respective timestep. |
| $K^c$ | $\max_{i\in\mathcal{I}} \overline{cap}_i$ | Investment at one candidate location cannot exceed its maximum installable capacity. |
| $K^{cm}$ | $\max_{g\in\mathcal{G}} \overline{cap}_g$ | A capacity market offer cannot exceed the generator's de-rated capacity. Since $\alpha_g \leq 1$, the largest generator capacity is a valid common bound. |
| $K^{dem}$ | $\max_{z\in\mathcal{Z}} \left(d^c_z + \sum_{(a,b)\in\mathcal{P}:z\in\{a,b\}} \overline{f}_{ab}\right)$ | The largest zonal procurement occurs where a zone covers its own requirement and takes on the maximum permitted obligation from all connected zones. |
| $K^{sys}$ | $\sum_{z\in\mathcal{Z}} \left(d^c_z + \sum_{(a,b)\in\mathcal{P}:z\in\{a,b\}} \overline{f}_{ab}\right)$ | This gives a conservative bound on the slack of the system-wide capacity floor. |
| $\widetilde{K}^{q,I}$ | $\max_{i\in\mathcal{I}} \overline{cap}_i$ | The unused output capability $c_i - q_{t,i}$ cannot exceed maximum installable capacity. |
| $\widetilde{K}^{q,J}$ | $\max_{t\in\mathcal{T},\, j\in\mathcal{J}} a_{t,j}\overline{cap}_j$ | The unused output capability of a legacy generator cannot exceed its maximum available output. |
| $\widetilde{K}^{cap}$ | $\max_{i\in\mathcal{I}} \overline{cap}_i$ | The investment slack $\overline{cap}_i - c_i$ cannot exceed maximum installable capacity. |
| $\widetilde{K}^{cm,I}$ | $\max_{i\in\mathcal{I}} \overline{cap}_i$ | Investable generators have $\alpha_i = 1$, so the unused capacity market capability cannot exceed maximum installable capacity. |
| $\widetilde{K}^{cm,J}$ | $\max_{j\in\mathcal{J}} \alpha_j\overline{cap}_j$ | The unused capacity market capability of a legacy generator cannot exceed its de-rated installed capacity. |
| $\widetilde{K}^f_{ab}$ | $2\overline{f}_{ab}$ | The transfer lies between $-\overline{f}_{ab}$ and $\overline{f}_{ab}$. Its maximum distance from either bound is the full interval width. |

**Table C.2:** Bounds on prices, dual variables, and stationarity expressions used in the disjunctive reformulation.

| Constant | Value | Reasoning |
|---|---|---|
| $\widehat{K}^{\lambda^e}$ | $VOLL^{em}$ | The energy price cannot exceed the willingness to pay represented by energy market load shedding. |
| $\widehat{K}^{\lambda^c}$ | $\overline{\lambda^c}$ | A capacity price above the highest investable-generator fixed cost is not required to support investment. Energy market rents can only lower the required capacity payment. |
| $\widehat{K}^{\mu^q}$ | $W^{\max} VOLL^{em}$ | Dispatch stationarity links the capacity shadow price to the weighted energy market margin. The largest possible margin is bounded by $VOLL^{em}$. |
| $\widehat{K}^{\mu^{cm}}$ | $\overline{\lambda^c}$ | Capacity-offer stationarity links the offer-bound dual to the zonal capacity price. |
| $\widehat{K}^{\mu^{cap}}$ | $W^{tot} VOLL^{em} + \overline{\lambda^c}$ | The upper investment-capacity dual can include scarcity rents accumulated over all represented hours and the capacity market contribution. |
| $\widehat{K}^{\nu}, \widehat{K}^{\rho}, \widehat{K}^{\phi}$ | $\overline{\lambda^c}$ | The capacity-demand and transfer duals represent changes in procurement expenditure and remain on the capacity-price scale. |
| $\widehat{K}^{\lambda^{c,sys}}$ | $\overline{\lambda^c}$ | The value of tightening the system-wide requirement cannot exceed the maximum capacity price used in the model. |
| $\overline{K}^{q,I}$ | $W^{\max}\left(VOLL^{em} + \max_{i \in \mathcal{I}} vc_i\right)$ | This covers the largest value of the investable-generator dispatch stationarity expression. |
| $\overline{K}^{q,J}$ | $W^{\max}\left(VOLL^{em} + \max_{j \in \mathcal{J}} vc_j\right)$ | The same reasoning applies to legacy-generator dispatch stationarity. |
| $\overline{K}^{c}$ | $\max_{i \in \mathcal{I}} fc_i + \widehat{K}^{\mu^{cap}} + \overline{\lambda^c}$ | The investment stationarity expression combines fixed cost, the upper-capacity dual, accumulated dispatch duals, and the capacity-offer dual. |
| $\overline{K}^{cm}$ | $\overline{\lambda^c}$ | The capacity-offer stationarity expression is the difference between the zonal capacity price and the offer-bound dual. |
| $\overline{K}^{dem}$ | $\overline{\lambda^c}$ | The procurement stationarity expression is largest when the zonal price is at its upper bound and the requirement duals are zero. |
| $\overline{K}^{ls}$ | $W^{\max} VOLL^{em}$ | The load-shedding stationarity expression is largest when the energy price is zero. |

The bounds are conservative common values rather than mathematically minimal bounds for every individual variable. Their adequacy is tested in the proof of concept by multiplying all values by 100.

# D

# Computational performance of the exploration runs

This appendix provides the detailed evidence supporting the computational-performance discussion in Section 5.1. Across both case studies, six capacity market designs and 80 exploration directions result in 960 first-stage runs. Every run returned a feasible incumbent, and the corresponding redispatch problem could subsequently be solved to optimality. All exploration outcomes remain included in the results analysis, irrespective of their final optimality gap.

## D.1. Overall computational performance

Table D.1 summarizes the solving performance for each scenario. The requested relative optimality gap was reached in only part of the exploration set, while most runs ended at the time limit. One run per scenario in Case Study 2, and one country-wide run in Case Study 1, did not return a finite relative gap.

**Table D.1:** Computational performance of all exploration runs.

| Scenario | Runs | Reached target gap | Time limit | No finite gap | Median gap | Maximum finite gap | Median time [s] |
|---|---|---|---|---|---|---|---|
| Case Study 1, $z1$ | 80 | 9 | 71 | 1 | 1.227 | 166.766 | 220.6 |
| Case Study 1, $z3$, $\sigma = 0$ | 80 | 21 | 59 | 0 | 0.146 | 35.301 | 220.5 |
| Case Study 1, $z3$, $\sigma = 0.25$ | 80 | 12 | 68 | 0 | 0.380 | 8.120 | 220.5 |
| Case Study 1, $z3$, $\sigma = 0.5$ | 80 | 10 | 70 | 0 | 0.348 | 5.256 | 220.6 |
| Case Study 1, $z3$, $\sigma = 0.75$ | 80 | 10 | 70 | 0 | 0.488 | 114.924 | 220.6 |
| Case Study 1, $z3$, $\sigma = 1$ | 80 | 10 | 70 | 0 | 0.752 | 99.792 | 220.6 |
| Case Study 2, $z1$ | 80 | 9 | 71 | 1 | 21.221 | 1095.719 | 120.6 |
| Case Study 2, $z3$, $\sigma = 0$ | 80 | 11 | 69 | 1 | 7.269 | 702.144 | 120.5 |
| Case Study 2, $z3$, $\sigma = 0.25$ | 80 | 11 | 69 | 1 | 15.226 | 687.545 | 120.5 |
| Case Study 2, $z3$, $\sigma = 0.5$ | 80 | 9 | 71 | 1 | 15.046 | 1201.550 | 120.5 |
| Case Study 2, $z3$, $\sigma = 0.75$ | 80 | 9 | 71 | 1 | 20.930 | $6.88 \times 10^8$ | 120.6 |
| Case Study 2, $z3$, $\sigma = 1$ | 80 | 9 | 71 | 1 | 18.547 | 950.937 | 120.6 |

The gaps refer to the PTDF-based exploration objective rather than to capacity market expenditure, redispatch cost, or another economically meaningful quantity. This objective can take values close to zero, which can produce very large relative gaps even where a feasible incumbent has been found. The reported gaps should therefore be interpreted as a measure of how far the solver progressed in the respective exploration direction, not as an equivalent uncertainty in the economic results.

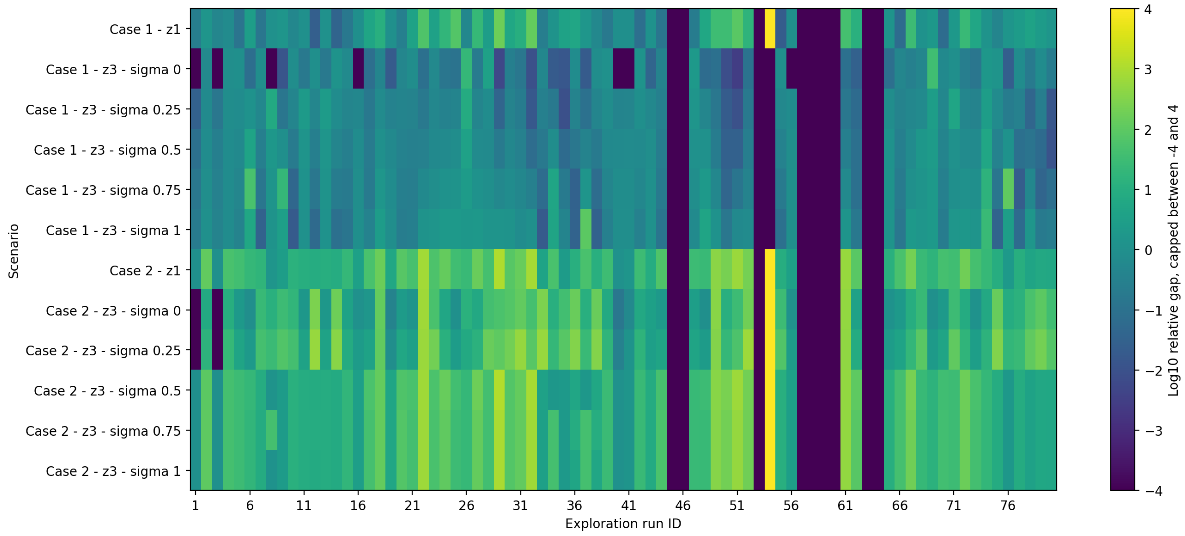


**Figure D.1:** Relative optimality gap by exploration run and scenario. Each column represents one PTDF-based exploration direction. Runs without a finite relative gap are displayed at the upper limit of the color scale. All runs remain included in the results analysis.

## D.2. Warm-start procedure for Case Study 2

Case Study 1 was solved with a standard time limit of 220 seconds per exploration direction. In Case Study 2, the complete MILP initially struggled to find feasible incumbents within the available solving time. A separate weight-independent LP was therefore solved once for every capacity market design and value of $\sigma$.

The LP contains the primal energy market, capacity market, and investment constraints, but excludes the dual variables and disjunctive constraints of the full MILP. Its primal solution was used to provide starting values for the continuous variables. Starting values for the binary variables were derived from whether the associated primal variables or constraint slacks were active. This resulted in a partial MIP start that was reused for all 80 exploration directions within the respective scenario.

The warm-start LP does not contain the PTDF-based exploration objective. The positive and negative exploration of each transmission line therefore begin from the same underlying starting point. The warm start does not alter the feasible set or any equilibrium condition. It can, however, affect the search path and the incumbent found before the time limit is reached, particularly for runs that do not achieve the requested gap.

## D.3. Mapping of exploration runs to PTDF directions

The exploration run IDs follow the order of the PTDF matrix. For each transmission line, the first run uses the positive PTDF direction and the second run uses the negative direction. Table D.2 provides the complete mapping. The number of significant entries is also reported to distinguish between sparse and dense PTDF rows.

**Table D.2:** Mapping of the PTDF exploration directions. $L_1$ is the sum of the absolute PTDF values in the row, while $n_{sig}$ counts entries with $|PTDF_{\ell,n}| > 0.05$.

| PTDF row order | Line index | $L_1$ | $n_{sig}$ | Positive run ID | Negative run ID |
|---|---|---|---|---|---|
| 1 | 0 | 14.76 | 33 | 1 | 2 |
| 2 | 1 | 18.24 | 33 | 3 | 4 |
| 3 | 10 | 4.85 | 20 | 5 | 6 |
| 4 | 11 | 3.10 | 10 | 7 | 8 |
| 5 | 12 | 2.91 | 10 | 9 | 10 |

Continued on next page

Table D.2 – continued from previous page

| PTDF row order | Line index | $L_1$ | $n_{sig}$ | Positive run ID | Negative run ID |
|---|---|---|---|---|---|
| 6 | 13 | 2.57 | 8 | 11 | 12 |
| 7 | 14 | 2.52 | 8 | 13 | 14 |
| 8 | 15 | 7.39 | 19 | 15 | 16 |
| 9 | 16 | 5.54 | 30 | 17 | 18 |
| 10 | 17 | 7.60 | 20 | 19 | 20 |
| 11 | 18 | 3.95 | 10 | 21 | 22 |
| 12 | 19 | 5.51 | 31 | 23 | 24 |
| 13 | 2 | 5.02 | 20 | 25 | 26 |
| 14 | 20 | 5.71 | 31 | 27 | 28 |
| 15 | 21 | 4.96 | 10 | 29 | 30 |
| 16 | 22 | 4.39 | 10 | 31 | 32 |
| 17 | 23 | 1.34 | 7 | 33 | 34 |
| 18 | 24 | 1.41 | 7 | 35 | 36 |
| 19 | 25 | 1.12 | 7 | 37 | 38 |
| 20 | 26 | 12.39 | 20 | 39 | 40 |
| 21 | 27 | 11.64 | 20 | 41 | 42 |
| 22 | 28 | 6.05 | 20 | 43 | 44 |
| 23 | 29 | 1.00 | 1 | 45 | 46 |
| 24 | 3 | 4.85 | 20 | 47 | 48 |
| 25 | 30 | 3.09 | 10 | 49 | 50 |
| 26 | 31 | 3.94 | 10 | 51 | 52 |
| 27 | 32 | 3.00 | 3 | 53 | 54 |
| 28 | 34 | 3.59 | 10 | 55 | 56 |
| 29 | 35 | 0.82 | 2 | 57 | 58 |
| 30 | 36 | 1.08 | 2 | 59 | 60 |
| 31 | 37 | 3.24 | 10 | 61 | 62 |
| 32 | 38 | 0.92 | 2 | 63 | 64 |
| 33 | 39 | 5.44 | 20 | 65 | 66 |
| 34 | 4 | 6.62 | 31 | 67 | 68 |
| 35 | 40 | 5.03 | 20 | 69 | 70 |
| 36 | 5 | 6.06 | 31 | 71 | 72 |
| 37 | 6 | 5.39 | 20 | 73 | 74 |
| 38 | 7 | 2.43 | 8 | 75 | 76 |
| 39 | 8 | 2.85 | 10 | 77 | 78 |
| 40 | 9 | 2.56 | 8 | 79 | 80 |

## D.4. Repeatedly difficult directions and PTDF structure

A clearer computational pattern appears when the gaps are compared by exploration run rather than only by scenario. Largely the same directions remain difficult across the different values of $\sigma$. In Case Study 1, run 74 is among the directions with the largest gaps for every investigated value of $\sigma$. In Case Study 2, runs 22, 49, 52, and 61 repeatedly appear among the most difficult directions. Both positive and negative PTDF directions are represented, so the sign of the exploration direction alone does not explain the difference in solving performance.

The clearest distinction is between highly radial and meshed PTDF rows. Five PTDF rows have significant entries at no more than three nodes, where an entry is treated as significant if $|PTDF_{\ell,n}| > 0.05$. Across the six designs, 59 of the 60 corresponding runs in Case Study 1 and 54 of 60 in Case Study 2 reach the requested gap. Among the remaining directions, only 13 of 420 runs in Case Study 1 and 4 of 420 in Case Study 2 reach the target. Exploration along radial directions is therefore considerably easier for the solver.

Beyond this distinction, solving difficulty does not increase mechanically with the density of the PTDF row. Several repeatedly difficult directions in Case Study 2 have ten significant entries and do not belong to the rows with either the largest $L_1$ norm or the largest value of $n_{sig}$. The PTDF structure therefore explains why the radial directions solve quickly, but not the full variation among the remaining meshed-network directions.

The repeated occurrence of the same difficult run IDs across the different values of $\sigma$ indicates that the selected network direction has a stronger influence on solving performance than the level of cross-zonal participation alone.

## D.5. Extended reruns

Runs 29 and 46 of Case Study 2 were rerun with an extended time limit of 1,500 seconds. The incumbent of the corresponding initial MILP run was used as the starting point. Table D.3 compares the original and extended results.

**Table D.3:** Comparison of the initial and extended Case Study 2 runs. A dash indicates that no finite relative gap was available.

| Design | $\sigma$ | Run | Initial status | Initial time $[s]$ | Initial gap | Rerun status | Rerun time $[s]$ | Rerun gap |
|---|---|---|---|---|---|---|---|---|
| $z1$ | 0 | 29 | Time limit | 120.8 | 1095.718 | Time limit | 1500.5 | 1095.719 |
| $z1$ | 0 | 46 | Time limit | 120.7 | – | Optimal | 176.9 | 0.000 |
| $z3$ | 0 | 29 | Time limit | 120.4 | 55.579 | Time limit | 1500.7 | 54.173 |
| $z3$ | 0 | 46 | Optimal | 18.3 | 0.000 | Optimal | 4.2 | 0.000 |
| $z3$ | 0.25 | 29 | Time limit | 120.6 | 108.195 | Time limit | 1500.6 | 106.648 |
| $z3$ | 0.25 | 46 | Optimal | 17.3 | 0.000 | Optimal | 4.0 | 0.000 |
| $z3$ | 0.5 | 29 | Time limit | 120.7 | 1201.550 | Time limit | 1500.9 | 1201.550 |
| $z3$ | 0.5 | 46 | Time limit | 120.3 | 42.934 | Optimal | 65.7 | 0.000 |
| $z3$ | 0.75 | 29 | Time limit | 120.7 | 950.936 | Time limit | 1501.2 | 950.937 |
| $z3$ | 0.75 | 46 | Time limit | 120.7 | – | Optimal | 236.4 | 0.000 |
| $z3$ | 1 | 29 | Time limit | 120.6 | 950.936 | Time limit | 1501.1 | 950.937 |
| $z3$ | 1 | 46 | Time limit | 120.6 | – | Optimal | 246.7 | 0.000 |

The extended solving time was effective for run 46. In four scenarios, it reached the requested gap after the initial run had ended at the time limit without doing so. Run 29 remained difficult across the scenario set despite the longer time limit and the use of the previous incumbent as a starting point. Additional solving time can therefore resolve some difficult directions, but it does not remove the structural difficulty of every exploration objective.

# E

# AI statement

For this thesis, AI was used in several ways. 1) Writefull's integration into Overleaf was used to improve the language of this thesis. Writefull not only points out spelling and grammar mistakes but also suggests improvements on how to improve readability by for example suggesting to switch the sentence structure. 2) GitHub Copilot was used for writing code to accelerate the coding process. Through the integration in VS Code, it was used to diagnose errors, clean up the structure but also write code itself. Importantly, it was only used to write code for the logic provided by the author beforehand. Therefore, it did not have any influence on the conceptual or formal model built by the author, but only the implementation of it in code. Especially for the creation of figures, the coding assistance saved a lot of time. 3) Claude (Opus 4.7) was used for clarity and report structure. In that it was primarily used to have an eye on the coherency of the report, suggesting what parts of a section should be switched in sequence for example or pointing out unnecessary repetitions across sections. It was therefore used to provide stylistic feedback improving the clarity of the report. To do so, sections of this thesis were periodically uploaded to check for coherency. However, no AI generated text was directly carried over into the report. 4) ChatGPT (GPT-5.5) was used to generate the cover image based on Figure 4.1 and Figure 4.3.

After using AI tools, I manually reviewed and critically assessed the results/suggestions and take full responsibility for the content of this report.